PhD degree in Molecular Medicine (curriculum in Molecular Oncology)

European School of Molecular Medicine (SEMM),

University of Milan and University of Naples "Federico II"

Settore disciplinare: BIO/11

Accessibility of genomic regulatory elements in macrophages

Silvia Bonifacio

IEO, Milan

Matricola n. R09404

Supervisor: Dr. Gioacchino Natoli

IEO, Milan

Added Supervisor: Dr. Serena Ghisletti

IEO, Milan

Anno accademico 2014-2015

TABLE OF CONTENTS

LIST OF ABBREVIATIONS

3C: Chromosome Conformation Capture

Ac: Acetylation

ARPs: Actin-Related Proteins

ATP: Adenosine-5’-triphosphate

BAC: Bacterial Artificial Chromosome

BMDM: Bone Marrow Derived Macrophages

bp: base pairs

BRM: Brahma

BRG1: Brahma-Related Gene 1

BSA: Bovine Serum Albumin

CENP-A; Centromere Protein A

C+G: Cytosine + Guanine content of a DNA stretch

CHD: CHromoDomain

ChIP: Chromatin Immuno-Precipitation

ChIP-seq: ChIP followed by HT-sequencing

CpG: CG dinucleotide

CTCF: CCCTC- binding factor zinc finger protein

DHSs: DNase Hypersensitivity Sites

DMEM: Dulbecco ‘s Modified Eagle’s’ Medium

DNA: Deoxyribonucleic Acid

Erα: estrogen receptor alpha

eRNA: enhancer RNA

ESC: Embrionic Stem Cell

FBS Fetal Bovine Serum

FISH: Fluorescence In Situ Hybridization

FPKM: Fragments Per Kilobase of transcript per Million mapped reads

H1: Histone1

H2: Histone2

H3: Histone3

H4: Histone4

H3K4me1: monomethylation of histone H3 Lysine 4

H3K4me3: trimethylation of histone H3 Lysine 4

H3K27me3: trimethylation of histone H3 on lysine 27

HAS: Helicase-SANT domain

HAT: Histone AcetylTransferase

HR: Homologous Recombination

HT: High-Throughput

Il6: Interleukin 6

IRF: Interferon-Regulatory Factor

ISW1: Imitation SWitch1

kbp kilo base pairs

LPS: Lipopolysaccaride

MEF: Mouse Embrionic Fibroblast

MNase: Micrococcal Nuclease

mRNA: messanger RNA

NDR: Nucleosome-Depleted Region

NFR: Nucleosome-Free Region

Nos2: Nitric oxide syntase 2

NPCs: Neural Progenitor Cells

nt: nucleotide

PBS: Phosphate Buffered Saline

PCR: Polymerase Chain Reaction

PDH: Plant homeodomains

polyA: poly Adenylated

PRG: Primary response gene

qPCR: quantitative PCRPu.1: Purine-rich box 1

PWM: Positioned Weight Matrix

RNA: Ribonucleic Acid

RNA pol II: RNA polymerase II

RPM: Revolutions Per Minute

RT: Room Temperature

shRNA: short hairpin RNA

SRG: Secondary Response Genes

SWi/SNF: SWItching defective/Sucrose Non-Fermenting

TF: Transcription Factor

TFBS: Transcription Factor Binding Site

TNFα: Tumor Necrosis Factor alpha

TSS: Transcription Start Site

UT: Untreated

FIGURES INDEX

Introduction

Results

TABLES INDEX

ABSTRACT

The packing of eukaryotic genomes into chromatin plays a fundamental role in controlling DNA accessibility, important for different processes such as transcription, DNA replication and repair. Faithful transcriptional control in eukaryotic cells relies on the precise interplay between regulatory elements in the DNA, nucleosomes and transcription factors (TFs). The aim of this study was to analyze: 1) the nucleosome organization and chromatin accessibility at regulatory elements in differentiated cell types (notably murine macrophages) and 2) the role of the macrophage master regulator Pu.1, ATP-chromatin remodelers and H2A.Z histone variant in regulating chromatin accessibility. We generated high-resolution genome-wide nucleosome maps (by Micrococcal Nuclease digestion) centered on TSS-distal Pu.1 binding sites. We found regularly spaced nucleosome arrays with a nucleosome-depleted region centered on Pu.1 binding peaks. On the contrary, high nucleosome occupancy overlapping regions bound by Pu.1 in macrophages was detected in cells depleted of, or not expressing Pu.1 or in in vitro-reconstituted chromatin. Our findings suggest that Pu.1 actively maintains nucleosome depletion at regulatory regions. We then focused on the role of chromatin remodelers highly expressed in macrophages in regulating nucleosome landscape. In particular, we found that Brg1 strongly co-localizes with Pu.1 at macrophage regulatory regions, suggesting its active role in organizing chromatin accessibility at regulatory elements. We then investigated the genomic localization of histone variant H2A.Z. We found that it is highly associated with regulatory regions and Pu.1-bound sites in macrophages and its binding to macrophage genomic regions is affected by inflammatory stimulus. Finally we generated genome-wide DNase-seq, FAIRE-seq and ATAC-seq maps to study DNA accessibility and its changes after inflammatory stimulus.

INTRODUCTION

The packing of eukaryotic genomes into chromatin plays a fundamental role in controlling DNA accessibility, important for different processes such as transcription, DNA replication and repair (reviewed in Ehrenhofer-Murray, 2004). In particular, eukaryotic gene regulation involves a balance between packaging of the genome into nucleosomes and enabling access to regulatory proteins (such as transcription factors) and RNA polymerase (Li et al., 2007) at regulatory elements.

Nucleosome stability at regulatory regions is modified in several ways including post-translational modification of histones (Zentner and Henikoff, 2013), ATP-dependent chromatin remodelers that move or displace nucleosomes (Hargreaves and Crabtree, 2011), replacement of canonical histones with histone variants (Talbert and Henikoff, 2010, 2014) and binding of pioneer transcription factors (Soufi et al., 2015; Zaret and Carroll, 2011), characterized by their ability to bind sites in a nucleosomal context and make them accessible.

1) Determinants of nucleosome positioning and occupancy

Compaction of genomic DNA into chromatin is a hallmark of all eukaryotic cells (Malik and Henikoff, 2003). Chromatin is a nucleoprotein complex, whose basic unit is the nucleosome, that comprises 146 base pairs of DNA wrapped 1.7 times around an octamer of histone proteins separated by shorter linker DNA (Luger et al., 1997). Linker DNA length varies in different species or even depending on the tissue considered (Valouev et al., 2011). The histone octamer is composed by a core constituted of an $(H3/H4)_2$ tetramer formed for a strong four-helix bundle interaction between the two H3 proteins. Interacting with the $(H3/H4)_2$ tetramer are

two heterodimers of H2A/H2B, which dock at the DNA entry and exit sites through the H2A C terminus-docking domain (Luger et al., 1997) (fig. 1).

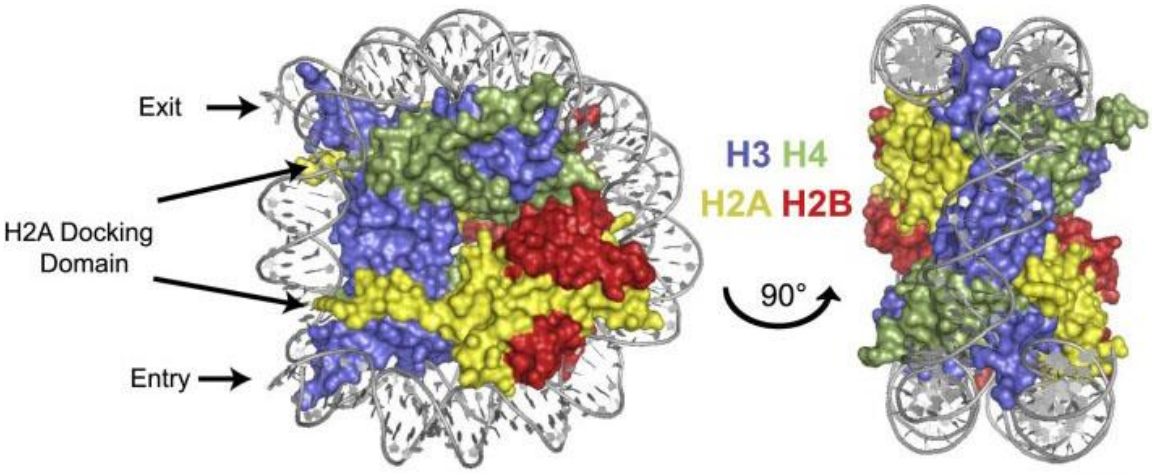

Fig. 1) Nucleosome structure. (Adapted from (Weber and Henikoff, 2014)).

Nucleosome positions are usually described through occupancy and positioning. Occupancy defines the probability that a DNA sequence is wrapped into a nucleosome in a population of cells. Given similar occupancy, the DNA can slide along the histone octamer, resulting in different conformations. The less conformations the nucleosome can assume, the better its positioning, and vice versa.

Nucleosome positioning and occupancy are dictated by the combined interplay of different factors: the intrinsic affinity for nucleosomes of DNA sequences (Kaplan et al., 2009; Segal et al., 2006), the barrier-induced statistical positioning (Mavrich et al., 2008a), the activity of ATP-dependent chromatin remodeling complexes and transcription factors (TFs) competing with nucleosomes for DNA binding (Gkikopoulos et al., 2011a; Valouev et al., 2011; Zhang et al., 2011). Pioneer studies showed a much larger contribution of the sequence to occupancy (Segal and Widom, 2009; Segal et al., 2006) than positioning (Zhang et al., 2009). In general, a moderate G/C content favors nucleosome assembly (Segal et al., 2006;

Tillo and Hughes, 2009) but the extreme guanine-cytosine content of some CpG islands is not compatible with efficient bending around the histone octamer and thus favors the formation of nucleosome-depleted areas (Fenouil et al., 2012; Ramirez-Carrozzi et al., 2009) that are rapidly accessible to stimulus-activated TFs as well as to the basal transcriptional machinery. Furthermore, Poly(dA:dT) tracts are virtually nucleosome-excluding sequence. They form stiff structures unable to bend around the histone octamer (Nelson et al., 1987; Segal and Widom, 2009). This in fact accounts for nucleosome depletion at poly(dA:dT) sequences commonly found in S. cerevisiae gene promoters. In human cells, nucleosome-repelling poly(dA:dT) tracts flanking moderately (dG:dC)-rich regions delimit container sites, defined as sequences able to accommodate positioned nucleosomes in in vitro assembly experiments (Valouev et al., 2011). Beside sequence itself, fixed barriers on chromosomes generate adjacent ordered arrays of nucleosomes, first described under the term of statistical positioning (Kornberg, 1981). A positioned nucleosome or another DNA-binding protein or complex as well as a repelling poly(dA:dT) tract can act as barriers.

Nucleosomal organization at regulatory elements has been the subject of intense studies, especially at transcriptional start sites (TSSs) and enhancers. Active and poised (namely those in which RNA polymerase II -RNA pol II- is engaged but is not elongating into the gene body) TSSs show a particular configuration in which a nucleosome free region (NFR) is flanked by two well-positioned nucleosomes (named +1 and -1 according to the direction of transcription), followed by a nucleosomal array overlapping the initial portion of the gene body (Jiang and Pugh, 2009).

Nucleosome positiosing sequences and poly(dA:dT) tracts upstream of TSSs were first ascribed as the barriers responsible for the positioning of the +1 nucleosome, from which an array of regularly spaced nucleosomes emanate (Yuan and Liu, 2008). While the NFR upstream TSSs is largely encoded by the sequence (Yuan and Liu, 2008), *in vitro* reconstitution of chromatin does not recapitulate the *in vivo* pattern. Several studies suggested that RNA Pol II may play a role in the maintenance of NFRs at promoters in various species, although this point was subject to discussion (Gilchrist et al., 2010; Mavrich et al., 2008b; Schones et al., 2008; Song et al., 2011a; Valouev et al., 2011; Weiner et al., 2010; Zhang et al., 2011). In particular, it has recently been shown that the RNA pol II complex is not responsible for the maintainance of this pattern (Fenouil et al., 2012). A crucial role for nucleosome organization is carried out by ATP-chormatin remodelers. Indeed Zhang et al. demonstrated that proper nucleosome positioning, spacing, and occupancy levels at 5' ends of most yeast genes was achieved by adding ATP to the reaction of *in vitro* reconstitution of chromatin (Zhang et al., 2011). The same authors showed a position-specific role (relative to the NFR) for many ATP-dependent chromatin remodelers (Yen et al., 2012). Another study demonstrated that Isw1 and Chd1 chromatin remodelers are required to maintain nucleosome organization at yeast genes (Gkikopoulos et al., 2011b). Arrays of positioned nucleosomes have also been shown to emanate from sites bound by TFs (Kundaje et al., 2012) but the contribution of co-factors and ATP-dependent chromatin remodeling at TSS-distal cis-regulatory elements still remains to be investigated.

2. ATP-dependent chromatin remodelers

ATP-dependent chromatin remodeling enzymes can re-position, evict, or alter the composition of nucleosomes (Clapier and Cairns, 2009a). Chromatin remodelers are large multi-subunit complexes with a common SF2 helicase ATPase domain comprised of two parts (DExx and HELICc regions) separated by a linker which catalyzes ATP-dependent restructuring and repositioning of nucleosomes. They are classified into four different families—SWI/SNF, ISWI, CHD and INO80—based on the arrangement of other domains in their catalytic subunit as well as their non-catalytic subunit composition (Hargreaves and Crabtree, 2011; Yodh, 2013). So far, studies of chromatin remodelers have predominantly focused on understanding the mechanism of ATP-mediated catalysis of nucleosome movement *in vitro* (Blosser et al., 2009; Deindl et al., 2013; Mueller-Planitz et al., 2013; Narlikar et al., 2001; Racki et al., 2014; Rippe et al., 2007; van Vugt et al., 2009). Less is known about their distribution throughout the genome and their individual roles in chromatin reorganization, in particular in mammals. Indeed, genome-wide functional *in vivo* studies have been performed mainly in yeast (Gkikopoulos et al., 2011; Yen et al., 2012; Zentner et al., 2013, Hughes and Rando, 2015; Parnell et al., 2015) or Drosophila (Moshkin et al., 2012).There are only a few genome-wide studies performed in mammals (Ho et al., 2009; Schnetz et al., 2009; Yildirim et al., 2011) including a recent report (Morris et al., 2013) that illustrates the cooperative nature of Brg1, Chd4 and Snf2h ATP-dependent chromatin-remodeling systems in mammalian cells. How remodelers are targeted to specific sites in chromatin has not been yet elucidated in details.

2.1) Families of ATP-dependent chromatin remodelers

Although all remodeler catalytic subunits share a conserved ATPase domain, each family member bears unique flanking domains, allowing their separation into the above-mentioned four distinct families (fig.2). In addition to the major subfamilies of ATP-dependent chromatin remodelers, at least 20 more subfamilies belong to the Snf2 family (Hargreaves and Crabtree, 2011; Yodh, 2013).

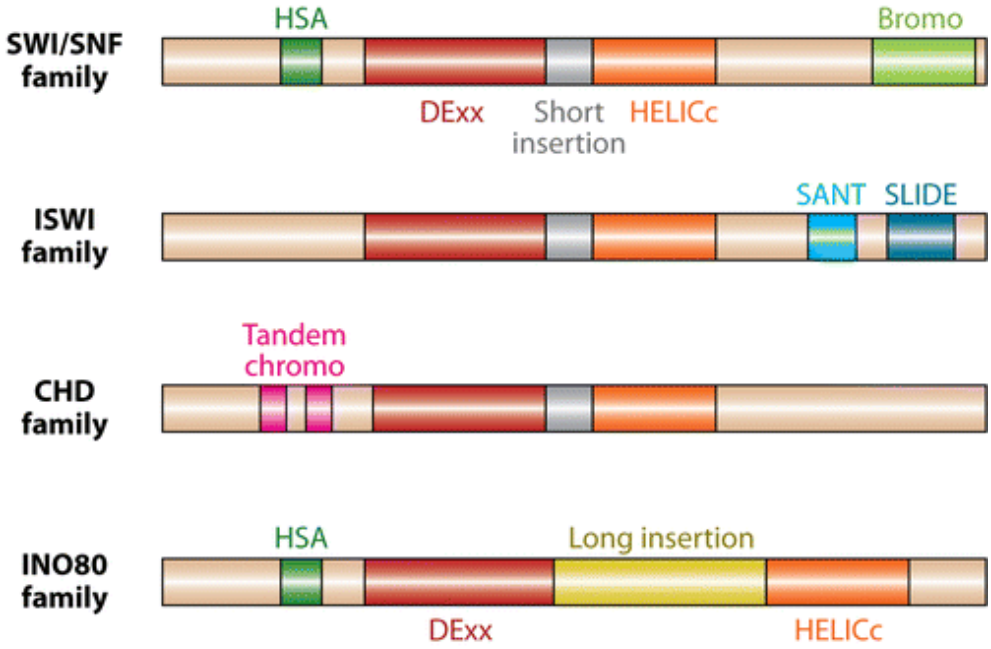

Fig.2) Different families of chromatin remodelers. (Adapted from Clapier and Cairns, 2009). ATPase subunits of the different families. All remodeler families contain an ATPase domain that is split in two parts: DExx (*red*) and HELICc (*orange*) divided by a short or long insertion. Each family contains different flanking domains: Bromodomain (*light green*), HSA (helicase-SANT) domain (*dark green*), SANT-SLIDE module (*blue*), tandem chromodomains (*magenta*).

SWI/SNF family

The SWI/SNF family (Clapier and Cairns, 2009a; Hopfner et al., 2012; Liu et al., 2011) was discovered through *S. cerevisiae* screening for suppression of transcriptional mutants with a mating-type *swi*tching defective/*s*ucrose *n*on-*f*ermenting phenotype (Neigeborn and Carlson, 1984; Stern et al., 1984). This family contains one or two ATPases (depending on the considered species): SWI2/SNF2 and STH1 in yeast, brahma (BRM) in *Drosophila melangaster*, and BRM and brahma-related gene 1 (BRG1) in mammalian. Purified SWI/SNF complexes contain 10–12 polypeptides and have an apparent molecular mass of ~2 MDa in mammals (Wang et al., 1996) and 1.14 MDa in yeast (Smith et al., 2003). The ATPase subunit together with other 8-14 regulatory subunits forms two tipes of complexes (yeast SWI/SNF and RSC; drosophila BAP/PBAP; human BAF/PBAF) (Cairns et al., 1996; Imbalzano et al., 1994; Kwon et al., 1994; Mohrmann and Verrijzer, 2005; Mohrmann et al., 2004; Papoulas et al., 1998). Both ATPase subunits have an N-terminal helicase-SANT (HSA) domain that interacts with actin-related proteins (ARP subunits), and a C-terminal Bromo/poly-Bromo domain, which recognizes the acetylated lysine residues on the N-terminal tails of histones (Hassan et al., 2002; de la Cruz et al., 2005) contributing to promoter targeting. In higher eukaryotes but not yeast, β-actin is also a subunit of the remodeling complex, and has been postulated to act as a nucleotide exchange factor for the ATPase subunit in human BAF (Hargreaves and Crabtree, 2011). SWI/SNF complexes remodel nucleosome structure and are capable of mobilizing nucleosomes both by sliding and by catalysing the ejection and insertion of histone octamers (Saha et al., 2006). Although *S. cerevisiae* SWI/SNF complexes were identified on the basis of their roles in the activation of transcription, evidence indicates that mammalian SWI/SNF complexes contribute to both repression and activation. For example, during

mammalian T lymphocyte development, BRG1 and BAF57 are required to both silence CD4 and activate CD8 expression (Chi et al., 2002). In embryonic stem cells (ESCs), BRG1 most commonly acts as a repressor to inhibit programmes that are associated with differentiation, but it also facilitates the expression of core pluripotency programmes (Ho et al., 2009).

ISW1 family

The ISWI (*i*mitation *swi*tch) family comprises different ATPases: ISW1 and ISW2 in yeast, ISWI in Drosophila and SNF2H and SNF2L in mammalians. The ISWI family of remodelers (Clapier and Cairns, 2009a; Hargreaves and Crabtree, 2011; Yodh, 2013) are smaller compared to SWI/SNF with only 2–4 subunits. The three major ISWI complexes (yeast ISW1a/ISW1b/ISW2; NURF, CHRAC, and ACF in drosophila and humans) are assembled around the different catalytic subunits. The ATPase subunit has unique C-terminal, adjacent SANT and SLIDE domains that are responsible for recognition of the nucleosome through interactions with nucleosomal and linker DNA and histone tails (de la Cruz et al., 2005).

The remaining subunits offer additional domains including DNA-binding motifs in hCHRAC and dNURF301, plant homeodomains (PDH) and bromodomains (hBPTF, hACF1). The ISWI family of remodelers uses DNA translocation to mobilize nucleosomes, though ISWI remodelers are typically restricted to movement/sliding only and not ejection (Clapier and Cairns, 2009a). Importantly, ISWI generates regularly spaced nucleosome arrays by ‘measuring’ the length of DNA linker between nucleosomes, and this property is thought to enable gene repression by ordering nucleosomes into closely spaced regular arrays that can restrict access to

DNA (Bartholomew, 2014; Gangaraju and Bartholomew, 2007; Grüne et al., 2003; Tirosh et al., 2010; Whitehouse and Tsukiyama, 2006).

CHD family

The CHD remodeler family (*c*hromodomain, *h*elicase, and *D*NA binding) includes a number of proteins that are highly conserved from yeast to humans (Hargreaves and Crabtree, 2011; Yodh, 2013). The presence of additional structural motifs is used to further divide the CHD family into three subfamilies (Hall and Georgel, 2007; Marfella and Imbalzano, 2007). CHD1 is the simplest remodeler in this family and is comprised of a single catalytic subunit (Chd1) across species (although it can be oligomeric in higher organisms). In higher eukaryotes, the NuRD complex contains up to ten subunits assembled around the catalytic subunit Mi-2 (Chd4) (Torchy et al., 2015). In both Chd1 and Mi-2 catalytic subunits, two tandem chromo-domains N-terminal to the ATPase region are involved in recognition of methylated H3 tails. Large variability exists in cellular functions of CHD remodelers—some activate transcription through nucleosome repositioning or removal, while others such as vertebrate Mi2/NuRD are involved in transcriptional repression via histone deacetylase (HDAC1/2) and methyl CpG-binding domains (MBD) (Torchy et al., 2015) .

INO80 family and H2A.Z

The INO80 chromatin remodelers comprise the most complex family in terms of subunit composition across species (Bao and Shen, 2007; Clapier and Cairns, 2009b; Yodh, 2013). Unlike the other three remodeler families, the INO80 family catalytic subunit is defined by a much longer insertion between the two parts of the ATPase domain. The ATPase subunit also has an N-terminal HSA domain for binding actin and ARPs, other subunits found in the remodelers of this family. Although INO80 and SWR have a split ATPase subunit that is otherwise similar to the SNF2 family of ATPases, the SWR complex is incapable of carrying out typical nucleosome remodeling reactions that involve sliding or eviction of the nucleosome (Gerhold and Gasser, 2014; Mizuguchi et al., 2004; Watanabe and Peterson, 2010). The INO80 complex is involved in several cellular processes, including transcription (Wang et al., 2014; Watanabe and Peterson, 2010; Wimalarathna et al., 2014). INO80 has multiple functions in transcriptional activation (via subunit histone acetylase (HAT) activity) as well as DNA repair. In fact, the INO80 member of the family is the only chromatin remodeling protein in which DNA helicase activity has been observed and evidence indicates a role for this complex in the facilitation of DNA repair (Gerhold et al., 2015). Similar to the ISWI remodeler family, INO80 remodelers interact with extranucleosomal DNA in order to mobilize nucleosomes. INO80 has been widely implicated in homologous recombination (Alatwi and Downs, 2015; van Attikum et al., 2004, 2007; Fritsch et al., 2004; Lopez-Perrote et al., 2014; Nishi et al., 2014; Tsukuda et al., 2005, 2009). Evidence suggests that members of this family are capable of histone exchange reactions (Watanabe and Peterson, 2010). Swr1, as part of the SWR complex, removes H2A/H2B dimers and replaces them with H2A.Z/H2B (Kobor et al., 2004; Mizuguchi et al., 2004). Mammalian SRCAP and p400 (as part of TIP60) are related to yeast SWR and

perform the same function (Ruhl et al., 2006a; Xu et al., 2012). In contrast to other chromatin remodelers, the ATP hydrolysis activity of SWR is stimulated not by the addition of DNA or nucleosomes but by the nucleosomal H2A–H2B dimer (Mizuguchi et al., 2004). The soluble H2A.Z–H2B dimer further stimulates ATP hydrolysis activity (Luk et al., 2010), whereas the nucleosome-incorporated variant dimer does not, which limits the SWR exchange reaction to one direction, making SWR incapable of replacing H2A.Z for H2A. The reaction proceeds in a two-step process, in which the H2A–H2B dimer is first removed from the nucleosome and the H2A.Z–H2B variant dimer bound to the Swc2 subunit (the human orthologue of which is YL1) of the yeast SWR complex is then deposited (Wu et al., 2005). Instability of the resultant heterotypic H2A.Z-containing nucleosome ensures replacement of the second H2A–H2B dimer with the variant (Luk et al., 2010) by the yeast SWR complex. Interestingly, acetylation of nucleosomal histones enhances this exchange reaction (Kusch, 2004; Ruhl et al., 2006b; Watanabe et al., 2013).

The budding yeast INO80 complex has been shown to catalyse the reverse reaction and replace H2A.Z/H2B dimers with H2A/H2B (Papamichos-Chronakis et al., 2011). Intriguingly, the INO80 complex, is also believed to be targeted to the +1 H2A.Z nucleosome by recognizing the adjacent NFR (Yen et al., 2013). The INO80 complex may have a role in preventing H2A.Z mislocalization by targeting the unacetylated histone variant. Given its localization to the coding regions of genes (Yen et al., 2013), INO80 may function to actively remove any H2A.Z–H2B dimer that is misincorporated into these regions. In mammalian cells, the histone chaperone ANP32E has been shown to remove H2A.Z from chromatin. In its absence there is a genome-wide accumulation of H2A.Z particularly at enhancers and insulators, and significantly also at the +1 nucleosome (Mao et al., 2014; Obri et al., 2014). Whether mammalian INO80 contributes to H2A.Z removal has not

been investigated in details. A recent work (Alatwi and Downs, 2015) demonstrated that in human cells the removal of H2A.Z from chromatin after DNA damage is dependent on INO80. They also report that the histone chaperone ANP32E similarly promotes homologous recombination (HR) and appears to work on the same pathway as INO80. The HR defect in cells depleted of INO80 or ANP32E can be rescued by H2A.Z co-depletion, suggesting that H2A.Z removal from chromatin is the primary function of INO80 and ANP32E in promoting homologous recombination.

3) Histone variants

Histones are highly conserved proteins, essential in all eukaryotes and encoded by multiple genes, often physically located in clusters (Albig and Doenecke, 1997; Marzluff et al., 2002; Schaffner et al., 1978), whose expression is confined during S-phase (Marzluff et al., 2008). In eukaryotic cells, in addition to canonical histones there are histone variants, whose protein levels are much lower than the canonical histones (~5–10%).

Histone variant expression is not restricted to S-phase because their genes are evolutionarily distinct from the canonical ones and physically located outside the replication-dependent histone clusters. This feature makes them available through all the cell cycle and they can be incorporated in chromatin in response to environmental stimuli, which typically are not synchronous with replication (Szenker et al., 2011; Zlatanova and Thakar, 2008). The synthesis of histone variants outside S-phase and in specific tissues also enables them to perform specialized functions such as DNA repair (H2A.X) (Yuan et al., 2010) or kinetochore assembly

(centromere protein A; CENP-A) (De Rop et al., 2012). Like the canonical histones, variants are generally highly conserved between species, although some variants have a restricted species distribution. Of the four core histones, variants of H3 and H2A are the most common, with the H2A family containing the highest number of variant forms including canonical H2A, H2A.Z, macroH2A, H2A.Bbd and H2A.X (reviewed in (Millar, 2013)).

3.1) H2A.Z histone variant

H2A.Z is highly conserved during evolution: it is found in organisms from *Plasmodium falciparum* to *Homo sapiens*, with sequence conservation of ~90% (Iouzalen, 1996). Its sequence identity to the major H2A is only ~60%, which suggests unique and important functions for H2A.Z (Jackson and Gorovsky, 2000; Thatcher and Gorovsky, 1994) (fig.3 shows regions divergent between H2A.Z and H2A and among H2A.Z in different species).

A

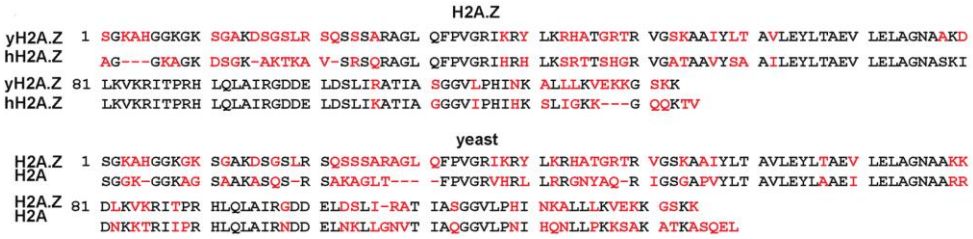

B

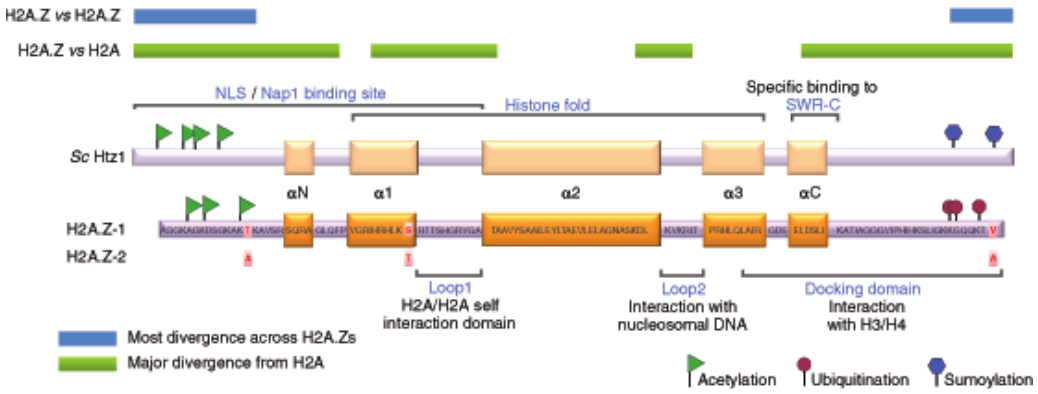

Fig.3) H2A.Z divergence from H2A and H2A.Z in different species. Adapted from (Mehta et al., 2010; Zlatanova and Thakar, 2008). (A) The amino acid sequences of H2A.Z (yeast versus human) and yeast H2A versus yeast H2A.Z are aligned (differences are presented in red). (B**)** A simplified view of H2A.Z structure and post-translational modifications**.** Bars indicate the major regions of divergence between H2A.Z proteins across species (blue) and between H2A.Z and H2A (green). Saccaromyces cerevisiae H2A.Z (ScHtz1) and the two human isoforms (H2AZ-1, H2A.Z-2) are shown.

The histone variant H2A.Z constitutes only a few percentage of the total H2A cellular pool (Ball et al., 1983; West and Bonner, 1980). However, H2A.Z is essential in several multi-cellular organisms (van Daal and Elgin, 1992; Faast et al., 2001; Ren and Gorovsky, 2001; Ridgway et al., 2004) and required for normal proliferation in *Schizosaccharomyces pombe* and *Saccharomyces cerevisiae* (Carr et al., 1994; Santisteban et al., 2000).

In vitro studies on H2A.Z containing nucleosome leaded to contrasting results. Using isolated budding yeast chromatin, a lower salt concentration was required to dissociate H2A.Z/H2B dimers compared to H2A/H2B dimers, suggesting that H2A.Z destabilizes the yeast nucleosome (Zhang et al., 2005). By contrast, using isolated chicken red blood cell chromatin, a higher salt concentration was required to remove H2A.Z (Li et al., 1993). Reconstitution of vertebrate chromatin *in vitro* using recombinant histones also demonstrated that H2A.Z clearly stabilizes the histone octamer within the nucleosome (Chen et al., 2013; Park et al., 2004).

The variant H2A.Z has been implicated in a wide range of DNA-mediated processes including transcription, DNA repair, and genomic stability such as repair machinery at the DNA double-strand breaks (Xu et al., 2012).

Numerous studies have shown that H2A.Z may play critical roles in heterochromatin formation. H2A.Z is required for proper centromere function by maintaining the integrity of pericentric heterochromatin, located in the boundary region to prevent

the spread of heterochromatin into euchromatin. H2A.Z also co-localized with heterochromatin protein HP1α at various constitutive heterochromatic domains in different mammalian cell types (Fan et al., 2004; Greaves et al., 2006; Meneghini et al., 2003). In mammalian cells, H2A.Z is involved in ESC biology (Creyghton et al., 2008a; Faast et al., 2001). In particular, recent reports define the importance of H2AZ and H2AZ-modifying enzymes in self-renewal of ESCs (Binda et al., 2013; Hu et al., 2013a; Li et al., 2012).

3.2) H2A.Z histone variant genomic localization

Genome-wide localization experiments in protozoa, fungi, animals, and plants (Albert et al., 2007; Creyghton et al., 2008b; Guillemette et al., 2005a; Li et al., 2005; Petter et al., 2011; Raisner et al., 2005; Siegel et al., 2009; Whittle et al., 2008; Zilberman et al., 2008) demonstrate that H2AZ is highly enriched within the few nucleosome surrounding transcriptional start sites (TSSs). There are some species-specific differences in the relative abundance of H2A.Z in the +1 and −1 nucleosomes, with the −1 nucleosome enriched in *Saccharomyces cerevisiae* and *Homo sapiens*, but not in *Drosophila melanogaster* or *S. pombe* (Lantermann et al., 2010; Mavrich et al., 2008b). Different tissues within the same species also have slightly different patterns, for example H2A.Z is absent from the +1 nucleosome in mouse testis but not in other mouse cell types that have been examined (Creyghton et al., 2008a; Kalocsay et al., 2009; Soboleva et al., 2012). H2A.Z is also enriched at gene enhancers in human and mouse cells (Barski et al., 2007; Hardy et al., 2009; Jin et al., 2009; Ku et al., 2012a) and the high enrichment of H2A.Z at genes and gene regulatory elements is the most generally conserved feature of H2A.Z localization. The chromatin remodeler Swr1 is responsible for H2A.Z deposition in

chromatin and INO80 (and AnpE in mammals) are responsible for its eviction (see INO80 family in the section on Chromatin Remodelers).

3.3) Effects on transcription of H2A.Z

The relationship between H2A.Z occupancy and gene activity levels is complex. In both budding and fission yeasts the presence of H2A.Z is negatively correlated with transcription (Buchanan et al., 2009; Guillemette et al., 2005b; Zhang et al., 2005), whereas in humans and mice it is positively correlated with transcriptional activity (for low to moderately expressed genes) (Cui et al., 2009; Nekrasov et al., 2012). This major difference appears to reflect when H2A.Z is incorporated into the +1 nucleosome. In yeast, H2A.Z is deposited when the promoter is in a repressed or basal state (Guillemette et al., 2005b; Raisner et al., 2005; Zhang et al., 2005). Following transcriptional activation and productive elongation by RNA Pol II, H2A.Z is displaced from the +1 nucleosome, thus yielding a negative correlation between H2A.Z and transcriptional activity. By contrast, a positive correlation for humans and mice implies that H2A.Z is deposited during the transcriptional activation process (most likely immediately before or concomitantly with RNA Pol II). However, analogous to the situation in yeast, as the transcription rate increases H2A.Z is displaced from the +1 nucleosome, thereby yielding a negative correlation (Cui et al., 2009; Nekrasov et al., 2012). In a recent study done using Drosophila cells, Weber et al. demonstrated that +1 nucleosome barrier correlates with nucleosome occupancy but anticorrelates with enrichment of histone variant H2A.Z and the depletion of H2A.Z results in a higher barrier to RNA pol II (Weber et al., 2014). These observations are supported by results in yeast, where H2A.Z increased the elongation rate of RNA pol II at a single fusion gene (Santisteban et al., 2011). In

contrast, human H2A.Z nucleosomes *in vitro* were completely refractory to transcription (Thakar et al., 2010).

H2A.Z located in the gene body has been shown to be correlated negatively with transcription (Cui et al., 2009; Hardy et al., 2009; Nekrasov et al., 2012) as well as being linked with gene silencing (Barski et al., 2007; Coleman-Derr and Zilberman, 2012; Farris, 2005; Jin et al., 2009). A role for H2A.Z in transcriptional repression has been established in plants where H2A.Z is specifically enriched in the bodies of repressed genes that are induced by environmental and developmental stimuli (Coleman-Derr and Zilberman, 2012; Kumar and Wigge, 2010).

H2A.Z has also been revealed to be involved in gene activation; H2A.Z enrichment in promoters is negatively correlated with CpG methylation in plant and mammalian cells and is enriched at the promoters of inducible genes to poise genes for rapid transcriptional activation (Conerly et al., 2010; John et al., 2008; Sutcliffe et al., 2009; Zilberman et al., 2008).

In particular, together with DNA-binding proteins such as Foxa2, H2A.Z regulates nucleosome depletion and promotes gene activation in differentiating cells. Knockdown of either FOXA2 or H2A.Z impairs nucleosome positioning, chromatin remodeling, and mouse ESC differentiation to endoderm/hepatic progenitor cells (Li et al., 2012). Another study further underscores the role of H2A.Z in promoting binding of TFs and chromatin modifiers at regulatory regions (Hu et al., 2013a). Knockdown of H2A.Z in mouse ESCs leads to increased nucleosomal occupancy, concomitant decrease in the Oct4 binding and diminished association of the MLL and PRC2 methyltransferase complexes with active and poised enhancers and promoters. Consequently, H2A.Z knockdown in mouse ESCs results in misregulation of both pluripotency and developmental genes, impairing self-renewal and differentiation (Creyghton et al., 2008; Hu et al., 2013).

A role of H2A.Z in maintaining chromatin accessibility is suggested by the evidence that H2A.Z depletion in murine embryonic stem cells increases overall nucleosome level at p300-intergenic sites and reduces the accessibility of ~20% of DNase Hypersensitivity Sites (DHSs) (Hu et al., 2013).

Recently Brunelle et al. demonstrated by genome-wide approaches that H2A.Z is present at a subset of active enhancers bound by the estrogen receptor alpha (ERα) (Brunelle et al., 2015). They also showed that H2A.Z-enriched enhancers are associated with chromatin accessibility, H3K122ac enrichment and hypomethylated DNA that upon estrogen stimulation produce enhancer RNAs (eRNAs), and recruit RNA pol II as well as RAD21, a member of the cohesin complex involved in chromatin interactions between enhancers and promoters. Importantly, their recruitment and eRNAs production are abolished by H2A.Z depletion.

Another aspect that is important to consider to understand H2A.Z role in nucleosome stability and control of transcription is its association with H3.3 histone variant. Nucleosomes containing H2A.Z and H3.3 appear to be less stable and therefore easier to displace from DNA than canonical nucleosomes (Jin and Felsenfeld, 2007). Jin et al. demonstrated that double-variant H3.3/H2A.Z-containing nucleosome is unstable *in vivo* and it is associated to active TSSs (Jin et al., 2009).

Numerous studies showed an enrichment of H2A.Z and H3.3 histone variants at both active and poised enhancer and promoter regions of multiple cell types, including ESCs (Barski et al., 2007; Creyghton et al., 2008b; Hu et al., 2013b; Jin and Felsenfeld, 2007; John et al., 2008; Ku et al., 2012b, Yukawa et al., 2014). Moreover, other highly accessible regions of the genome, which included DNase I hypersensitive sites and CTCF (CCCTC- binding factor zinc finger protein) binding sites, also contained this H3.3/H2A.Z-containing nucleosome (Jin et al. 2009) and

might be important for the bindings of CTCF and cohesin to mediate higher-ordered chromatin organization (Millau and Gaudreau, 2011; Nekrasov et al., 2012).

Another aspect to be taken into consideration is that H2AZ is post-translationally modified by acetylation, SUMOylation, ubiquitination, and methylation of lysines (reviewed in Sevilla and Binda, 2014).

H2A.Z sumoylation has been implicated in DNA repair in *S. cerevisiae* (Kalocsay et al., 2009), ubiquitination correlates with localization to the inactive X chromosome (Xi) in mammals (Sarcinella et al., 2007), whereas N-terminal acetylation leads to nucleosome destabilization (Thambirajah et al., 2006). It was suggested that H2A.Z acetylation works as a switch-like mechanism to modulate H2A.Z nucleosome stability, ascribing repressive functions to the unmodified and activating functions to the acetylated form (Marques et al., 2010). Furthermore, acetylated H2A.Z was found associated with active genes, but its role at these sites is not yet completely understood (Sevilla and Binda, 2014). For example Valdés-Mora et al. showed that acetylated H2AZ is solely found at the TSS of actively transcribed genes (Valdés-Mora et al., 2012).

4) Murine macrophages as a model to study genome accessibility and gene regulation

Bone marrow derived macrophages (BMDMs) from M. musculus represent a very suitable system to study genome organization and regulation of transcription.

In particular, macrophages constitute a very well studied and dynamic system where massive transcriptional and epigenomic changes can be induced by external stimuli. For example, stimulating macrophages with lipopolysaccharide (LPS) can mimic the innate immune response to bacteria *in vitro*. This results in massive reorganization of chromatin and transcription on a very short time scale. Furthermore, genomic regulatory elements and the master regulators of macrophage identity (in particular

the lineage determining factor Purine rich box 1-Pu.1-) are known (Smale and Natoli, 2014 , Lawrence and Natoli, 2011).

4.1) Transcriptional regulation of inflammatory response in macrophages

Macrophage stimulation by LPS has been extensively used to study their response to inflammatory stimulus. The complexity of the inflammatory response requires several hundreds of genes to be activated in a kinetically complex fashion, with some genes rapidly activated immediately after the stimulus (‘primary’ response genes, PRGs) and others induced with slower kinetics (‘secondary’ response genes -SRGs- and some slowly activated primary response genes).

PRGs are formally defined as genes that can be induced without de novo protein synthesis, while SRGs require new protein synthesis for inducible expression (Herschman, 1991). The promoters of most PRGs such those encoding tumor necrosis factor alpha (TNFα), superoxide dismutase 2 (SOD2), and prostaglandin G/H synthase 2 (PTGS2)—contain a CpG island (Deaton and Bird, 2011; Hargreaves et al., 2009; Ramirez-Carrozzi et al., 2009). The very high CG content of CpG islands tends to directly interfere with the assembly of stable nucleosomes (Fenouil et al., 2012; Ramirez-Carrozzi et al., 2009), allowing the rapid activation of these genes without nucleosome eviction by chromatin remodeler complexes. CpG island promoters show also high level of H3K4me3, histone acetylation and RNA Pol II already in unstimulated macrophages, indicating that are transcribed at low basal level (Ramirez-Carrozzi et al., 2009). An increase in H3K4me3 and H4K5/8/12Ac occurs upon stimulation and is associated with an increase in Ser2-phosphorylated RNA Pol II, productive elongation and generation of normally

spliced transcripts (Hargreaves et al., 2009; Medzhitov and Horng, 2009). The promoters of SRGs, such as the Nitric oxide syntase 2 (*Nos2*) and the Interleukin 6 (*Il6*) genes, as well as of some PRGs with delayed activation kinetics such as *Ccl5*, show low basal levels of H3K4me3 and H3/H4Ac (Escoubet-Lozach et al., 2011; De Santa et al., 2009). SRG promoters are also characterized by a comparatively lower G+C content and a sequence context that favors nucleosome occupancy, explaining the requirement for a nucleosome remodeling step triggered by the SWI/SNF chromatin-remodeling for their activation (Hargreaves et al., 2009; Ramirez-Carrozzi et al., 2009).

A recent genome-scale analysis of nascent transcripts in LPS-induced macrophages revealed that CpG islands are in fact also present at some SRG promoters not constitutively transcribed probably because of the lack/inactivity in the basal state of TFs required for their transcription (Bhatt et al., 2012). However, non-CpG island genes differ from CpG island-containing genes because they are induced by a larger magnitude after stimulation (Bhatt et al., 2012), possibly because of their tighter control in the basal state.

4.2) Macrophage genome organization

Studies of regulatory elements in macrophages have indicated that competence for responses to an inflammatory stimulus is programmed at an early stage of differentiation by factors involved in lineage commitment and macrophage identity, which are responsible for the organization of the macrophage-specific cis-regulatory repertoire (Ghisletti and Natoli, 2013; Lichtinger et al., 2012; Natoli, 2010; Smale and Natoli, 2014). In macrophages, the same genomic location includes binding

sites for macrophage-specific lineage-determining TFs and for ubiquitously expressed TFs, which are recruited on these regions upon stimulation.

4.2.1) Chromatin features of distal cis-regulatory elements

In general, gene expression is regulated through many *cis*-regulatory elements, including core promoters and promoter-proximal elements, as well as *cis*-regulatory modules localized at greater distances from the TSSs, such as enhancers, silencers and insulators.

These cis-regulatory elements are relatively nucleosome depleted, as demonstrated by DNAse I-hypersensitivity-based approaches or by FAIRE (formaldehyde-assisted isolation of regulatory elements) assay which allows the recovery of the soluble (i.e. nucleosome-free) fraction of the chromatin (Ernst et al., 2011; Giresi and Lieb, 2009; Neph et al., 2012a; Sabo et al., 2006; Song et al., 2011b).

Enhancers were first identified as stretches of DNA that, when inserted up- or downstream of transgenes, were able to augment gene expression irrespective of orientation (Banerji et al., 1981). Enhancers can increase basal transcription levels from gene promoters and TSSs at distances ranging from hundreds of bases to megabases (Heinz et al., 2015). Enhancers regulate transcription by looping into close 3D proximity with target gene promoters (Su et al., 1991). This model is supported by several independent experimental observations, such as the frequencies of distal DNA sequence ligation using chromatin conformation capture (3C), and by florescence *in situ* hybridization (FISH) (Cubeñas-Potts and Corces, 2015; Pombo and Dillon, 2015). Terminally differentiated cells have a unique repertoire of enhancers (Heintzman et al., 2009; Rada-Iglesias et al., 2011; Stergachis et al., 2013; Visel et al., 2009a) that is generated by TFs that control lineage specification (Calo and Wysocka, 2013a; Natoli, 2010). Indeed, enhancers

function as integrated TF binding platforms containing clustered recognition sites for multiple TFs (reviewed in Spitz and Furlong, 2012). Most TFs are unable to bind their cognate sites when embedded in a nucleosomal context, except for pioneer factors. Pioneer factors are functionally defined as sequence-specific DNA-binding proteins able to bind to their target sites covered by nucleosomes. Subsequent recruitment of chromatin remodelers by pioneer factors results in stable local opening of the chromatin, thus making it competent for other factors to bind. Once bound, pioneer factors act in some cases as placeholders that will be replaced by other TFs at later stages of development (Zaret and Carroll, 2011).

Enhancers are characterized by high levels of mono-methylation of histone H3 Lysine 4 (H3K4me1) in the absence of significant levels of tri-methylation of the same residue (H3K4me3), which is instead highly enriched at promoters (Barski et al., 2007; Heintzman et al., 2007, 2009; Zhou et al., 2011). Specifically, in a given cell, enhancer elements can be broadly categorized as inactive, primed, poised, or active (Barski et al., 2007; Ernst et al., 2011; Heintzman et al., 2007). An inactive enhancer is defined as DNA that is either sequestered as heterochromatin, actively repressed by DNA methylation or generally lacks the marks of an alternate enhancer state. A primed enhancer is defined by mono- or dimethyl modifications on histone H3 lysine 4 (H3K4me1/2) (He et al., 2010) but lacks additional active marks (see below). Particularly during early embryogenesis, poised enhancers can additionally be marked with tri-methylation of histone H3 on lysine 27 (H3K27me3), which is a marker of active repression and is mutually exclusive with acetylation on the same residue (Rada-Iglesias et al., 2011). Finally, active enhancers generally exhibit acetylation of histone H3 lysine 27 (H3K27ac) (Creyghton et al., 2010; Rada-Iglesias et al., 2011). Interestingly, active enhancers are also actively transcribed by RNA pol II giving rise to enhancer RNA, or eRNA (Andersson et al., 2014; Kim et al., 2010; Lam et al., 2013; De Santa et al., 2010). Additional marks associated with

active enhancers include binding of histone acetyltransferases (HATs) such as p300 and CBP (Ghisletti et al., 2010; Heintzman et al., 2009; Visel et al., 2009b). Interestingly, enhancers are also characterized by a distinctive nucleosomal composition, being enriched in noncanonical histone variants, mainly the H2A variant H2A.Z and H3.3 (Calo and Wysocka, 2013b; Zlatanova and Thakar, 2008). Enhancers are located non-uniformly with respect to genes, such that some genes are located in enhancer-rich regions of the genome, whereas others have few or no enhancers in their proximity. Super-enhancers were initially defined as large (tens of kilobases in length) genomic loci with an unusually high density of enhancer-associated marks, such as binding of the Mediator complex, relative to most other genomic loci (Hnisz et al., 2013; Pott and Lieb, 2015; Whyte et al., 2013). These regions can also be defined by high-density and/or extended (>3 kb) depositions of the histone mark H3K27ac (Hnisz et al., 2013; Parker et al., 2013). A substantial fraction of super-enhancers and nearby genes are cell type-specific, and the gene sets that are associated with super-enhancers in a given cell type are highly enriched for the biological processes that define the identities of the cell types (Hnisz et al., 2013; Parker et al., 2013).

The initial characterization of enhancers involved in LPS-inducible gene expression in macrophages was based on the ability of stimulus-activated TFs, such as NF-κB and IRFs, to promote the recruitment of the p300 HAT. LPS-inducible p300 recruitment unveiled thousands of enhancers and revealed their underlying sequence features. In addition to binding sites for LPS-activated TFs such as NF-κB, AP-1, and IRF, these enhancers were almost invariably associated with binding sites for Pu.1, an ETS family protein that controls myeloid development and is expressed at very high levels in terminally differentiated macrophages (Ghisletti et al. 2010).

4.2.2) Pu.1: the master regulator of macrophage differentiation

Pu.1 is the essential macrophage-determining TF: it is constantly expressed at high levels in macrophages and is required to induce and to maintain macrophage differentiation and viability (Nerlov and Graf, 1998).

Pu.1 is exclusively expressed in cells of the hematopoietic lineage and belongs to the ETS family of TFs, one of the largest families of winged helix-loop-helix DNA-binding proteins. The ETS family includes almost 30 members that can be assigned to four classes based on their binding specificity (Wei et al., 2010).

Pu.1 (Spi1) and its paralogs SpiB and SpiC recognize both *in vitro* and *in vivo* highly specific sequences that differ at a few critical positions (mainly at the 5' of the binding site) from the binding sites of all other ETS proteins (Wei et al., 2010, fig.4).

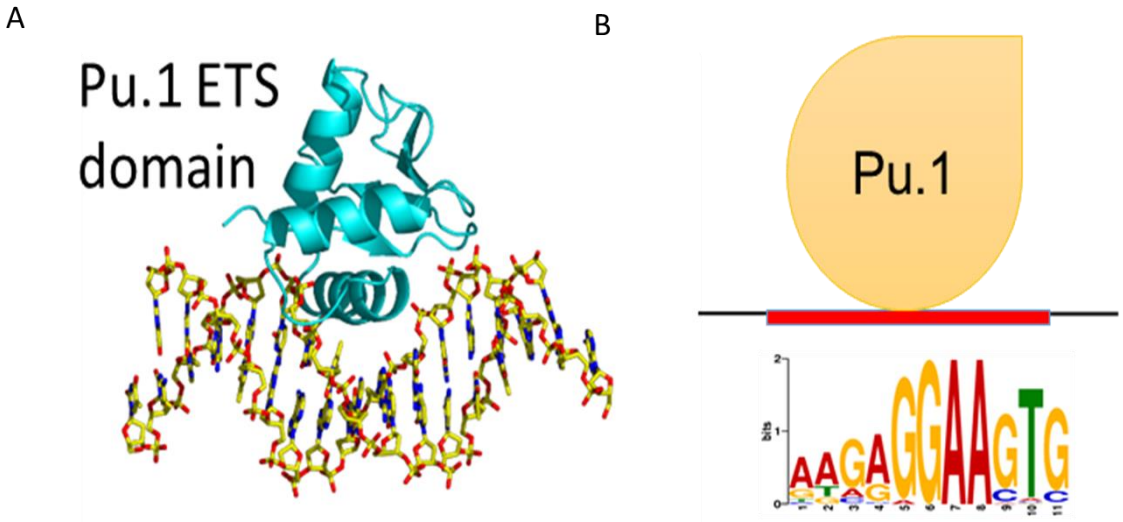

Fig.4) Pu.1 binding on DNA*.Pu.1* ETS domain binding to DNA (adapted from 1PUE PDB entry) (a) and Pu.1 binding to its positioned weight matrix (PWM) (b) are represented.

Several studies with Pu.1 gene-disrupted mice indicate that Pu.1 is a critical regulator of differentiation within the hematopoietic system and is particularly important for myeloid and B lymphocyte lineage development (Nerlov and Graf, 1998). Pu.1_/_mice, which are born alive but die of severe septicemia within 48 h,

are characterized by a normal amount of erythrocytes and megakaryocytes, but they lack mature myeloid and B cells (McKercher et al., 1996; Scott et al., 1994). More recently, conditional knockout mouse models indicated that Pu.1 is not essential for myeloid and lymphoid lineage commitment, but it is absolutely required for the normal differentiation of most myeloid lineages and B cells (Carotta et al., 2010; Iwasaki et al., 2005). Pu.1 is expressed at different levels in mature blood cells. Precisely, high levels favor macrophage differentiation, whereas about tenfold lower levels of Pu.1 are associated with B-cell development (Bakri et al., 2005; Dahl et al., 2003; DeKoter, 2000). Pu.1 overexpression in fibroblasts induces their trans-differentiation into macrophage-like cells, while its absence blocks terminal macrophage differentiation from myeloid precursors indicating that its activity is necessary and sufficient to specify macrophage identity (Ghisletti et al., 2010; Heinz et al., 2010).

4.2.3) Pu.1 role in controlling macrophage genomic landscape

Genome-wide mapping of Pu.1 binding revealed that its distribution is widespread in the macrophage genome (Ghisletti et al. 2010; Heinz et al. 2010) and that is constitutively associated with nearly all TSSs and enhancers marked by H3K4me1 (Ghisletti et al. 2010; Heinz et al. 2010). A recent study (Ostuni et al., 2013) showed that Pu.1 is also recruited after different inflammatory stimuli to regulatory elements that were unbound by TFs and unmarked in unstimulated cells (namely latent enhancers). These latent enhancers acquire H3K4me1 and H3K27Ac and undergo an increase in accessibility over several hours after stimulation, thus reflecting a slow process of chromatin reorganization that depends on the functional

cooperation between stimulus-activated TFs (such as Stat1 and Stat6 induced in response to IFN-γ and IL-4, respectively) and Pu.1.

Other two recent studies elucidated that environment dictates tissue-specific epigenetic enhancer signatures independently of cellular origin and thus plays a dominant role in specifying cellular identity (Gosselin et al., 2014; Lavin et al., 2014). Upon transfer of differentiated macrophages from one tissue to another (Lavin et al., 2014) or upon tissue culture with factors specific for a different tissue (Gosselin et al., 2014), macrophages can acquire to a large extent the newly induced identity. In particular, Gosselin et al. demonstrated that distinct tissue environments drive divergent programs of gene expression by differentially activating a common enhancer repertoire and by inducing the expression of divergent secondary transcription factors that collaborate with Pu.1 to establish tissue-specific enhancers. Lavin et al. elucidated that the environment is capable of shaping the chromatin landscape of transplanted bone marrow precursors, and even differentiated macrophages can be reprogramed when transferred into a new microenvironment.

In B cells, where Pu.1 concentration is about 10-fold lower than in macrophages, Pu.1 distribution (as well as the enhancer repertoire) is completely different, which might reflect a higher dependence on cooperative interactions provided by B-cell-specific partner TFs (Heinz et al, 2010).

Several experimental evidences suggested that Pu.1 could act as a pioneer factor during macrophage differentiation. Interestingly, Pu.1 binding is able to promote the deposition of H3K4me1 and to create small open regions of accessible DNA that can be bound by other TFs, such as those activated by inflammatory stimuli. Indeed, Pu.1 expression in non-myeloid cells or in Pu.1-negative myeloid progenitors is sufficient to induce nucleosome-free DNA sequences at the same genomic regions identified as enhancers in macrophages (Ghisletti et al., 2010; Heinz et al., 2010a).

The unique distribution of Pu.1 in macrophages suggests that it could also directly promote the looping of distant enhancers onto cognate TSSs.

3C in Hematopoietic Stem Cells demonstrated that Pu.1 autoregulation through its distal regulatory element, the 14 kB URE (Upstream Regulatory Element), is due to the formation of a chromosome loop that allows promoter–enhancer interactions and consequently gene activation (Leddin et al., 2011; Staber et al., 2013). Also in dendritic cells, Pu.1 was recently reported to control long distant contacts between regulatory elements and the IRF8 gene (Schönheit et al., 2013). However the role of Pu.1 in 3D organization remains to be clarified.

AIMS OF THE WORK

The aim of this study was to clarify the nucleosome organization and DNA accessibility at regulatory elements in mouse macrophages and the role of the lineage determining transcription factor Pu.1, chromatin remodelers and histone variants in controlling it. We used mouse primary macrophages as a highly specialized cell type in which the master regulator of the myeloid lineage Pu.1 acts as a global genome organizer. As already described in the previous section, Pu.1 binds virtually the entire repertoire of H3K4me1-positive regions and a large fraction of TSSs (Ghisletti et al., 2010; Heinz et al., 2010b). Pu.1 expression in fibroblasts (Ghisletti et al., 2010) or in Pu.1-negative myeloid precursors (Heinz et al., 2010) is sufficient to drive the deposition of H3K4me1 and to locally increase DNA accessibility. This suggests that Pu.1 may act as a pioneer factor to create the macrophage-specific repertoire of accessible cis-regulatory elements together with other TFs expressed at different phases of myeloid differentiation (Lichtinger et al., 2012). Indeed the role of Pu.1 in actively open condensed chromatin and to recruit other TFs, chromatin modifiers and nucleosome remodelers was not still demonstrated. Given these premises, our first goal was to elucidate the role of Pu.1 in nucleosome organization at macrophage enhancers. Our second aim was to understand which factors are involved together with Pu.1 in nucleosome organization at macrophage regulatory regions, in particular ATP-dependent chromatin remodelers and H2A.Z histone variant. ATP-dependent remodelers are fundamental to obtain nucleosome arrays (Zhang et al., 2011) and their role in nucleosome organization in macrophages has not been yet elucidated. H2A.Z histone variant was another important factor to study in defining macrophage landscape at regulatory elements. Indeed H2A.Z is a specialized histone variant

associated with enhancers (Jin et al., 2009; Yukawa et al., 2014), whose role is still controversial. Finally, we wanted to study the opening of chromatin at regulatory sites and its regulation after inflammatory stimulus by DNA accessibility techniques (DNase I digestion of chromatin, FAIRE and ATAC-seq).

MATHERIAL AND METHODS

Cell culture. Animal experiments were performed in accordance with the Italian Laws (D.L.vo 26/2014), which enforce the EU 2010/63 Directive.

Bone marrow cells were isolated from C57B6/Jhsd mice and plated in 10 cm dishes for 6 days in 10 ml of BM-medium (Dulbecco's Modified Eagle's Medium (DMEM)) supplemented with 20% low-endotoxin fetal bovine serum (FBS), 30% L929 conditioned medium, 1% glutamine, 1% penicillin-streptomicin, 0.5% sodium pyruvate and 0.1% β-mercaptoethanol). Stimulations were carried out at day 6 with LPS from E.Coli serotype EH100 (Alexis) at 10 ng/ml.

Antibodies. The anti-Pu.1 rabbit polyclonal antibody was generated in-house against the N-terminus of mouse Pu.1 (aa. 1-100; NP_035485.1) and affinity purified. Brg1, Chd4 and H2A.Z antibodies from Abcam (ab70558, Ab72418 and ab4174) were used in ChIP experiments. Normal Rabbit IgG (Santa Cruz, SC2027) were used as control in ChIP. Anti-vinculin antibody (Sigma V9131) or anti-histone H3 (Abcam Ab1791) were used as loading control in Western blots. Secondary IRDye antibodies were from Li-Cor (#926-68021 and 926-32210); Odyssey scanner and software (Li-Cor) were used for infrared fluorescence acquisition and quantification.

Nucleosome mapping. MNase digestion was performed starting from 8-12 x 10^6 cells. All the steps before MNase digestion were performed on ice and centrifugation at 4° C. After 2x washes with PBS, cells were scraped in PBS and pelleted at 1200 RPM for 5 minutes. Cell pellets were then resuspended in a 15 mM NaCl, 15 mM Tris-HCl [pH 7.6], 60 mM KCl, 2 mM EDTA, 0.5 mM EGTA, 0.3 M sucrose buffer (0.5 mM PMSF, 1 mM DTT, 0.2 mM spermine, 1 mM spermidine). Intact nuclei were obtained by lysing the cells with NP40 (0.2% final concentration, 5 min incubation

on ice). After centrifugation and supernatant removal, nuclei were washed with a 15 mM NaCl, 15 mM Tris-HCl [pH 7.6], 60 mM KCl, 0.3 M sucrose buffer (0.5 mM PMSF, 1 mM DTT, 0.2 mM spermine, 1 mM spermidine). A limited MNase digestion was carried out on intact macrophage nuclei to generate a mixture of mono- and poly-nucleosomes (mainly mono-nucleosomes). In particular, digestion was performed with 1.3 units of MNase (Roche 10107921001) in a 20 mM Tris-HCl [pH 7.6], 5 mM CaCl2 digestion buffer, for 100 minutes at 37°C. Digestion was stopped by adding EDTA to a final concentration of 50 mM. DNA was purified from octamer proteins with the Qiagen PCR purification kit. Purified DNA was then run in a 1% agarose gel and the mononucleosomal band cut and purified first with Millipore DNA Gel Extraction Kit and then with the Qiagen PCR purification kit. Mononucleosomal DNA was prepared for HiSeq2000 sequencing using the Illumina standard protocol. Paired-end sequencing with a 100 bp read length and high sequencing depth (200 M filtered, uniquely aligned reads/sample) was performed.

ChIP sequencing. ChIP was carried out starting from 5-8 x 10^6 cells (for Pu.1 ChIP-seq), or 25-50 x 10^6 cells (for Brg1, Chd4 and H2A.Z) using a previously described protocol (Ghisletti et al., 2010). Briefly, BMDM were fixed 10 minutes at RT with formaldehyde (SIGMA F8775) at 1% final concentration. Crosslinking was stopped by addition of Tris-HCl pH 7.6 (125 mM as final concentration). After three washes with PBS, cells were collected and lysated. Cross-linked nuclear lysate was then sonicated to share cross-linked DNA to 300-500 bp fragments and then immunoprecipitated with 5 µg of specific antibody or normal rabbit IgG. Antibodies were pre-bound to G protein-coupled paramagnetic beads (Dynabeads) in PBS-0.5% BSA and incubated with lysates overnight at 4°C. Beads were washed six times in a modified RIPA buffer (50 mM HEPES [pH 7.6], 500 mM LiCl, 1 mM EDTA, 1% NP-40, 0.7% Na-deoxycholate) and once in TE containing 50 mM NaCl. DNA

was eluted in TE-2% SDS and crosslinks reversed by incubation overnight at 65°C. DNA was then purified by QIAquick PCR purification kit (Qiagen) and quantified with PicoGreen (Invitrogen). ChIP validation was performed by qPCR analysis with specific primers and Syber Green Master Mix (Applied Biosistems). ChIP DNA was prepared for HiSeq2000 sequencing following standard protocols.

Retroviral infection for H2A.Z depletion. The hairpin used in this study to deplete H2A.Z was selected among five designed using a publicly available software (http://katahdin.mssm.edu/siRNA). The sequence is available upon request. The shH2A.Z sequence was cloned in the MSCV-based pLMP retroviral vector (Dickins et al., 2005). The empty vector containing a scrambled sequence was used as control. At day 0 bone marrow cells were isolated and 4 x 10^6 cells/plate were seeded in 10 cm dishes in TET-free BM medium. Cells were infected twice (in two consecutive days after plating) using supernatants from transfected Phoenix-ECO packaging cells. Puromycin selection (3 µg/ml) started on day 3. Cells were recovered at day 7.

Recombinant retroviruses were produced by transient transfection of ecotropic Phoenix cells. In brief, Phoenix cells were plated at 2x10^6 cells/10-cm plate 24h before transfection. Calcium phosphate transfection was performed with 10 µg of the retroviral plasmid of interest. The medium of Phoenix cells was replaced with 10ml of medium with 20 µM chloroquine. Plasmid DNA was added to 2.8 µg of pCL-Eco packaging vector, 61 µl of 2M CaCl2 and water up to 500 µl. Then 500 µl of HBS Buffer2x were dripped into the mix. The mixture was dispensed on the phoenix cells by dripping. After 16h of incubation, the medium was replaced with 5 ml of target cell medium. After 24h and 48h from the medium changing the supernatant

of Phoenix cells supplemented with Polybrene (8 µg/ml) and HEPES pH 7.5 was added to BMDM cells.

Inducible retroviral infection for Pu.1 depletion. The hairpin used in this study to deplete Pu.1 was selected among five designed using a publicly available software (http://katahdin.mssm.edu/siRNA). The sequence is available upon request. The shPU.1 sequence was cloned in a modified version of TtRMPVIR inducible retroviral vector (Genbank HQ456318) (Zuber et al., 2011) in which the puromycin resistance gene was inserted. The empty vector, containing an sh-Renilla sequence was used as control. At day 0 bone marrow cells were isolated and 4 x 10^6 cells/plate were seeded in 10 cm dishes in TET-free BM medium. Cells were infected twice (in two consecutive days after plating) using supernatants from transfected Phoenix-ECO packaging cells. Puromycin selection (3 µg/ml) started on day 3. At day 5, shPU.1 expression was induced for 48 hours using doxycycline (0.5 µg/ml).

DNase I digestion. We applied the method described in Neph et al., 2012 with minor modifications. Briefly, DNase digestion was performed starting on 10 x 10^7 cells. Cell pellets were resuspended in a 15 mM NaCl, 15 mM Tris-HCl [pH 8], 60 mM KCl, 1 mM EDTA, 0.5 mM EGTA, 0.15 mM spermine, 0.5 mM spermidine buffer and lysed upon addition of a 0.2% NP40 (final concentration). Nuclei were washed and resuspended at a concentration of 1 x 10^8/ml in the initial solution without NP-40. Parallel limited DNase digestion were carried out with 1 x 10^7 nuclei, 60 units of DNase I (Roche, 04716728001) in the provided DNase buffer, for 10 minutes at 37°C. The reactions were stopped with an equal volume of a 100 mM NaCl, 50 mM Tris-HCl [pH 8], 0.1% SDS, 100 mM EDTA, 0.3 mM spermine,1 mM spermidine, RNAse A 10 µg/ml solution for 15 minutes at 55° C, Proteinase K was added at final concentration of 0.5 mg/ml and the samples were incubated for 2-16 h at 55° C.

After a standard phenol-chloroform DNA extraction, a 10-40% sucrose gradient ultra-centrifugation was performed for 24 h at 25000 rpm, 25° C (described in detail in Sabo et al., 2006). DNA from the fractions with fragments smaller than 1.2 kb was purified with Qiaquick PCR purification kit (Qiagen) and loaded on a 1% agarose gel. All the fragments <500 bp were purified from the gel with standard methods (Qiagen gel exraction kit) and prepared for sequencing on HiSeq2000. Single-read sequencing with a 50 bp read length and high sequencing depth (400 M filtered, uniquely aligned reads/sample) was performed.

Protein extraction and western blot. Whole cell lysate was obtained with a lysis buffer “Buffer 1”(250mM NaCl, NP40 0,2%, Tris-HCl pH8 50mM, EDTA 0,5mM and EGTA 0,5mM) for Pu.1 experiments and UREA 8M for H2A.Z experiments. The proteins obtained were separated according to their molecular weight by electrophoresis in a polyacrylamide gel and transferred into a Protran nitrocellulose filter of 0.45 microns. After the blocking of the non specific sites by incubation in TBST buffer (20mM Tris-HCl pH7.5, 500mM NaCl, 0.1% Tween-20) supplemented with 5% milk, the filter were subjected to hybridization with specific antibodies. Quantified images were acquired either using Li-Cor with secondary IR-Dye antibodies or the Chemidoc from Bio-Rad.

***In vitro* nucleosome assembly.** Naked genomic DNA was purified from mouse macrophages by three consecutive phenol/chloroform extractions. DNA was sonicated to obtain fragments smaller than 2 kb, and fragments ranging from 600 to 2,000 bp were purified with Solid-Phase Reversible Immobilization (SPRI) beads (Agencourt AMPure XP, Beckman Coulter). DNA was combined with recombinant histones (EpiMark™ Nucleosome Assembly Kit, NEB E5350) to generate nucleosomes by salt dialysis (Luger et al., 1999). DNA molecules were considered as multiple of 150 bp nucleosome-assembling units. Assembly reaction was

performed mixing octamers and nucleosome-assembling units in a 1:2 molar ratio so that DNA was not limiting and octamer would assemble according to the sequence preference.

FAIRE-seq. We applied the method described in Giresi and Lieb, 2009 with minor modifications. Briefly, we fixed 5-8 x 10^6 cells for 10 minutes at RT with 1% formaldehyde (SIGMA F8775). Crosslinking was stopped by addition of Tris-HCl pH 7.6 (125 mM as final concentration). After three washes with PBS, cells were collected and lysated. Cross-linked nuclear lysate was then sonicated to share cross-linked DNA to 100-1000 bp fragments. After a phenol/clorophorm extraction, we purified free DNA in aqueous phase with Qiagen Minelute PCR columns and quantified it with Nanodrop. FAIRE validation was performed by qPCR analysis with specific primers and Syber Green Master Mix (Applied Biosistems). FAIRE DNA was prepared for HiSeq2000 sequencing following standard protocols.

ATAC-seq. We performed ATAC-seq using the method described in Buenrostro et al., 2015 with minor modifications. Briefly, 50.000 cells were scraped in PBS and pelleted by centrifugation for 20 min at 500g and 4º C. Cell pellets were washed once with 1x PBS and cells were pelleted by centrifugation using the previous settings. Cell pellets were re-suspended in 25 µl of cold lysis buffer (10mM Tris-HCl pH 7.4, 10mM NaCl, 3mM MgCl2, 0.1% Igepal CA-630) and nuclei were pelleted by centrifugation for 20 min at 500g, 4 ºC. Supernatant was discarded and nuclei were re-suspended in 25 µl reaction buffer containing 2 µl of Tn5 transposase and 12.5 µl of TD buffer (Nextera Sample preparation kit from Illumina). The reaction was incubated at 37ºC for one hour. Then 5 µl of clean up buffer (900mM NaCl, 300mM EDTA), 2ul of 5% SDS and 2 µl of Proteinase K (NEB) were added and incubated for 30 min at 40 ºC. Tagmentated DNA was isolated using 2x SPRI beads cleanup.

For library amplification, two sequential 9-cycle PCR were performed in order to enrich small tagmentated DNA fragments. We used 2 µl of indexing primers included in the Nextera Index kit and KAPA HiFi HotStart ready mix. After the first PCR, the libraries were selected for small fragments (less than 600 bp) using SPRI cleanup. Then a second PCR was performed with the same conditions in order to obtain the final library. DNA concentration was measured with a Qubit fluorometer (Life Technologies) and library sizes were determined using Bioanalyzer (Agilent Technologies). Libraries where sequenced on a Hiseq 2000 for an average of 20 million reads per sample.

Computational methods.

All the analyses were performed by Bioinformatician lab members (I. Barozzi, C. Balestrieri and A. Termanini).

ChIP-seq. After quality filtering, 51 nt long single-end reads were aligned onto the mm9 release of the murine genome using Bowtie v0.12.7 (Langmead et al., 2009). Only unique alignments were retained, allowing up to two mismatches compared to the reference genome. Peak calling was performed using MACS v1.4 (Zhang et al., 2008). Cell type specific inputs were used as controls. In order to visualize the raw profiles on the Genome Browser (Meyer et al., 2013), wiggle files were generated with MACS v1.4 and converted to Bigwig (Fujita et al., 2011). Induced and repressed regions were found using MACSv1.4, with the untreated sample as control.

MNase-seq. Paired-end reads were mapped to the mouse genome using Bowtie (Langmead et al., 2009). Wiggle tracks at single bp resolution were generated with BedTools (Quinlan and Hall, 2010). PeakSplitter (Salmon-Divon et al., 2010) was used to extract nucleosomal positions from this population-averaged profile. Paired-end fragments for ESCs, NPCs and MEFs were retrieved from the literature (Teif et

al., 2012). Pu.1-bound regions were sorted according to the NDR occupancy level. The number of midpoints of the nucleosomal fragments falling into the central 300 bp of each region was calculated and used as a proxy for the overall occupancy of the area.

DNase-seq, FAIRE-seq and ATAC-seq. Reads alignment and peak calling was performed as for ChIP-seq data. Briefly, Reads were aligned to the mouse genome using Bowtie and Peak calling was performed using MACSv1.4 (Zhang et al., 2008) using default parameters and the option –no-lambda. Induced and repressed regions were found using MACSv1.4, with the untreated sample as control.

TFBSs over-representation analysis. We used Pscan (Zambelli et al., 2009) to detect statistically significant over-represented DNA motifs. Given a dataset of position weight matrices (PWMs), representing experimentally determined binding preferences for known transcription factors (TFs), Pscan scans each input sequence for the best match to each one of these PWMs. It then uses these values to build a distribution and compare it with that obtained applying the same procedure to a background set. Pscan returns a *p*-value for each PWM so that significantly over-represented binding motifs can be identified.

Functional Annotations Using GREAT. GREAT 1.8 (McLean et al., 2010) was run with standard parameters against the whole mm9 genome as background. GO Biological Process ontology was considered.

Statistics and plots. All plots were drawn and statistics was performed using the R package.

RESULTS

1) Role of Pu.1 in nucleosomal organization at macrophage regulatory regions

1.1) Nucleosomal organization at Pu.1-bound TSS-distal regions

Pu.1 is the master regulator of macrophage differentiation and mediates the deposition of H3K4me1 and an increase in accessibility at its binding sites (Ghisletti et al., 2010; Heinz et al., 2010b). To clarify the role of Pu.1 as global organizer of nucleosomes in macrophages, we obtained high-resolution nucleosome maps and centered them on Pu.1-bound TSS-distal regulatory regions. A MNase digestion was carried out on intact macrophage nuclei at different times of digestion (20 and 100 minutes, fig.1). We chose the digestion that generated a mixture of mono- and poly-nucleosomes with mainly mono-nucleosomes. (fig. 1, 100 min digestion).

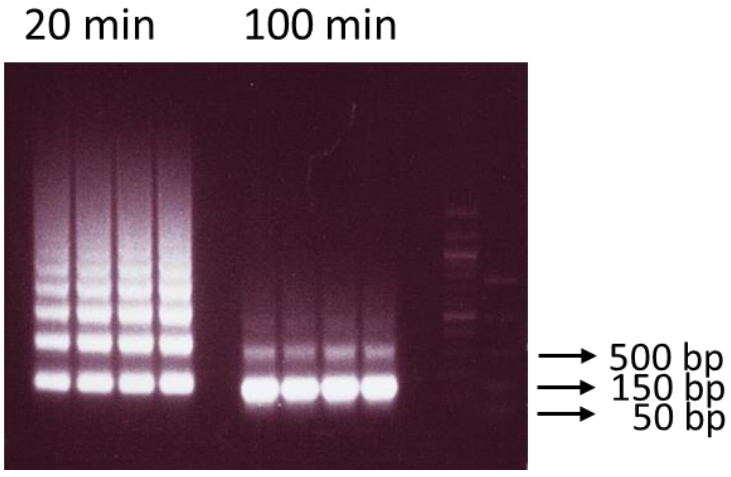

Fig. 1) MNase digestion and selection of the mononucleosomal band from agarose gel.

A Mnase digestion on intact nuclei was performed at different time points (20 and 100 minutes). A prolonged digestion to obtain mainly mononucleosomes (100 min) was chosen and

mononucleosomal DNA was recovered from agarose gel. Samples coming from 8 millions of untreated macrophages were loaded on each of the four lanes per time point .

Mononucleosome-sized DNA fragments were then purified from agarose gel and subjected to paired-end 100 bp read length sequencing at high sequencing depth. By pooling four replicates, we obtained 825 millions of uniquely aligned, filtered and properly paired sequencing reads that allowed us to generate a high-resolution view of nucleosome arrays. TSS-distal sites were defined upon annotation of the Pu.1-bound sites to Ensembl genes (Flicek et al., 2012), resulting in 59'481 regions. TSS-distal Pu.1 peaks corresponding to macrophage-specific enhancers (Ostuni et al., 2013) were used as central anchoring points for the generation of nucleosome maps (fig. 2).

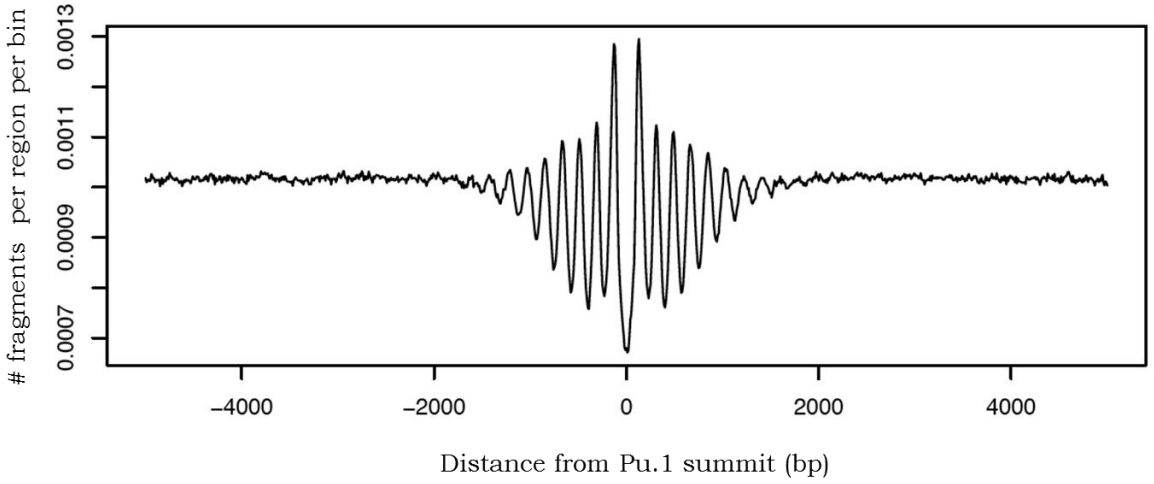

Fig. 2) Regular arrays of nucleosomes centered at Pu.1-bound enhancers in macrophages. Cumulative distribution of midpoints of nucleosomal sequencing fragments centered on the summit of TSS-distal Pu.1 sites in macrophages. The number of fragments in each 10-bp bin was normalized by the total number of fragments in the area.

We detected regular arrays of nucleosomes (with up to seven nucleosomes on each side of the Pu.1-bound region) with a nucleosome-depleted region (NDR) centered on the Pu.1 summit, which indirectly suggests a role for Pu.1 as a nucleosomal

barrier. Notably, nucleosome depletion surrounding Pu.1-bound sites was independently observed in ChIP-seq experiments based on sonicated chromatin (Ghisletti et al., 2010; Heinz et al., 2010), thus suggesting that it was not due to digestion of labile nucleosomes with high sensitivity to MNase.

Since this cumulative distribution is not informative of the behavior of individual genomic regions, we generated a heatmap in which Pu.1 summit-centered nucleosome patterns were sorted based on the decreasing width of the central NDR and split into deciles (fig. 3). Regions at the bottom of the heatmap (10th decile) are characterized by a narrow NDR surrounded by two well-positioned nucleosomes and other nucleosomes with overall high occupancy. Regions at the top of the heatmap (1st decile) showed a wider NDR less clearly demarcated because of the much lower degree of occupancy of the flanking nucleosomes.

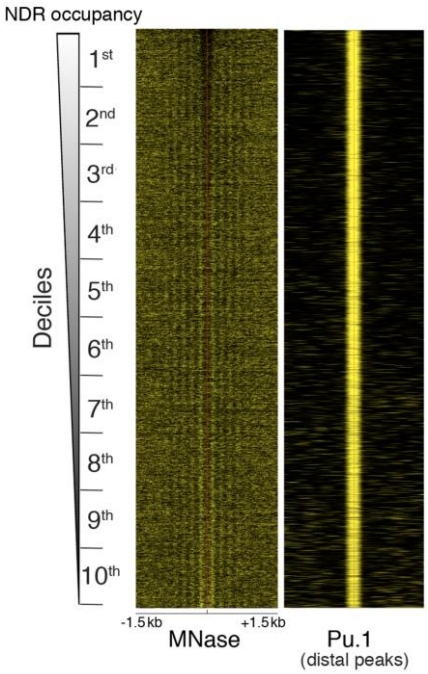

Fig. 3) TSS-distal Pu.1-bound sites in macrophages were sorted according to the induced NDR. Nucleosome patterns (MNase) and Pu.1 binding profiles are shown as heatmaps. MNase heatmaps ordered from top to bottom based on decreasing occupancy of the NDR and divided in deciles. The counts exceeding the 95th percentile of the overall distribution were set to its value. Considering MNase data, these counts were then normalized in the range 0–1 separately for each

region. The same procedure was applied to ChIP-seq data, except that the 0–1 normalization was applied to the entire data set.

Pu.1 occupancies were relatively similar in magnitude across all deciles, with slightly higher scores only in the first decile (fig. 4). This suggest that different degrees of Pu.1 occupancy are not a major determinant of the width of the NDR. Other factors such as chromatin remodelers or other partner TFs could be responsible for the different width of NDR at Pu.1-bound enhancers.

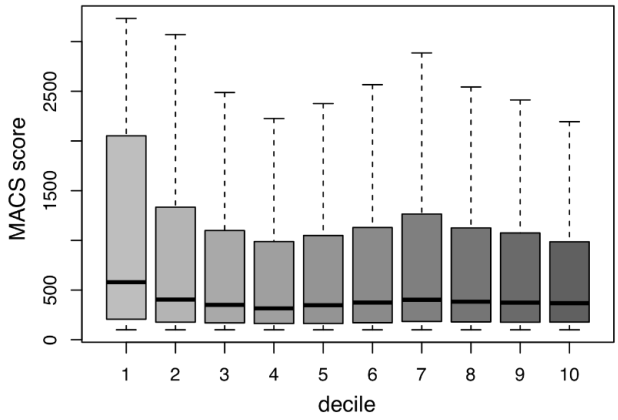

Fig. 4) Binding of Pu.1 in in the different deciles. Pu.1 ChIP-seq score (according to MACS) of the peaks in different deciles are shown. Groups are significantly different (p = 7.89e-95 in a Kruskal-Wallis test) even though only the first decile (larger NDRs) displays a marked increase in ChIP-seq determined occupancies.

1.2) Nucleosomal patterns in unrelated cell-types and in in vitro reconstituted chromatin

To better determine the role of Pu.1 in nucleosome organization, we then analyzed nucleosome occupancy at macrophage Pu.1-bound sites in cell types that do not express Pu.1. Nucleosome sequences from embryonic stem cells (ESCs), neural precursors (NPCs) and mouse embryonic fibroblasts (MEFs) (Teif et al., 2012) were aligned to the summit of Pu.1 peaks. In all the three cases, high nucleosome occupancy extending for about a single nucleosome length and precisely

overlapping the macrophage Pu.1-bound, nucleosome-depleted regions was detected (fig. 5).

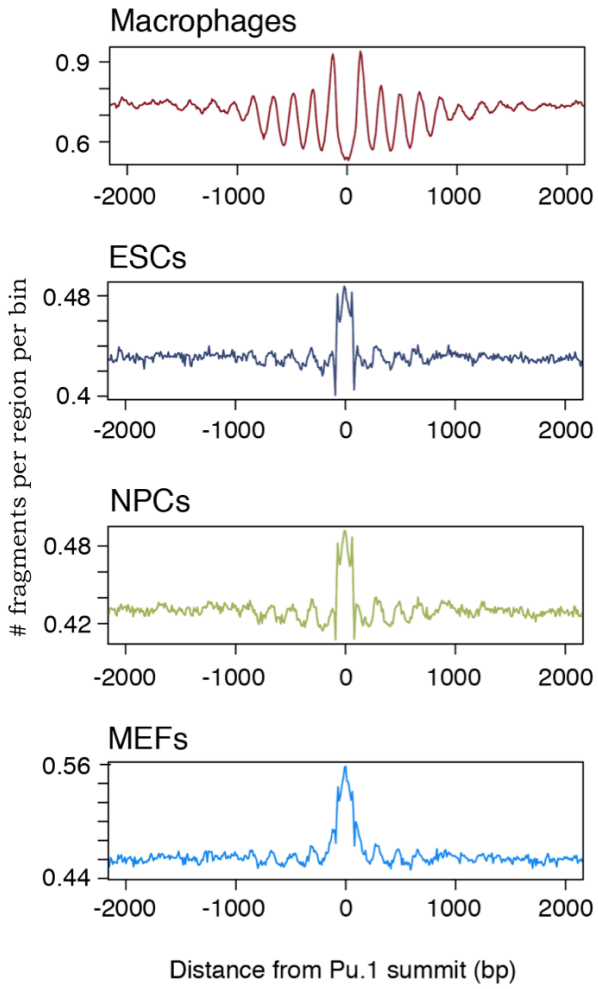

Fig. 5) Pu.1-bound, nucleosome-depleted macrophage enhancers are covered by nucleosomes in unrelated cell types. Cumulative distributions of the midpoints of the nucleosomal fragments centered on distal Pu.1 sites in macrophages and in unrelated cells that do not express Pu.1 (ESCs=embrionic stem cells, NPCs=neural precursors and MEFs=mouse embrionic fibroblasts). The number of midpoints in each 10-bp bin was scaled according to the total number of regions and sequencing depth.

To investigate the role of DNA sequence in controlling the nucleosomal landscape at Pu.1 sites, we assembled nucleosomes *in vitro* (experiment done by M. Simonatto). Naked genomic DNA extracted from mouse macrophages was sonicated and a smear of 600 to 2'000 bp fragments was purified and combined

with recombinant histones to generate nucleosomes by salt dialysis (Luger et al., 1999). Assembly conditions in which DNA was not limiting were used to specifically focus on the effects of the primary sequence on nucleosome positioning (Luger et al., 1999; Valouev et al., 2011). The cumulative distribution of fragments bound to nucleosomes *in vitro* (fig. 6) shows an overall high nucleosome occupancy (compared to random data) and a nucleosome positioned over the Pu.1-binding site in macrophages. Although nucleosome occupancy is affected by several factors, these data suggest that Pu-1-bound regions have an intrinsic high nucleosome occupancy (dictated by sequence features) that is overcome by Pu.1 binding in macrophages.

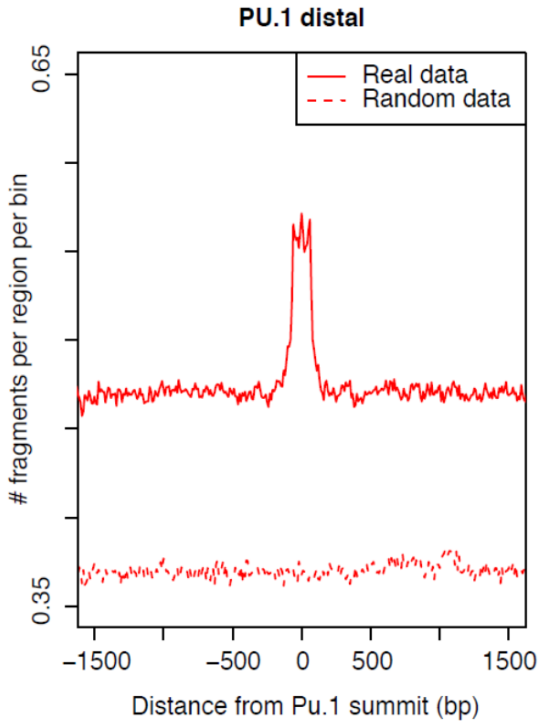

Fig. 6) TSS-distal Pu.1-bound regions show an increase in nucleosomal density in *in vitro* reconstituted chromatin. Cumulative midpoints distribution from in vitro assembled nucleosomes (bin = 10 bp).

1.3) Effects of Pu.1 Depletion on Nucleosome Occupancy

To better clarify the role of Pu.1 in counteracting DNA sequence-driven nucleosome occupancy and maintaining nucleosome depletion and accessibility of the underlying regulatory regions, we generated nucleosome maps in Pu.1-depleted macrophages. We first obtained a retroviral vector for inducible, doxycycline-regulated expression of an shRNA targeting Pu.1. We chose an inducible system in order to deplete Pu.1 only in differentiated macrophages, because Pu.1 is essential for macrophage differentiation (Nerlov and Graf, 1998). A vector containing a scrambled shRNA was used as a control (empty vector). Bone marrow-derived cells (that proliferate and differentiate in macrophages in M-CSF-containing medium) were infected at day 1 and 2 after plating, selected in puromycin and then induced to express the Pu.1-shRNA at day 5. 48h after shRNA induction, a ca. 60% depletion of Pu.1 protein was obtained in two independent experiments (repl. 1 and 2 in fig. 7; notably, a complete depletion of Pu.1 would not be compatible with macrophage survival).

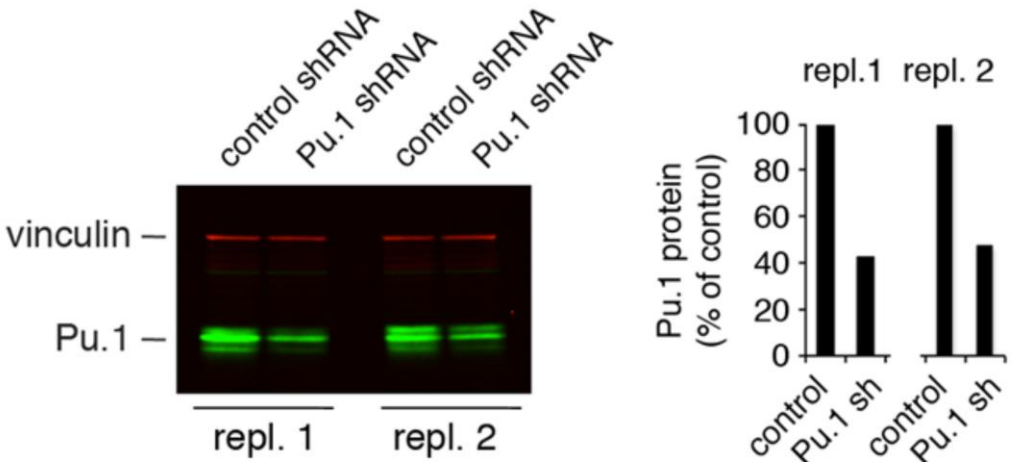

Fig.7. Evaluation of Pu.1 depletion in retrovirally infected cells. Acute depletion of Pu.1 in terminally differentiated macrophages using a retrovirus-encoded Tet-regulated shRNA. Data from

two biological replicates are shown. Vector with scrambled shRNA was used as a control. Protein levels measured by Western blot (vinculin was used as loading control).

We then performed a Pu.1 ChIP-seq experiment on Pu.1-depleted cells compared to the control to classify regulatory regions based on the level of reduction of Pu.1 binding. The reduction of Pu.1 binding controlled by qPCR on selected targets is shown in figure 8.

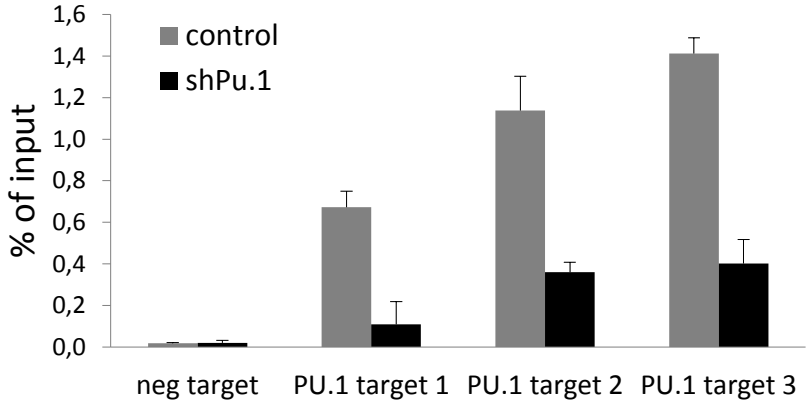

Fig. 8) Pu.1 binding reduction in shPu.1 cells compared to the control. Pu.1 binding reduction measured by ChIP-qPCR on selected targets (neg=negative target) as % on input. Standard deviation is shown.

TSS-distal Pu.1 peaks identified by ChIP-seq were then divided in quartiles based on the Pu.1 signal ratio in Pu.1-depleted *vs.* control cells, the fourth quartile corresponding to the stronger reduction in Pu.1 binding. After generating MNase high-resolution nucleosome maps in Pu.1 depleted and control cells, we investigate the nucleosome distribution at the TSS-distal Pu.1 binding sites found by ChIP-seq divided in the above-described quartiles (fig. 9). A strong and statistically significant ($p << 0.01$, Wilcoxon signed-rank test) increase in nucleosomal reads at Pu.1-bound enhancers was detected in both experiments, particularly in the fourth quartile.

These data indicate that Pu.1 is necessary to maintain the NDR at genomic regions that tend to be reincorporated into nucleosomes upon its depletion.

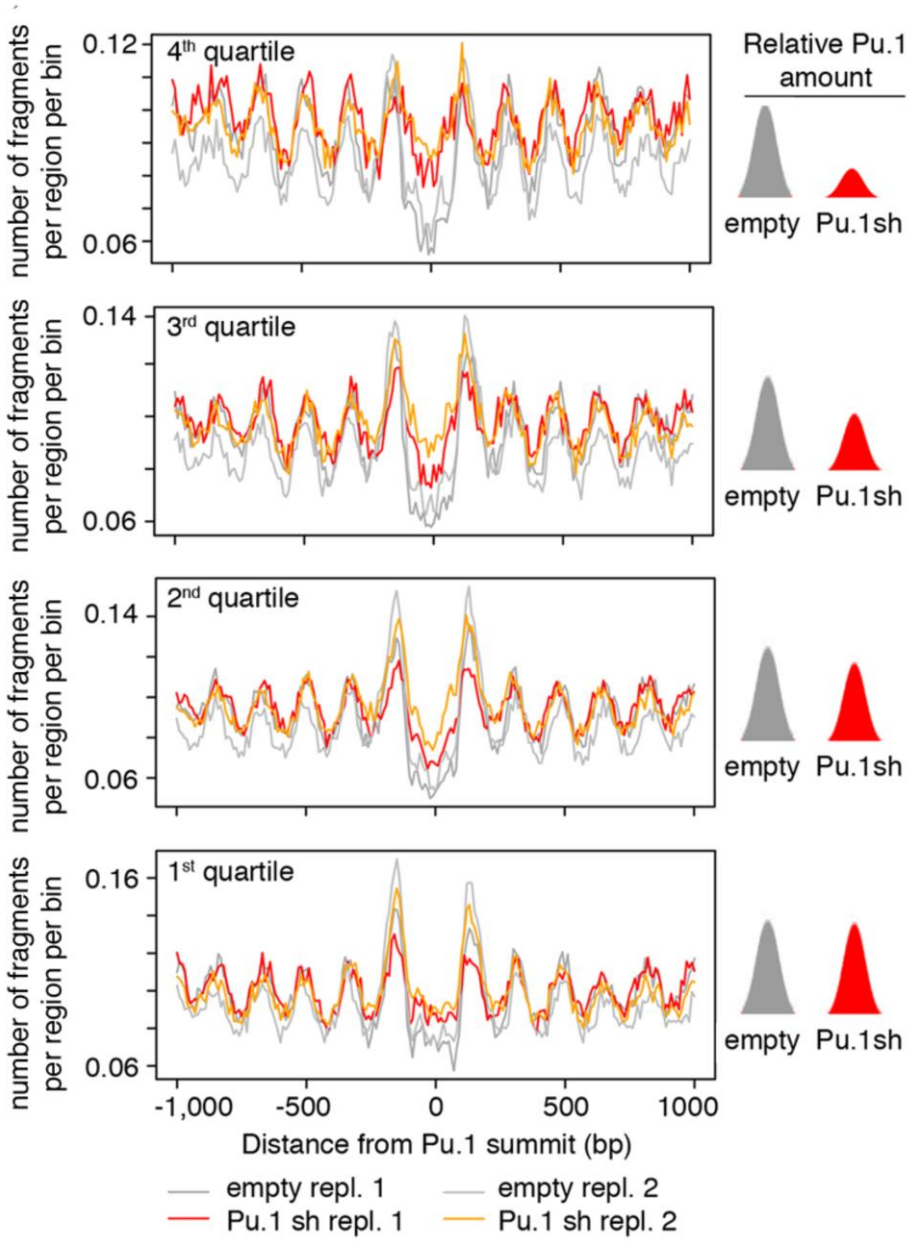

Fig. 9) Nucleosome occupancy in Pu.1-depleted macrophages. Pu.1 peaks were divided in quartiles based on the degree of signal reduction in Pu.1-depleted vs. control cells. The 4th quartile corresponds to Pu.1 peaks with the higher reduction in binding occupancy in depleted cells. Distributions of the midpoints of the nucleosome fragments were centered on the summit of Pu.1 peaks. MNase-seq data from two different biological replicates were independently analyzed.

2) Role of chromatin remodelers at macrophage regulatory regions

Chromatin remodelers may be differentially required for full Pu.1 binding to sequences characterized by high nucleosomal occupancy. Consistent with the notion that displacement of nucleosomes and formation of nucleosome arrays requires the activity of ATP-dependent remodelers (Zhang et al., 2011), we next wanted to investigate their impact on nucleosome organization and chromatin opening at Pu.1 distal elements in macrophages.

2.1) Chromatin remodeler expression in macrophages

Looking at the expression profiles of ATPase subunits of chromatin remodeler complexes in RNA-seq data of BMDM previously produced in the laboratory, we noticed that Chd4/Mi2b, Brg1/Smarca4 and Brm/Smarca2 were the most expressed in macrophages (table 1, FPKM of total polyA RNA in basal state respectively 29, 13.3 and 11.7). Furthermore, the induction of Chd4/Mi2b and Brg1/Smarca4 expression after 4h LPS treatment suggested a specific role of these factors in the rearrangement of macrophage chromatin after the inflammatory stimulus.

ATPase subunit	Alternative name	FPKM polyA RNA	
		UT	4 h
BRG1	SMARCA4	13.29	36.36
BRM	SMARCA2	11.70	3.19
Chd1		1.78	17.44
Chd1l		2.22	0.91
Chd2		2.58	6.63
Chd3		5.93	8.40
Chd4	Mi2b	29.08	58.63
Chd5		0.04	0.02
Chd6		1.40	2.70
Chd7		0.46	4.00
Chd8		5.99	12.55
Chd9		1.33	7.61
snf2l	SMARCA1	0	0
snf2h	SMARCA5	3.26	8.67
	SMARCA5-PS	0.90	4.19

Table 1) Expression of chromatin remodeler ATPase subunits.

Total polyA RNA FPKM (Fragments Per Kilobase of transcript per Million mapped reads) for different ATPase subunits of chromatin remodelers are shown for BMDM in basal conditions (UT) and after 4h LPS stimulation.

Notably, a Mass Spectrometry analysis of Pu.1 binding partners previously done in our laboratory identified Chd4/Mi2b, Brg1/Smarca4 and Brm/Smarca2 (together with other regulatory subunits of the corresponding complexes) as top scoring proteins interacting with Pu.1 (table 2).

Complex/Family	Subunit/Component
Mi2/Nurd complex	**Chd4/Mi2b**, MTA1, MTA2, HDAC1, HDAC2, Rbbp4, Gatad2
Swi/Snf complex	Arid1a, **Brm/Smarca2**, **Brg1/Smarca4**, Baf180/PBRMI, Baf170/Smarcc2, Baf155/Smarcc1, Baf60a/Smarcd1, Baf60b/Smarcd2, Baf57/Smarcc1
Condensin complex	Smc2, Smc4
Cohesin complex	Smc1, Wap1, Stag2, Pds5a, Pds5gb, Smc3
RNA pol II components	Rpb1, Rpb2, Trim33, Spt5, Spt6
DNA polymerases	DNA pol alpha and delta
Lamina/nuclear matrix components	Tmpo/Lap2, prohibitin, Laminb2, Safb-like modulator Sltm

Table 2) Interactome of Pu.1 identified by high resolution mass spectrometry. Top scoring protein identified by mass spectrometry are shown. Pu.1 was immunoprecipitated with specific andtibody on crosslinked chromatin. After an I-Gel protein digestion, mass spectrometry was performed.

2.2) Chromatin remodelers occupancy on macrophage genome in basal conditions

According to these evidences, we focused our analysis on Brg1, Brm and Chd4 role in mouse macrophage genome remodeling. To this aim, we performed ChIP-seq experiments to investigate their genome-wide localization in macrophages in basal conditions. Only Brg1 and Chd4 Chip-seq experiments produced good datasets which have been analyzed.

For Brg1, 43,213 binding sites were identified in the mouse macrophage genome (MACS score> 50) (a representative snapshot is reported in fig.10b). 48% of total Brg1 binding regions were localized in intergenic regions and 52% in promoters and intragenic regions (16% in promoters, 6% in exons and 30% in introns, fig. 10a).

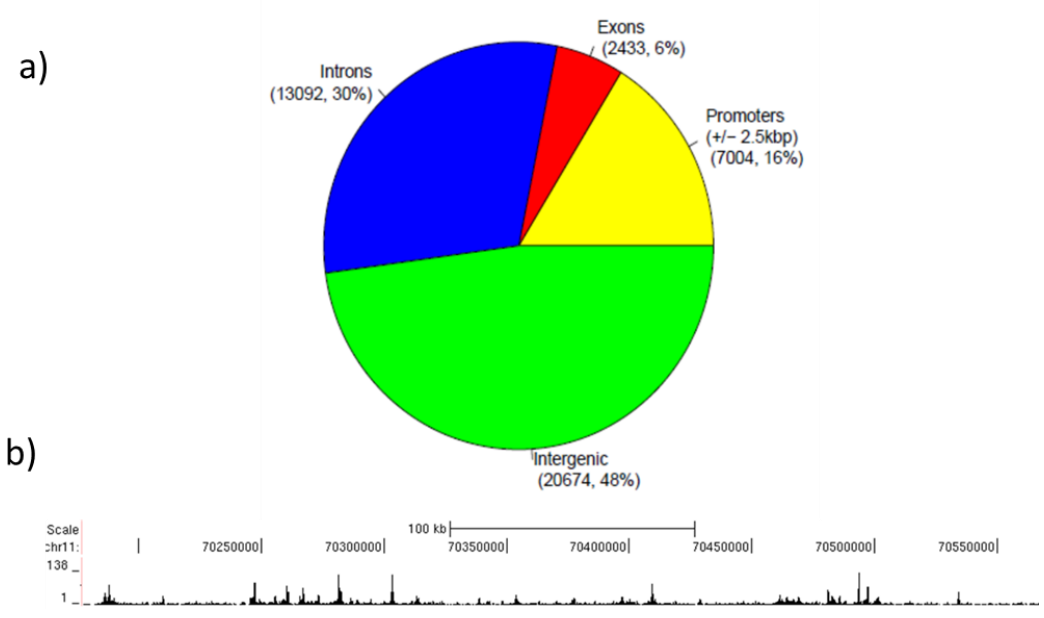

Fig. 10) Brg1 genomic occupancy. Genomic distributions of Brg1 at annotated genic regions (number of regions and percentage) (a) and a representative ChIP-seq snapshot (b) are shown.

For Chd4, 13,044 peaks were identified (MACS score> 100). 24% of them are localized in promoters, 41% in intergenic regions and 35% in intragenic ones (fig. 11a). For this analysis, MACS score> 100 was used instead of >50 as for Brg1, since Chd4 ChIP-seq resulted in broader peaks as represented in fig 11b.

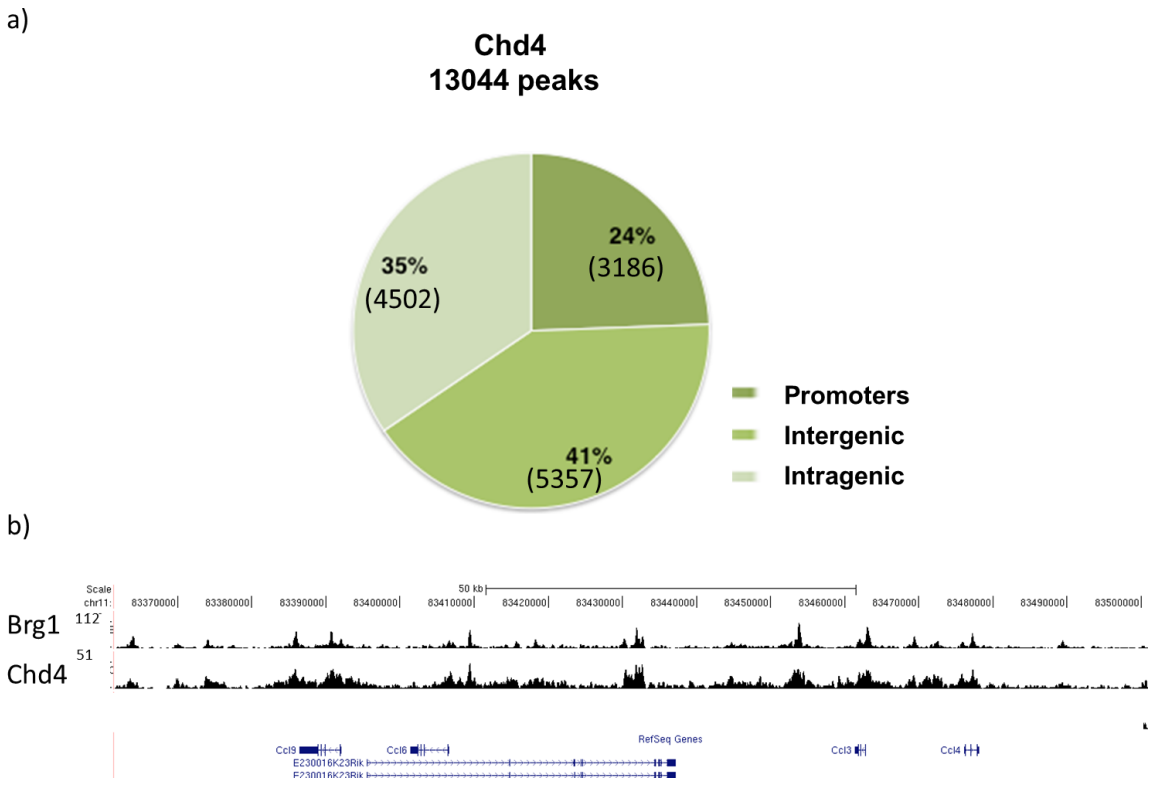

Fig.11) ***Chd4 genomic occupancy***. Genomic distributions of Chd4 remodeler at annotated genic regions (number of regions and percentage) (a) and a representative ChIP-seq snapshot (b) are shown.

We then investigated the co-localization of Brg1 and Chd4 and we found that 81% of Chd4 peaks overlap with Brg1 peaks (MACS score> 100) (fig 12). This high co-occupancy between the two factors may suggest a cooperative role of Chd4 and Brg1 in most of the regions bound. Conversely, only 58% of total Brg1 peaks overlap with Chd4, suggesting that Brg1 could have specific functions in regulating the opening of a distinct regulatory region subset. It would be interesting to better

elucidate which subsets are specifically bound only by Brg1 or Chd4 to better determine their functions on chromatin opening.

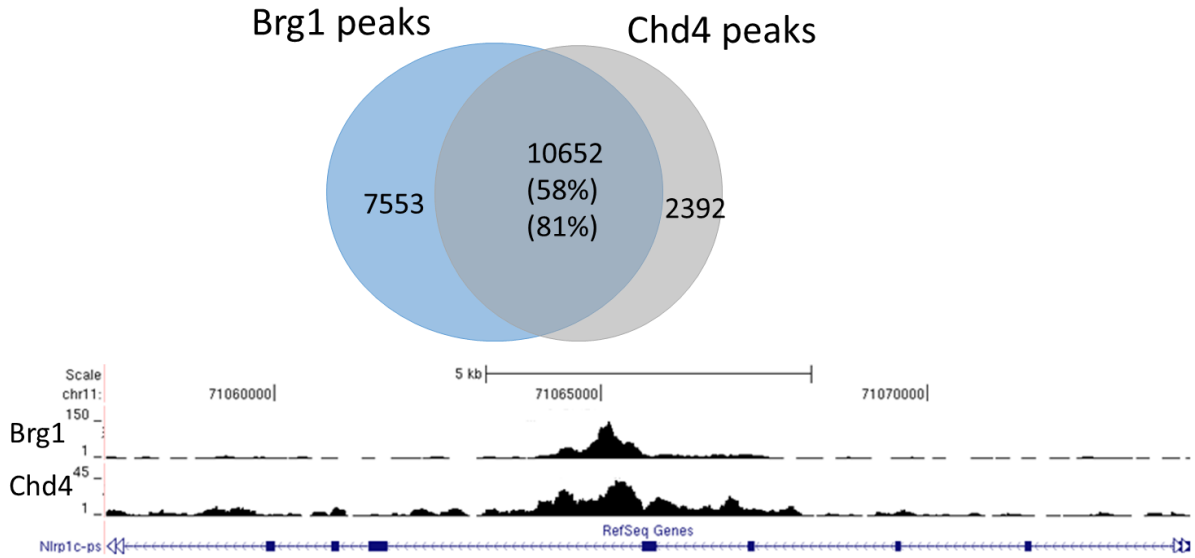

Fig. 12) Co-localization of Brg1 and Chd4 on genomic targets. Venn diagram displaying overlaps of binding-site occupancy between Brg1 and Chd4 (a) and a representative ChIP-seq snapshot of an overlapping peak (b) are shown.

2.3) Brg1 binding to Pu.1-bound regulatory elements

We then moved to investigate the role of Brg1 in cooperating with Pu.1 in opening chromatin at its binding regions and in particular at regulatory elements.

First, we looked at the co-localization between total Brg.1 and Pu.1-bound regions in macrophage genome. Notably, 85% of Brg.1 peaks overlapped with Pu.1 binding sites, suggesting an involvement of Brg1 in nucleosome organization at Pu.1-bound regulatory regions (fig. 13).

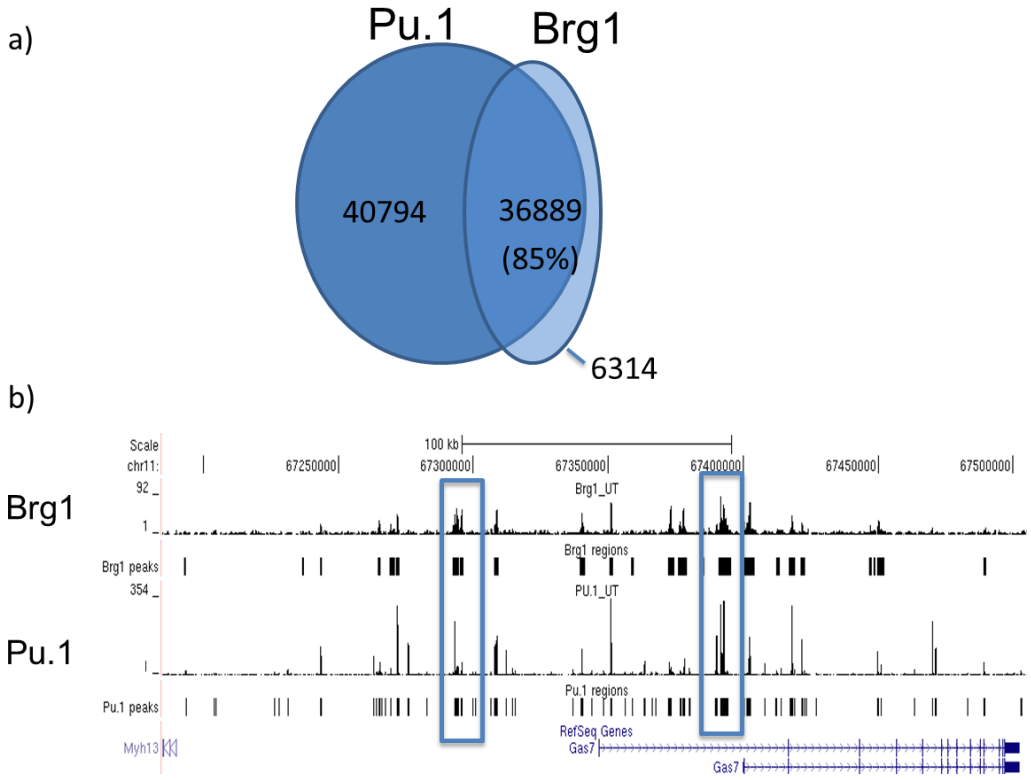

Fig. 13) Brg1 binding to Pu.1 sites. Venn diagram displaying overlaps of binding-site occupancy between Pu.1 and Brg1 (a) and a representative ChIP-seq snapshot of overlapping peaks (b) are shown.

We then investigated the recruitment of Brg1 at macrophage regulatory regions bound by Pu.1. We focused our analysis on TSS-distal Pu.1-bound regulatory regions. Heatmap of fig.14 shows the binding of Brg.1 at TSS-distal Pu.1 sites compared to the opening of the chromatin observed by MNase digestion. Notably, regulatory regions bound by Pu.1 are significantly enriched for the binding of Brg1, confirming its role in remodeling nucleosomes at these regions.

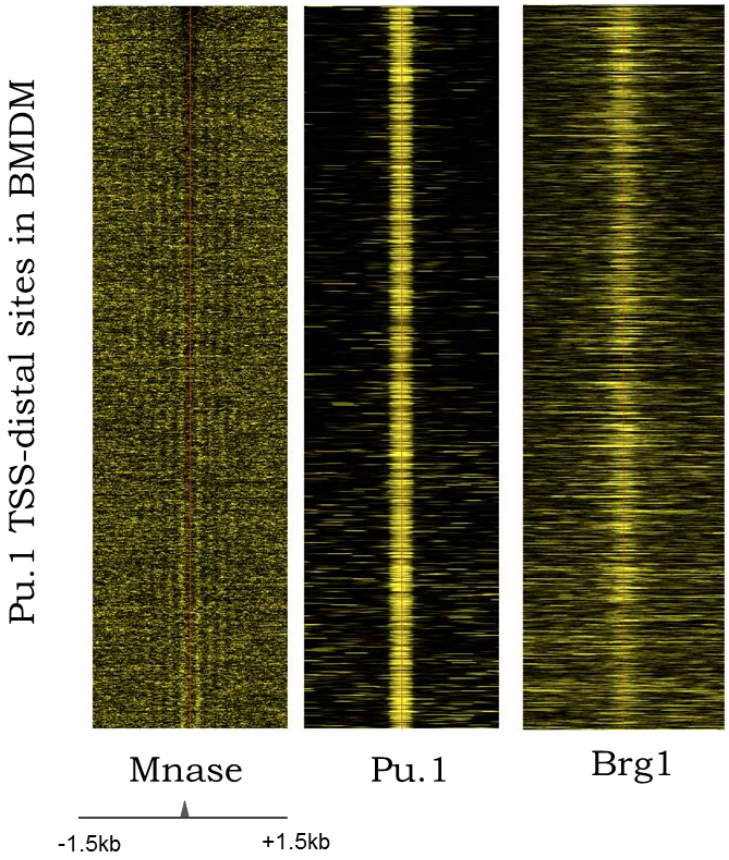

Fig. 14) Brg1 binding at TSS-distal regulatory regions bound by Pu.1. Heatmap showing MNase, Pu.1 and Brg1 signal at TSS-distal Pu.1 binding sites. MNase heatmaps are ordered from top to bottom based on decreasing occupancy of the NDR. MNase signal was normalized per row and the others are shown as absolute values. Bin=10 bp. The counts exceeding the 95th percentile of the overall distribution were set to its value. Considering MNase data, these counts were then normalized in the range 0–1 separately for each region. The same procedure was applied to ChIP-seq data, except that the 0–1 normalization was applied to the entire data set.

3) Role of H2A.Z histone variant at regulatory regions

Regulatory regions are associated with the presence of histone variants, in particular H2A.Z and H3.3 (Jin et al., 2009; Yukawa et al., 2014), but the role of H2A.Z in transcription and gene regulation has not been completely clarified.

3.1) H2A.Z genomic binding to chromatin

In order to elucidate the role of the H2A.Z histone variant at regulatory regions, we mapped its genomic locations through a ChIP-seq experiment in mouse macrophages. We detected 31,335 H2A.Z binding sites in the mouse genome (MACS score> 50), 43% of which were localized in intergenic regions and 57% in promoters and intragenic regions (35% in promoters, 6% in exons and 16% in introns, fig. 15).

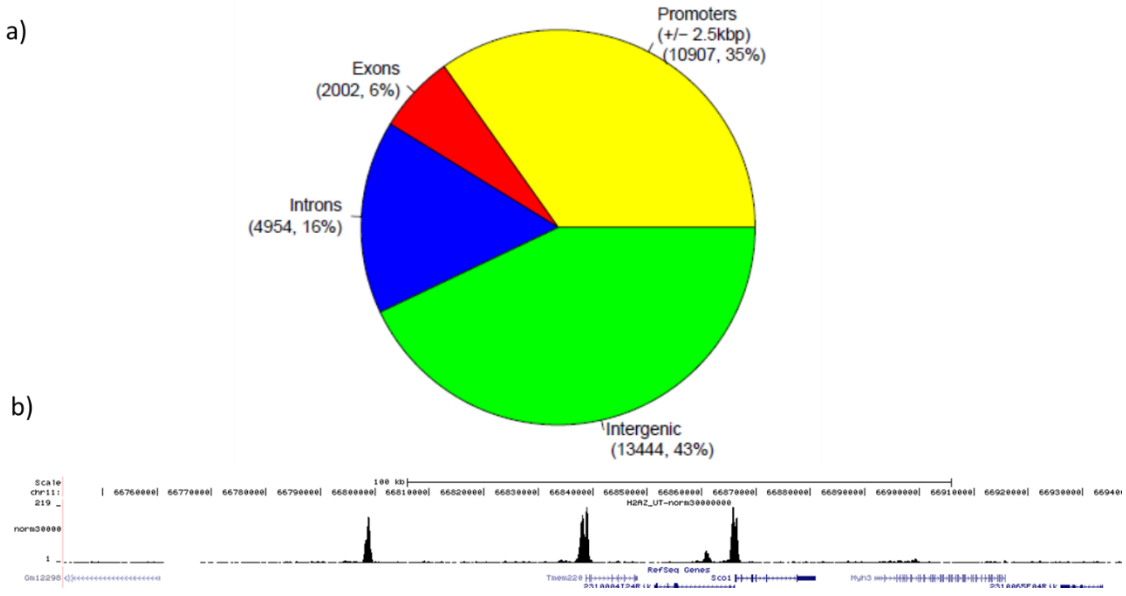

Fig.15) H2A.Z genomic binding to chromatin. Distributions of H2A.Z binding at annotated genic regions (number of regions and percentage) (a) and a representative ChIP-seq snapshot (b) are shown.

3.2) H2A.Z binding at macrophage regulatory regions

In order to elucidate the role of H2A.Z at macrophage regulatory regions, we evaluated its distribution at open regulatory regions. Notably, 80% of the H2A.Z peaks overlap with DNase I hypersensitivity regions (see section 4 for the details on this technique) underlying its functions at regulatory elements.

The strong presence of H2A.Z in open chromatin leaded us to investigate its co-localization with typical marks of genomic regulatory elements. Notably, H2A.Z binding sites showed very high overlap with the selected marks. In particular, 91.3% of H2A.Z binding regions overlap with H3K4me1 (that generally marks enhancers and promoters), 43.75% with H3K4me3 (that mostly marks promoters), 68% with H3K27ac (that marks active enhancers) and 37.5% with RNA pol II (that indicates transcribed regions) (table 3 and in fig. 16 representative snapshots are shown).

	%	# peaks
Total		31,335
Overlap H3K4me1	91.3	28,621
Overlap H3K27ac	68	21,328
Overlap H3K4me3	43.75	13,708
Overlap RNA Pol II	37.5	11,747
Overlap Pu.1	75	23,573

Table 3) H2A.Z co-localization with marks of regulatory regions. Overlaps of binding-site occupancy between H2A.Z and histone marks, RNA pol II and Pu.1 are shown.

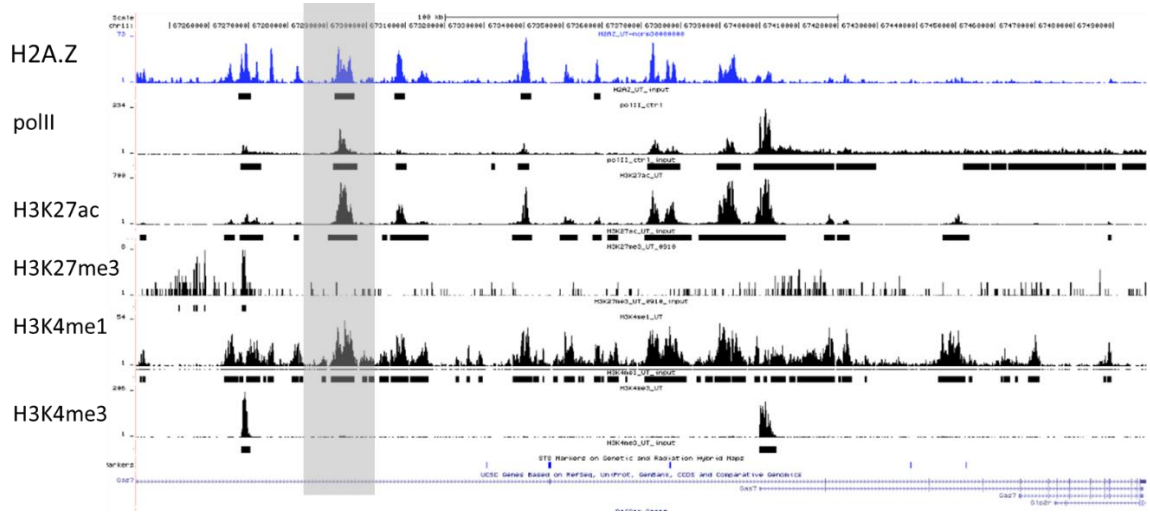

Fig. 16) H2A.Z co-localization with marks of regulatory regions. A representative snapshot is shown.

We also investigated the co-localization of H2A.Z with Pu.1 (table 3) and we obtained that 75% of the H2A.Z peaks overlapped with Pu.1 binding sites, suggesting a specific role of H2A.Z at Pu.1-bound macrophage regulatory regions that needs to be further investigated.

To understand the function of H2A.Z binding to TSS and in particular the association of its binding with macrophage specific TFs, we performed a motif finding analysis on H2A.Z positive versus H2A.Z negative TSS (the best 10 TF matrixes rescued by the Pscan are shown in table 4). From this analysis, we found as over-represented in H2A.Z-positive TSS some members of ETS family (ETV5, ELK1, ELK4) and members of kruppel-like family (Klf7) and E2F3, which is involved in cell cycle progression. This is consistent with data previously produced in the laboratory that identified ETS proteins as overrepresented in TSS of genes basally expressed in macrophages.

TF matrix	Z score	P value
HC_E2F3_si	16,68	1,20E-124
HC_low_RBL1_f1	17,48	1,70E-117
ETS0009 h-Elk4	15,40	6,14E-108
BU0039 Klf7_primary	16,06	3,54E-105
HC_E2F5_do	13,16	1,29E-104
JMB_GC_box	15,45	1,25E-102
HC_MBD2_si	15,87	5,96E-102
TA0136_ETV5_DBD_monomer	14,23	8,55E-97
MA0028.1 ELK1	14,05	3,39E-94
BMC_MTE	14,49	3,34E-92

Table 4. TFBS over-representation analysis on H2A.Z positive TSSs. We used Pscan (Zambelli et al., 2009) to detect statistically significant over-represented DNA motifs in H2A.Z positive TSSs versus negative one. Top 10 best score TFBSs are shown. Background= H2A.Z negative TSSs.

3.3) Dynamic changes of H2A.Z genomic occupancy after LPS treatment

To better evaluate the role of H2A.Z in maintaining macrophage regulatory landscape under perturbations, we performed ChIP-seq experiments in macrophages under inflammatory conditions. In particular, we stimulated cells with LPS at different time points (30 min, 2h and 4 h) to investigate H2A.Z binding changings after short and longer stimulations.

As shown in table 5, after LPS treatment we obtained a number of regions compatible with those obtained in basal conditions. We found that H2A.Z binds 24,986 regions after 30 min of LPS treatment, and respectively 26,596 after 2h and 27,702 after 4h. Considering the regions differentially bound by H2A.Z in stimulated macrophages compared to untreated ones, LPS stimulus induced H2A.Z de novo binding in 103 regions after 30 minutes of treatment, 1,332 after 2h and 2,690 after 4h (a representative snapshot of induced regions is shown in fig 17a). On the contrary, a huger number of H2A.Z binding sites were repressed after LPS stimulus (1,394, 2,809 and 4,604 regions respectively after 30 minutes, 2 h and 4 h of LPS stimulus, a representative snapshot of induced region is shown in fig 17b). The fact that a fraction of the total number of H2A.Z binding sites is induced (ca 10% at 4h LPS) or repressed (ca 20% at 4h LPS) after inflammatory stimulation suggested a role of H2A.Z at regulatory regions of LPS-regulated genes.

# peaks	untreated	0.5h LPS	2h LPS	4h LPS
Total	31,335	24,986	26,596	27,702
Induced (vs UT)		103	1,332	2,690
Repressed (vs UT)		1,394	2,809	4,604

Table 5. H2A.Z-bound regions after LPS stimulus. Total number of H2A.Z bound regions (MACS score> 50) in UT, 0.5 h, 2h and 4h LPS treated cells and induced and repressed peaks in LPS treated compared to untreated macrophages are shown.

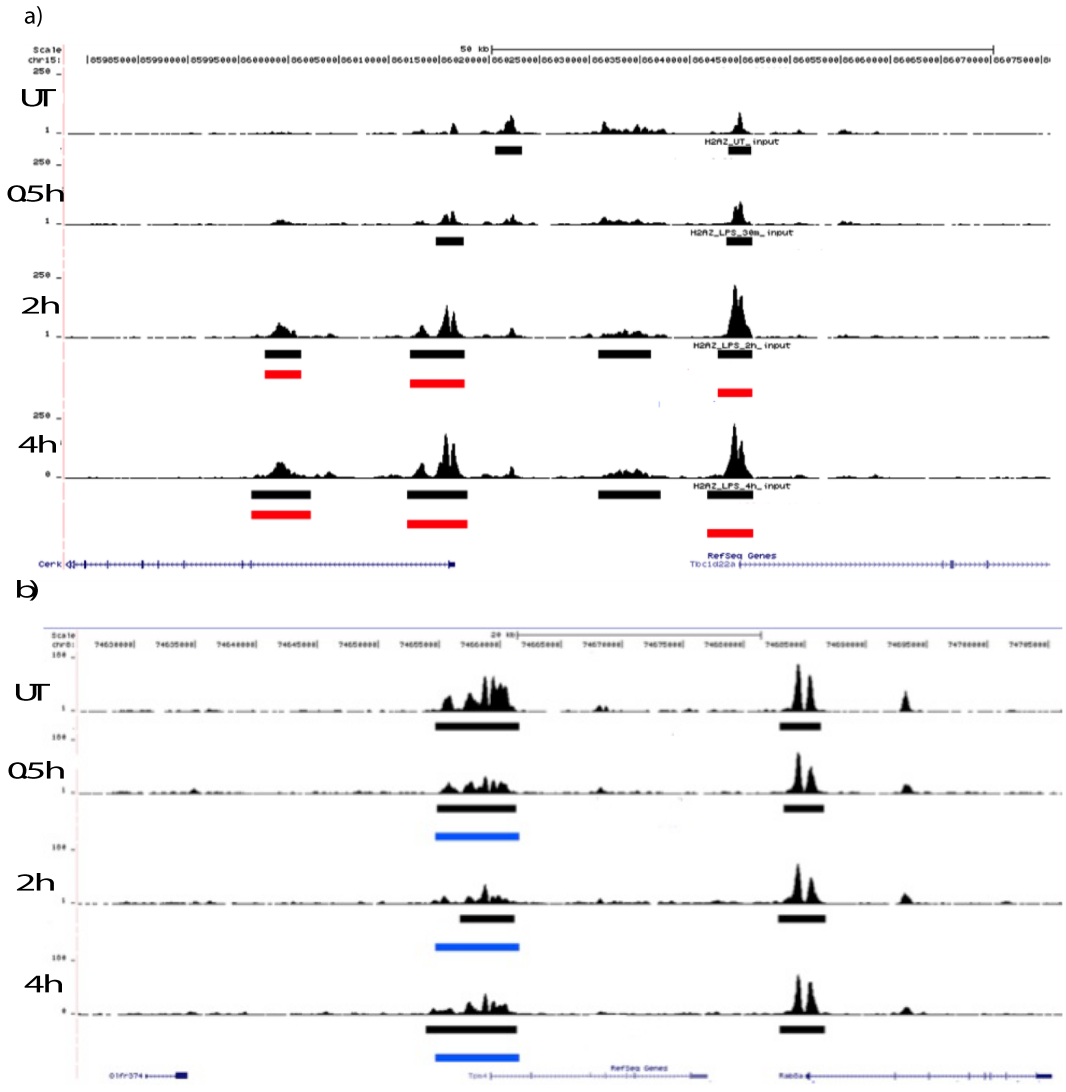

Fig. 17) Representative snapshots of regions induced (a) or repressed (b) after LPS treatment. Black box: significant vs background, red box: induced peaks compared to untreated sample, blue box: repressed peaks compared to untreated sample.

3,3.1) Colocalization of H2A.Z with Pu.1 after LPS treatment

To better clarify the interactions between H2A.Z and Pu.1 in macrophages in basal state and after LP overrepresentation of distinct ontology terms associated with the neighboring genes. GREAT (genomic regions enrichment of annotations tool) computes the enrichment of ontology terms in a set of genomic regions extracted from sequencing data (McLean et al. 2010). When considering the S treatment, we divided the Pu.1-bound sites found at MACS score> 100 in proximal (+/- 2500 bp) and distal (> 2500 bp) from TSS. In untreated macrophages, 78% of total H2A.Z peaks (19,850/25,436) overlap with Pu.1 sites. In particular, 59.8% of these overlapping peaks (11,864/19,850) are located at Pu.1-bound distal sites and 40.2% (7,986/19,850) at proximal ones.

A gene ontology performed on these overlapping peaks was performed using GREAT (genomic regions enrichment of annotations tool) GREAT computes the enrichment of ontology terms in a set of genomic regions extracted from sequencing data (McLean et al. 2010). GO biological processes best score terms revealed that in untreated macrophages the TSS-distal, H2A.Z-PU.1 overlapping peaks are related mainly to regulation of cytokine biosynthesis, toll-like receptor signaling and negative regulation of immune response. (table 6, on the left). On the contrary, TSS-proximal H2A.Z-Pu.1 peaks are mainly related to protein folding and RNA export from the nucleus (table 6, right part).

untreated macrophages	
TSS-distal	TSS-proximal
positive regulation of cytokine biosynthetic process	ncRNA processing
regulation of cytokine biosynthetic process	protein folding
regulation of toll-like receptor signaling pathway	nuclear export
Ras protein signal transduction	tRNA processing
negative regulation of protein serine/threonine kinase activity	RNA export from nucleus
positive regulation of T cell proliferation	spindle organization
cellular response to inorganic substance	mRNA export from nucleus
negative regulation of immune response	GPI anchor biosynthetic process
establishment of endothelial barrier	spindle assembly
negative regulation of MAP kinase activity	GPI anchor metabolic process

Table 6. Gene Ontology on H2A.Z-Pu.1 overlapping peaks in macrophages in basal conditions. Best 10 GREAT results for GO biological processes are represented for H2A.Z and Pu.1 common peaks in UT macrophages, divided in TSS-distal (>2500 bp from TSS) and proximal ones (+/- 2500 bp from TSS).

After 4 hours of LPS treatment a total of 22,147 H2A.Z peaks were detected at MACS score >100, 74% of which overlap with Pu.1-bound sites (16,394/22,147). 53% of these overlapping peaks are located at Pu.1-bound distal sites (8,683/16,394) and 47% at proximal ones (7,711/16,394). A gene ontology performed on these overlapping peaks was performed using GREAT. GO biological processes best results revealed that in 4h LPS treated macrophages the TSS-distal, H2A.Z-PU.1 overlapping peaks are related mainly to regulation of cytokine biosynthesis, cytoskeleton and microtubule transport and ser/tre kinase activity, all processes related to LPS response (table 7, on the left). TSS-proximal H2A.Z-Pu.1 peaks are mainly related to protein folding, rRNA and tRNA processing and export from the nucleus (table 7, right part), according to new protein synthesis after stimulus .

4h LPS TSS-distal	TSS-proximal
DNA methylation or demethylation	ncRNA processing
microtubule-based transport	protein folding
cytoskeleton-dependent intracellular transport	rRNA processing
cellular response to reactive oxygen species	nuclear export
positive regulation of CD4-positive, alpha-beta T cell activation	tRNA processing
positive regulation of CD4-positive, alpha-beta T cell differentiation	RNA export from nucleus
regulation of cyclin-dependent protein serine/threonine kinase activity	spindle organization
positive regulation of cytokine biosynthetic process	GPI anchor biosynthetic process
cAMP metabolic process	spindle assembly
cellular response to hydrogen peroxide	GPI anchor metabolic process

Table 7. Gene Ontology on H2A.Z-Pu.1 overlapping peaks in macrophages after 4 hours of LPS. Best 10 GREAT results for GO biological processes are represented for H2A.Z and Pu.1 common peaks in LPS-treated macrophages, divided in TSS-distal (>2500 bp from TSS) and proximal ones (+/- 2500 bp from TSS).

We then analyzed peaks induced and repressed after 4h LPS treatment. A total of 3,986 repressed and 2,304 induced peaks was identified at MACS score>100. At 4h of LPS treatment, 630 of total 2,304 H2A.Z induced peaks overlap with Pu.1 genomic sites, of which 478 (75.9%) co-localize with Pu.1 TSS-distal peaks and 152 (24.1%) with proximal ones. 2,344 of total 3,986 repressed genes overlap with Pu.1 peaks, of which 86.2% (2021) overlap with TSS-distal Pu.1 peaks and 323 (13.8%) with TSS-proximal ones. A gene ontology on H2A.Z-Pu.1 overlapping peaks was performed. For LPS-induced peaks no statistically significant results were obtained. For LPS-repressed peaks, GO biological processes revealed that TSS-distal peaks are related mainly to response to bacteria, cell activation and citochine production (table 8, left side). TSS-proximal peaks are mainly related to immune response (table 8, right side).

4h LPS repressed peaks	
TSS-distal	TSS-proximal
response to other organism	immune response
regulation of cytokine production	defense response
immune response	immune system process
response to biotic stimulus	innate immune response
leukocyte activation	response to other organism
cell activation	response to biotic stimulus
immune effector process	immune effector process
response to molecule of bacterial origin	defense response to virus
response to bacterium	regulation of immune response
lymphocyte activation	multi-organism process

Table 8. Gene Ontology on repressed H2A.Z peaks overlapping with Pu.1 in macrophages after 4 hours of LPS. Best 10 GREAT results for GO biological processes are represented for H2A.Z-repressed, Pu.1 overlapping peaks in 4h LPS-treated macrophages, divided in TSS-distal (>2500 bp from TSS) and proximal ones (+/- 2500 bp from TSS).

In basal conditions and after 4h LPS, distal peaks are associated with tissue/macrophage specific functions and proximal peaks are mostly associated to housekeeping functions (e.g. RNA processing). 4h-LPS repressed peaks are mainly associated to inflammatory response activation.

3.4) H2A.Z depletion

The obtained results suggest a specific role of H2A.Z at macrophage regulatory regions in basal conditions and after LPS stimulus. To understand the impact of H2A.Z on regulatory regions function, we depleted it in mouse macrophages. We first generated a retroviral vector for an shRNA targeting H2A.Z. A vector containing a scrambled shRNA was used as a control (empty vector). Bone marrow-derived cells (that proliferate and differentiate in macrophages in M-CSF-containing medium) were infected at day 1 and 2 after plating, selected in puromycin and then collected at day 7 after seeding to allow a complete differentiation of BMDMs. A ca. 75% depletion of H2A.Z protein was obtained in independent experiments (fig.18).

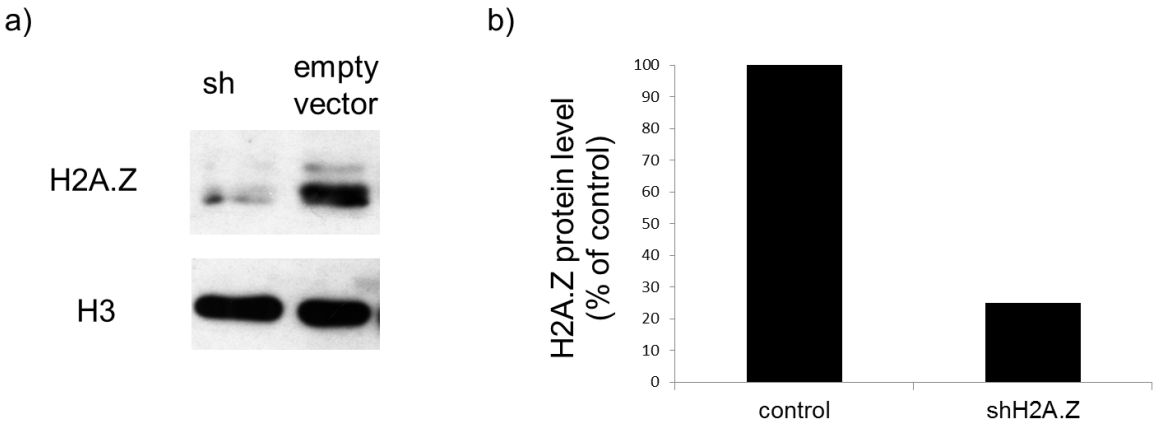

Fig. 18) Evaluation of H2A.Z depletion in retrovirally infected cells. Depletion of H2A.Z in macrophages using a retrovirus-encoded shRNA. Vector with scrambled shRNA (empty vector) used as a control. Protein levels measured by Western Blot (histone H3 was used as loading control) (a) and quantification of H2A.Z depletion (b) are shown.

We then performed a ChIP experiment to evaluate the decrease in H2A.Z chromatin binding in the shH2A.Z cells compared to control. We evaluate the binding of H2A.Z at selected targets and we found that H2A.Z binding is not affected in the shH2A.Z cells compared to the control (fig. 19). These results may indicate that an H2A.Z depletion of 75% is not enough to exert an impact on H2A.Z binding to DNA.

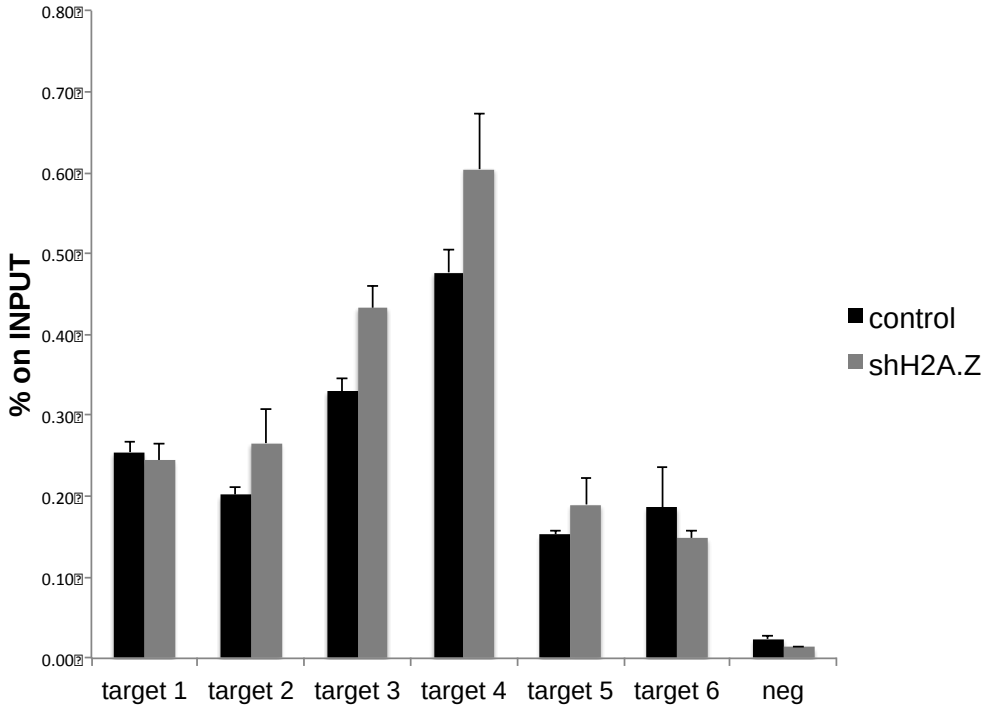

Fig. 19) Effects of H2A.Z depletion on binding to target regions. H2A.Z binding reduction measured by ChIP-qPCR on selected targets (neg=negative target) as % on input. Standard deviation is shown.

4) Techniques for mapping DNA accessibility

4.1) DNase hypersensitivity sites in macrophage genome

Generally, enhancer activation requires the presence of multiple TFs, including lineage-specific TFs (such as Pu.1) and sequence-dependent effectors of signaling pathways, ensuring integration of intrinsic and extrinsic environmental cues at these

elements. As mentioned above, occupancy of TFs at enhancers is associated with regions of nucleosomal depletion, exhibiting high sensitivity to DNA nucleases such as DNase I. Indeed, mapping DNase I hypersensitive sites has historically been a valuable tool for identifying all different types of regulatory elements, including promoters and enhancers (Boyle et al., 2008; Galas and Schmitz, 1978; Gross and Garrard, 1988; Hesselberth et al., 2009a; Sabo et al., 2006; Song and Crawford, 2010). More recently, DNase I hypersensitivity experiments at high sequencing depth have been adapted to obtain base-pair resolved TF footprints (Neph et al., 2012a, 2012b; Piper et al., 2014; Sherwood et al., 2014; Sung et al., 2014; Yardımcı et al., 2014). Indeed, the binding of sequence-specific TFs protects the underlying DNA from DNase cleavage, leaving footprints within the hypersensitive sites.

To characterize open chromatin sites corresponding to regulatory regions in macrophage genome and TFs that bind along with (or without) Pu.1 at regulatory elements, we performed a DNase I-seq experiment based on a mild DNase I digestion. According to the method used in (Neph et al., 2012a), we carefully select the concentration of DNase and time of digestion in order to have a very small portion of genomic DNA digested. We did the digestion with the selected limited concentration of DNAse I on intact nuclei. As shown in fig. 20a, after digestion almost all the genomic DNA was at high molecular weight (>10 Kb), with a little smear under the major high molecular weight band. After a sucrose gradient centrifugation of the digested DNA to separate low form high molecular weight DNA, small DNase hypersensitivity fragments (<500 bp) were purified from agarose gel (fig. 20b). The recovered fragments were then sequenced at high sequencing depth.

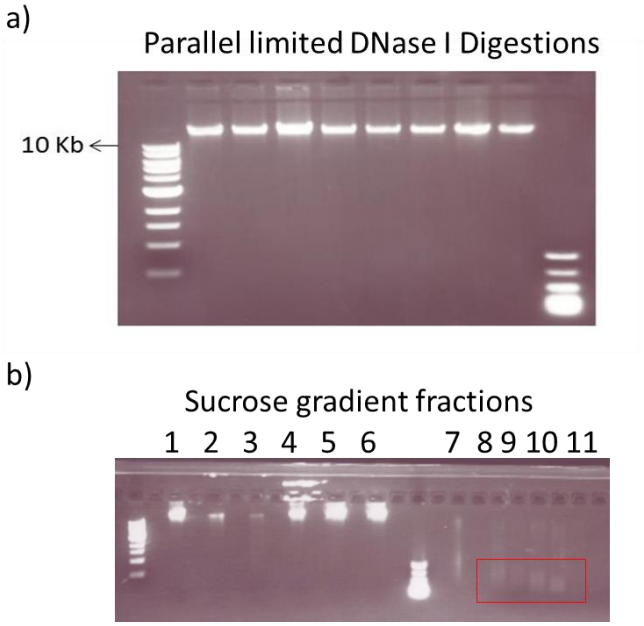

Fig. 20) DNase digestion of chromatin and separation of small DNase hypersensitivity fragments. Parallel limited DNase digestion were carried out on 1 x 10^7 intact nuclei each, 10 minutes at 37°C to obtain a limited digestion of genomic DNA (a). Fractions recovered after sucrose gradient are shown (b). Fractions from 8 to 11 contained small DNase hypersensitivity fragments (<500 bp) that were recovered from agarose gel and sent to sequencing.

Samples from BMDMs in basal conditions and treated with LPS (0.5, 2h and 4h) were obtained to study the dynamic changes in chromatin opening after inflammatory stimulus. After sequencing, we obtained respectively 411, 283, 237 and 259 millions of PCR filtered and uniquely aligned reads for the different samples. Using MACS (score>50) we identified respectively 158,176 DNase hypersensitivity regions in the untreated sample, 129,297 after 0.5 h of LPS treatment, and respectively 116,426 after 2h and 177,511 after 4h. Considering the regions differentially open in stimulated macrophages compared to untreated ones, LPS stimulus induced 4278 de novo DNase hypersensitivity regions after 30 minutes of treatment, 7,533 after 2h and 12,600 after 4h. A lower number of DNase hypersensitivity regions were repressed after LPS stimulus (1,432, 2,168 and 3,015 regions respectively after 30 minutes, 2 h and 4 h of LPS stimulus) (table 9).

# peaks	Untreated	0.5 h LPS	2h LPS	4h LPS
Total	158,176	129,297	116,426	177,511
Induced		4,278	7,533	12,600
Repressed		1,432	2,168	3,015

Table 9. Open chromatin regions identified by DNase-seq after LPS stimulus. Total number of DNase hypersensitivity regions (MACS score>50) in UT, 0.5 h, 2h and 4h LPS treated cells and induced and repressed peaks in LPS treated compared to untreated macrophages are shown.

After evaluating the power of different available TF footprint identification tools (Barozzi et al., 2014a), TF footprint identification trough Wellington (Piper et al., 2014) is ongoing in order to find TFs binding to macrophage regulatory regions alone or in combination with Pu.1 in basal conditions and after inflammatory stimulus.

4.2) Set up of other DNA accessibility techniques

In order to develop cheaper and easier techniques to investigate DNA accessibility we set up FAIRE (Formaldehyde Assisted Isolation of Regulatory Elements)-seq and ATAC (Assay for Transposase-Accessible Chromatin)-seq on macrophages in basal conditions and after inflammatory stimulus.

FAIRE is a simple procedure for genome-wide isolation of nucleosome-depleted DNA from chromatin. It is based on formaldehyde fixation of chromatin and phase-separation of protein-free DNA. We performed a FAIRE experiment on BMDMs (protocol adapted from Giresi and Lieb, 2009), on formaldehyde-fixed cells. After cell lysis and chromatin sonication, we performed a phenol-chloroform extraction of the nucleosome-free DNA (Figure 21). The recovered DNA was sequenced by single-end sequencing with a 50 nt read length and a sequencing depth of 90M raw reads. As a first attempt aimed at identifying differences in DNA accessibility in each

condition versus a theoretical random distribution and among conditions, we used MACS (Zhang et al., 2008) with a high stringency (p-value <1e-10). Even though these are very preliminary analyses, we could already identify thousands of constitutively open regions, as well as hundreds of regions undergoing changes in accessibility after LPS treatment (fig. 22).

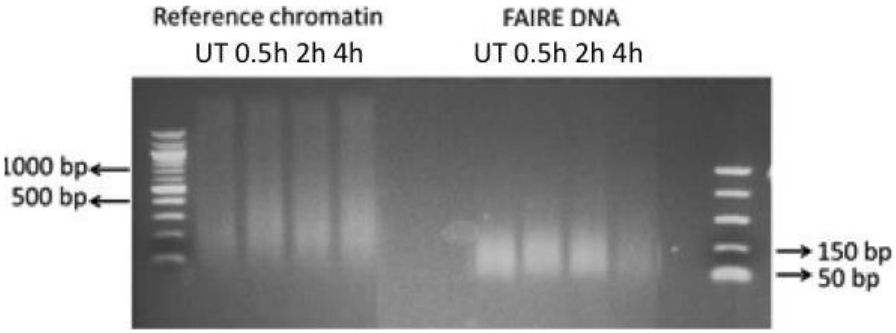

Fig. 21) Control of FAIRE DNA on agarose gel. FAIRE was performed on 15 millions of BMDMs untreated (UT) and treated 0.5h, 2h and 4h with LPS. Reference chromatin: chromatin after sonication (100 bp-1000 bp fragment size range); FAIRE DNA: nucleosome-free DNA fragments recovered after phenol-chloroform extraction (75-200 bp fragment size distribution).

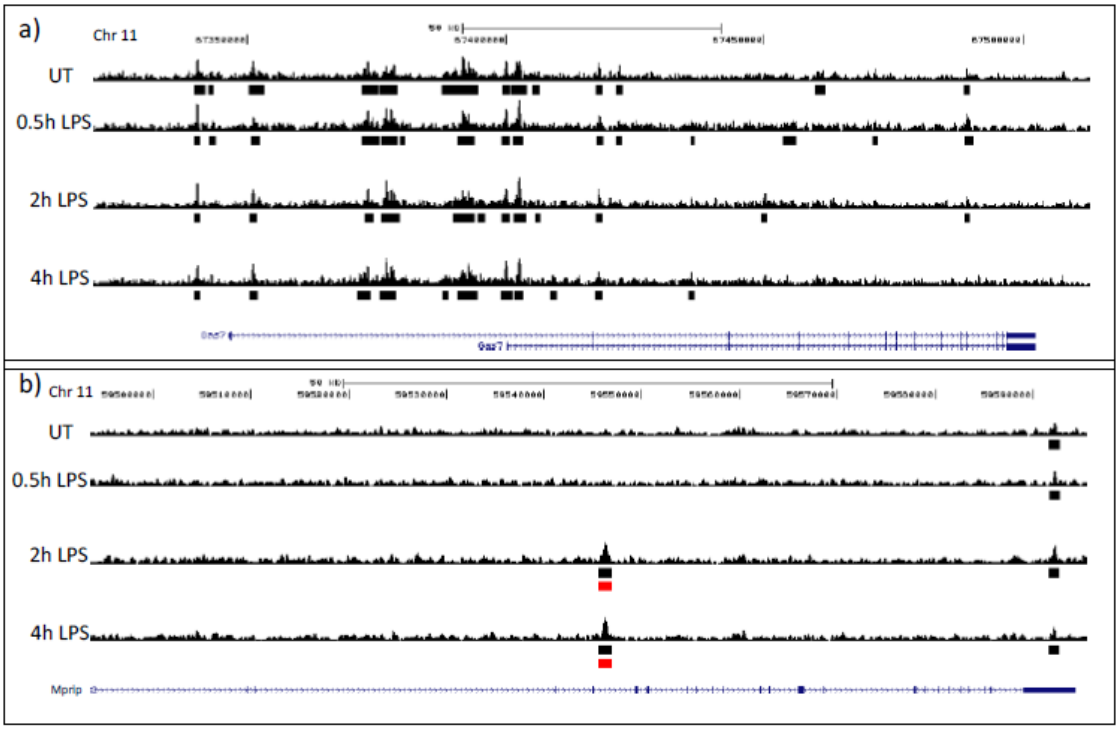

Fig. 22. Examples of a FAIRE constitutively open region (a) and a region undergoing changes in accessibility after LPS treatment (b). Representative snapshots of FAIRE-seq. Samples untreated and treated with LPS are indicated. Black box: significant vs. random distribution, red box: significantly more accessible after LPS treatment.

ATAC-seq (Buenrostro et al., 2013 and 2015) is a very powerful technique to investigate open chromatin sites with a very low amount of cells. It is based on direct in vitro insertion of sequencing adapters into accessible regions of chromatin by Tn5 transposase. We performed ATAC-seq on BMDMs in basal conditions and after inflammatory stimulus. After cell lysis, tagmentation reaction with Tn5 transposase was performed on 50,000 cells. DNA library was obtained from tagmented fragments using Nextera kit (Illumina) and it was sequenced on Hiseq 2000 for an average of 20 million reads per sample. We obtained good data and bioinformatics analyses are ongoing. ATAC-seq peaks are highly overlapping with open chromatin regions found by DNAse-seq (fig, 23).

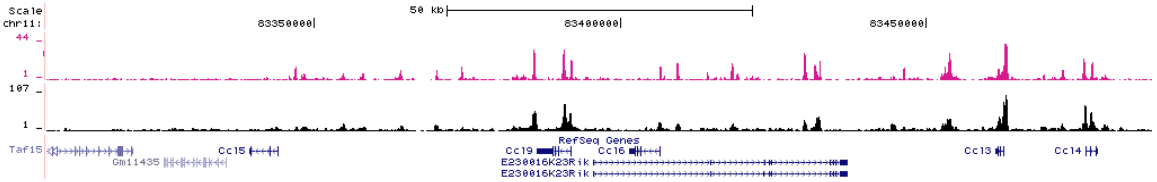

Fig.23. Comparison between ATAC-seq and DNAse-seq. Representative snapshot of ATAC-seq (pink) and DNAse.seq (black) peaks in macrophages in basal conditions are shown.

DISCUSSION

1) Nucleosome organization at regulatory regions

Our findings on nucleosome organization at macrophage enhancers allowed us to clarify the interplay between nucleosome occlusion of regulatory DNA sequences and TF binding. In particular, we demonstrated that the lineage-determining TF Pu.1 is necessary to maintain a NDR at bound sites in macrophages that tends to be reincorporated into nucleosomes upon its depletion. Moreover, the NDR corresponding to Pu.1-bound sites is absent in cells that do not express Pu.1. Notably, high nucleosome occupancy at regulatory regions is overcomed by Pu.1 in macrophages, the specific cell type in which the activity of the enhancers is required to drive their gene expression program. This could suggest that high nucleosome occupancy in unrelated cell types may prevent the binding of TFs to macrophage-specific regulatory regions and the unscheduled activation of macrophage genes. Indeed, we demonstrated through a computational model that a minimal set of DNA sequence and shape features accurately predicted both Pu.1 binding and nucleosome occupancy genome-wide in unrelated cell types (Barozzi et al., 2014b). This finding implies that the same evolutionary forces that act to maintain the functionality of TF binding sites jointly control nucleosome deposition, thus preserving the gatekeeper function of nucleosomes during the evolution of regulatory DNA.

All the study was performed in macrophages in basal conditions. It would be interesting to investigate the changes in nucleosome positioning and occupancy after LPS stimulus at regulated genes and the role of Pu.1 in orchestrating nucleosome changes. Even though we reached an unprecedented sequencing

depth for a nucleosomal pattern in a single cell type, the number of fragments describing each nucleosome in the population is too low to define nucleosome positions with high confidence at regulatory regions of specific genes whose transcription is perturbed after LPS stimulation. To this regard, MNase-ChIP technique (already set up in the laboratory) can be used to obtain a higher resolution. Briefly, after the digestion of chromatin with MNase, a ChIP on markers of regulatory regions (e.g. H3K4me1, H3K4me3 or H3K27ac normalized on total H3) is performed and sequenced, allowing to obtain resolution at single nucleosomes with low sequencing depth. As a second strategy, target enrichment (TE) can be utilized. Target enrichment is commonly used in next generation sequencing (NGS) workflows to eliminate genomic DNA regions that are not of interest for a particular experiment. By only targeting specific regions, one can obtain greater depth of DNA sequencing coverage for regions of interest. Considering the high range of G+C that must be covered and the extensive overlap with repetitive elements (Tewhey et al., 2009) standard TE strategies will be inappropriate. Instead, locus-specific enrichment of mononucleosomal DNA using hybridization to BACs could be used. BAC-based enrichment increases the coverage up to 500 fold, compared to previous genome-wide sequencing efforts (Yigit et al., 2013).

2) Functions of chromatin remodelers at regulatory regions

Data previously obtained in the laboratory identified Brg1, Brm and Chd4 as the most expressed ATPase subunits of chromatin remodeler complexes in BMDMs. The finding that they were found as top scoring proteins interacting with Pu.1 underlies their role in defining macrophage nucleosome landscape. Our results confirmed that Brg1 strongly co-localizes with Pu.1 on macrophage genome, in particular at distal Pu.1-bound regulatory regions. Brg1 and Chd4 also co-localize on genomic regions suggesting cooperative functions. Our results are in accordance with a previous study (Morris et al., 2013) performed in a mouse mammary epithelial cell line in which they found an overlap of 76% of Chd4 sites with Brg1. In their study, Brg1 overlap with Chd4 is higher than what we found (74% versus 58%), suggesting unique specific functions of Brg1 in mouse macrophages. Conversely, another study performed in Drosophila (Moshkin et al., 2012) came to diametrically different conclusions, as distinct remodelers were found to have non-overlapping genome-wide distributions. This could be due to differences in chromatin remodeler functions in insect versus mammalian cells.

An interesting issue that needs to be addressed is to understand the distinct roles of Brg1 and Brm, the two ATPase subunits of the SWI/SNF complex, almost 75% identical to each other, whose specific functions in macrophages are not yet elucidated. Another key experiment that needs to be done to clarify the division of labor among the different chromatin remodelers is to deplete each of them and to evaluate their impact on chromatin organization and transcription. Interestingly, Chd4 and Brg1 total RNA was induced after LPS stimulus, suggesting a dynamic role in response to inflammatory stimulus that needs to be further investigated. Notably, previous studies demonstrated that Brg.1 regulates gene expression

programs in response to interferon stimulation (Cui et al., 2004; Liu et al., 2002) and Toll-like receptor signaling pathways (Lai et al., 2009; Ramirez-Carrozzi et al., 2009).

In particular, Ramirez-Carrozzi et al. performed Brg1/Brm knock-down in murine macrophages followed by stimulation with LPS through Toll-like receptor 4 (TLR4) that revealed that only a subset of TLR4-induced genes require SWI/SNF complexes for activation. Almost all secondary response genes (i.e., genes requiring new protein synthesis for activation) exhibited strong SWI/SNF dependence, whereas primary response genes (i.e., genes activated in the absence of new protein synthesis) could be divided into SWI/SNF-dependent and independent classes. Notably, in a previous study it was demonstrated that Chd4 (Mi-2beta) was selectively recruited in macrophages after LPS stimulus along with the SWI/SNF complexes to the control regions of secondary response and delayed primary response genes, acting antagonistically to limit the induction of these gene classes (Ramirez-Carrozzi et al., 2006).

Finally, a crucial aspect that is important to elucidate is the direct role of Pu.1 in recruiting the chromatin remodelers, through the evaluation of their binding to Pu.1-bound sites in Pu.1-depleted macrophages.

3) Role of H2A.Z histone variant at regulatory regions

H2A.Z role in regulating transcription is controversial. Our results indicate that it is associated with regulatory regions in macrophages and strongly co-localize with Pu.1 (75% of overlap at bound genomic regions). We also demonstrated that H2A.Z binding to genomic regions is regulated by LPS treatment, suggesting a dynamic role in regulating gene expression after inflammatory stimulus. We obtained a good depletion of H2A.Z (75%) with a retroviral vector, but this had no effect on its binding on selected targets. To exclude that the unseen effect is due to the fact that only a small fraction of H2A.Z is incorporated in chromatin, we performed a preliminary western blot on cytoplasmic, nucleoplasmic and chromatin fractions that confirmed that H2A.Z is all associated to chromatin (data not shown). However, it would be possible that the residual H2A.Z level is sufficient to exert its functions. To bypass the variability and difficulty to obtain high level of protein knockdown in BMDMs, we could use the CRISPR/Cas9 tecnhology (Ran et al., 2013) to obtain the complete H2A.Z knockout in macrophage cell lines (e.g. RAW cells). However, results in cell lines might not fully recapitulate the depletion effects obtained in primary cells. To this regard, a valuable tool now available in our laboratory is a Cre-dependent Cas9 knockin mouse (Platt et al., 2014) that could allow to obtain gene knock-out directly in BMDMs, through the ex vivo delivery of guideRNAs on bulk population. Using this tool, we could have a full H2A:Z knock-out, not reachable with retroviral infection.

4) DNase hypersensitivity sites

The identification of DNase hypersensitivity regions in basal conditions and after inflammatory stimulus could allow us to study dynamic changes in DNA accessibility. A major issue of this technique is the number of cells (10×10^7) to obtain sufficient quantity of DNase hypersensitivity fragments to be sequenced, due to the loss of material in the laborious steps of sucrose gradient fractionation and recovery of fragments from agarose gel. We tried to optimize the protocol using Ampure Beads (Agencourt) instead of sucrose gradient to separate small digested fragments, but we obtained a higher background. To study open chromatin sites, we also performed FAIRE-seq (Giresi and Lieb, 2009). FAIRE-seq is based on formaldehyde fixation of chromatin and phase-separation of protein-free DNA. Compared to DNAse-seq, FAIRE is a simpler technique and allows the recovery of a higher amount of DNA starting with a smaller number of cells, but it also leads to higher background and has a bias in identifying promoters of active genes (Song et al., 2011c). Recently we set up ATAC-seq (Buenrostro et al., 2013) as an alternative technique to DNAse-seq. ATAC-seq has the advantage to capture open chromatin sites using a simple two-step protocol with 500–50,000 cells. It was also demonstrated that ATAC-seq allows the detection of TF footprints and individual nucleosomes at nucleotide resolution (Buenrostro et al., 2013; Schep et al., 2015).

We performed DNase-seq at high sequencing depth to identify footprints of TFs cooperating with Pu.1 in defining the macrophage accessible regulatory landscape (Hesselberth et al., 2009b; Neph et al., 2012a). After evaluating the power of different available TF footprint identification tools (Barozzi et al., 2014a), TF footprint identification trough Wellington (Piper et al., 2014) is ongoing. Through TF footprints, we potentially could identify the binding of hundreds of different TFs to

their genomic motifs from a single DNase-seq experiment. In this way, we could elucidate regulatory circuits and partner TFs cooperating with Pu.1 in defining macrophage-specific gene expression program. In particular we will be able to identify partner TFs binding with Pu.1 at regulatory regions and TF that binds Pu.1 negative regions important for gene regulation in BMDMs. It will be also interesting to elucidate the changings in recruiting TF at regulatory regions after LPS treatment.

ACKNOWLEDGMENTS

First of all, I would like to thank my boss GIoacchino Natoli, because he gave me the great opportunity to be enrolled in the SEMM PhD program and to carry on this interesting PhD project.

I would like also to acknowledge my internal advisor Saverio Minucci and my external advisor Jean Christophe Andrau for useful discussion about the project.

I would like also to thank all the GN members, in particular Serena for supervising me in these years and Iros, Marta, Chiara and Alberto who shared with me some parts of the project. A special thank goes to all the other researchers who helped me with everyday problem solving and experimental set up and to IEO Genomic Unit, kitchen and administrative staff.

Finally, I am really grateful to my friends and family that supported me during these years.

BIBLIOGRAPHY

latwi, H.E., and Downs, J.A. (2015). Removal of H2A.Z by INO80 promotes homologous recombination. EMBO Rep. *16*, 986–994.

Albert, I., Mavrich, T.N., Tomsho, L.P., Qi, J., Zanton, S.J., Schuster, S.C., and Pugh, B.F. (2007). Translational and rotational settings of H2A.Z nucleosomes across the Saccharomyces cerevisiae genome. Nature *446*, 572–576.

Albig, W., and Doenecke, D. (1997). The human histone gene cluster at the D6S105 locus. Hum. Genet. *101*, 284–294.

Andersson, R., Gebhard, C., Miguel-Escalada, I., Hoof, I., Bornholdt, J., Boyd, M., Chen, Y., Zhao, X., Schmidl, C., Suzuki, T., et al. (2014). An atlas of active enhancers across human cell types and tissues. Nature *507*, 455–461.

van Attikum, H., Fritsch, O., Hohn, B., and Gasser, S.M. (2004). Recruitment of the INO80 complex by H2A phosphorylation links ATP-dependent chromatin remodeling with DNA double-strand break repair. Cell *119*, 777–788.

van Attikum, H., Fritsch, O., and Gasser, S.M. (2007). Distinct roles for SWR1 and INO80 chromatin remodeling complexes at chromosomal double-strand breaks. EMBO J. *26*, 4113–4125.

Bakri, Y., Sarrazin, S., Mayer, U.P., Tillmanns, S., Nerlov, C., Boned, A., and Sieweke, M.H. (2005). Balance of MafB and PU.1 specifies alternative macrophage or dendritic cell fate. Blood *105*, 2707–2716.

Ball, D.J., Slaughter, C.A., Hensley, P., and Garrard, W.T. (1983). Amino acid sequence of the N-terminal domain of calf thymus histone H2A.Z. FEBS Lett. *154*, 166–170.

Banerji, J., Rusconi, S., and Schaffner, W. (1981). Expression of a β-globin gene is enhanced by remote SV40 DNA sequences. Cell *27*, 299–308.

Bao, Y., and Shen, X. (2007). INO80 subfamily of chromatin remodeling complexes. Mutat. Res. Mol. Mech. Mutagen. *618*, 18–29.

Barozzi, I., Bora, P., and Morelli, M.J. (2014a). Comparative evaluation of DNase-seq footprint identification strategies. Front. Genet. *5*, 278.

Barozzi, I., Simonatto, M., Bonifacio, S., Yang, L., Rohs, R., Ghisletti, S., and Natoli, G. (2014b). Coregulation of Transcription Factor Binding and Nucleosome Occupancy through DNA Features of Mammalian Enhancers. Mol. Cell.

Barski, A., Cuddapah, S., Cui, K., Roh, T.-Y., Schones, D.E., Wang, Z., Wei, G., Chepelev, I., and Zhao, K. (2007). High-resolution profiling of histone methylations in the human genome. Cell *129*, 823–837.

Bartholomew, B. (2014). Regulating the chromatin landscape: structural and

mechanistic perspectives. Annu. Rev. Biochem. *83*, 671–696.

Bhatt, D.M., Pandya-Jones, A., Tong, A.-J., Barozzi, I., Lissner, M.M., Natoli, G., Black, D.L., and Smale, S.T. (2012). Transcript dynamics of proinflammatory genes revealed by sequence analysis of subcellular RNA fractions. Cell *150*, 279–290.

Binda, O., Sevilla, A., LeRoy, G., Lemischka, I.R., Garcia, B.A., and Richard, S. (2013). SETD6 monomethylates H2AZ on lysine 7 and is required for the maintenance of embryonic stem cell self-renewal. Epigenetics *8*, 177–183.

Blosser, T.R., Yang, J.G., Stone, M.D., Narlikar, G.J., and Zhuang, X. (2009). Dynamics of nucleosome remodelling by individual ACF complexes. Nature *462*, 1022–1027.

Boyle, A.P., Davis, S., Shulha, H.P., Meltzer, P., Margulies, E.H., Weng, Z., Furey, T.S., and Crawford, G.E. (2008). High-resolution mapping and characterization of open chromatin across the genome. Cell *132*, 311–322.

Brunelle, M., Nordell Markovits, A., Rodrigue, S., Lupien, M., Jacques, P.-É., and Gévry, N. (2015). The histone variant H2A.Z is an important regulator of enhancer activity. Nucleic Acids Res. gkv825 – .

Buchanan, L., Durand-Dubief, M., Roguev, A., Sakalar, C., Wilhelm, B., Strålfors, A., Shevchenko, A., Aasland, R., Shevchenko, A., Ekwall, K., et al. (2009). The Schizosaccharomyces pombe JmjC-protein, Msc1, prevents H2A.Z localization in centromeric and subtelomeric chromatin domains. PLoS Genet. *5*, e1000726.

Buenrostro, J.D., Giresi, P.G., Zaba, L.C., Chang, H.Y., and Greenleaf, W.J. (2013). Transposition of native chromatin for fast and sensitive epigenomic profiling of open chromatin, DNA-binding proteins and nucleosome position. Nat. Methods *10*, 1213–1218.

Cairns, B.R., Lorch, Y., Li, Y., Zhang, M., Lacomis, L., Erdjument-Bromage, H., Tempst, P., Du, J., Laurent, B., and Kornberg, R.D. (1996). RSC, an Essential, Abundant Chromatin-Remodeling Complex. Cell *87*, 1249–1260.

Calo, E., and Wysocka, J. (2013a). Modification of Enhancer Chromatin: What, How, and Why? Mol. Cell *49*, 825–837.

Calo, E., and Wysocka, J. (2013b). Modification of enhancer chromatin: what, how, and why? Mol. Cell *49*, 825–837.

Carotta, S., Dakic, A., D'Amico, A., Pang, S.H.M., Greig, K.T., Nutt, S.L., and Wu, L. (2010). The transcription factor PU.1 controls dendritic cell development and Flt3 cytokine receptor expression in a dose-dependent manner. Immunity *32*, 628–641.

Carr, A.M., Dorrington, S.M., Hindley, J., Phear, G.A., Aves, S.J., and Nurse, P. (1994). Analysis of a histone H2A variant from fission yeast: evidence for a role in chromosome stability. Mol. Gen. Genet. *245*, 628–635.

Chen, P., Zhao, J., Wang, Y., Wang, M., Long, H., Liang, D., Huang, L., Wen, Z., Li, W., Li, X., et al. (2013). H3.3 actively marks enhancers and primes gene

transcription via opening higher-ordered chromatin. Genes Dev. *27*, 2109–2124.

Chi, T.H., Wan, M., Zhao, K., Taniuchi, I., Chen, L., Littman, D.R., and Crabtree, G.R. (2002). Reciprocal regulation of CD4/CD8 expression by SWI/SNF-like BAF complexes. Nature *418*, 195–199.

Clapier, C.R., and Cairns, B.R. (2009a). The biology of chromatin remodeling complexes. Annu. Rev. Biochem. *78*, 273–304.

Clapier, C.R., and Cairns, B.R. (2009b). The biology of chromatin remodeling complexes. Annu. Rev. Biochem. *78*, 273–304.

Coleman-Derr, D., and Zilberman, D. (2012). Deposition of Histone Variant H2A.Z within Gene Bodies Regulates Responsive Genes. PLoS Genet. *8*, e1002988.

Conerly, M.L., Teves, S.S., Diolaiti, D., Ulrich, M., Eisenman, R.N., and Henikoff, S. (2010). Changes in H2A.Z occupancy and DNA methylation during B-cell lymphomagenesis. Genome Res. *20*, 1383–1390.

Creyghton, M.P., Markoulaki, S., Levine, S.S., Hanna, J., Lodato, M.A., Sha, K., Young, R.A., Jaenisch, R., and Boyer, L.A. (2008a). H2AZ is enriched at polycomb complex target genes in ES cells and is necessary for lineage commitment. Cell *135*, 649–661.

Creyghton, M.P., Markoulaki, S., Levine, S.S., Hanna, J., Lodato, M.A., Sha, K., Young, R.A., Jaenisch, R., and Boyer, L.A. (2008b). H2AZ is enriched at polycomb complex target genes in ES cells and is necessary for lineage commitment. Cell *135*, 649–661.

Creyghton, M.P., Cheng, A.W., Welstead, G.G., Kooistra, T., Carey, B.W., Steine, E.J., Hanna, J., Lodato, M.A., Frampton, G.M., Sharp, P.A., et al. (2010). Histone H3K27ac separates active from poised enhancers and predicts developmental state. Proc. Natl. Acad. Sci. U. S. A. *107*, 21931–21936.

Cubeñas-Potts, C., and Corces, V.G. (2015). Architectural proteins, transcription, and the three-dimensional organization of the genome. FEBS Lett.

Cui, K., Tailor, P., Liu, H., Chen, X., Ozato, K., and Zhao, K. (2004). The chromatin-remodeling BAF complex mediates cellular antiviral activities by promoter priming. Mol. Cell. Biol. *24*, 4476–4486.

Cui, K., Zang, C., Roh, T.-Y., Schones, D.E., Childs, R.W., Peng, W., and Zhao, K. (2009). Chromatin signatures in multipotent human hematopoietic stem cells indicate the fate of bivalent genes during differentiation. Cell Stem Cell *4*, 80–93.

van Daal, A., and Elgin, S.C. (1992). A histone variant, H2AvD, is essential in Drosophila melanogaster. Mol. Biol. Cell *3*, 593–602.

Dahl, R., Walsh, J.C., Lancki, D., Laslo, P., Iyer, S.R., Singh, H., and Simon, M.C. (2003). Regulation of macrophage and neutrophil cell fates by the PU.1:C/EBPalpha ratio and granulocyte colony-stimulating factor. Nat. Immunol. *4*, 1029–1036.

Deaton, a. M., and Bird, a. (2011). CpG islands and the regulation of transcription. Genes Dev. *25*, 1010–1022.

Deindl, S., Hwang, W.L., Hota, S.K., Blosser, T.R., Prasad, P., Bartholomew, B., and Zhuang, X. (2013). ISWI remodelers slide nucleosomes with coordinated multi-base-pair entry steps and single-base-pair exit steps. Cell *152*, 442–452.

DeKoter, R.P. (2000). Regulation of B Lymphocyte and Macrophage Development by Graded Expression of PU.1. Science (80-.). *288*, 1439–1441.

Dickins, R. a, Hemann, M.T., Zilfou, J.T., Simpson, D.R., Ibarra, I., Hannon, G.J., and Lowe, S.W. (2005). Probing tumor phenotypes using stable and regulated synthetic microRNA precursors. Nat. Genet. *37*, 1289–1295.

Ehrenhofer-Murray, A.E. (2004). Chromatin dynamics at DNA replication, transcription and repair. Eur. J. Biochem. *271*, 2335–2349.

Ernst, J., Kheradpour, P., Mikkelsen, T.S., Shoresh, N., Ward, L.D., Epstein, C.B., Zhang, X., Wang, L., Issner, R., Coyne, M., et al. (2011). Mapping and analysis of chromatin state dynamics in nine human cell types. Nature *473*, 43–49.

Escoubet-Lozach, L., Benner, C., Kaikkonen, M.U., Lozach, J., Heinz, S., Spann, N.J., Crotti, A., Stender, J., Ghisletti, S., Reichart, D., et al. (2011). Mechanisms establishing TLR4-responsive activation states of inflammatory response genes. PLoS Genet. *7*, e1002401.

Faast, R., Thonglairoam, V., Schulz, T.C., Beall, J., Wells, J.R., Taylor, H., Matthaei, K., Rathjen, P.D., Tremethick, D.J., and Lyons, I. (2001). Histone variant H2A.Z is required for early mammalian development. Curr. Biol. *11*, 1183–1187.

Fan, J.Y., Rangasamy, D., Luger, K., and Tremethick, D.J. (2004). H2A.Z alters the nucleosome surface to promote HP1alpha-mediated chromatin fiber folding. Mol. Cell *16*, 655–661.

Farris, S.D. (2005). Transcription-induced Chromatin Remodeling at the c-myc Gene Involves the Local Exchange of Histone H2A.Z. J. Biol. Chem. *280*, 25298–25303.

Fenouil, R., Cauchy, P., Koch, F., Descostes, N., Cabeza, J.Z., Innocenti, C., Ferrier, P., Spicuglia, S., Gut, M., Gut, I., et al. (2012). CpG islands and GC content dictate nucleosome depletion in a transcription-independent manner at mammalian promoters. Genome Res. *22*, 2399–2408.

Flaus, A., and Owen-Hughes, T. (2001). Mechanisms for ATP-dependent chromatin remodelling. Curr. Opin. Genet. Dev. *11*, 148–154.

Flicek, P., Amode, M.R., Barrell, D., Beal, K., Brent, S., Carvalho-Silva, D., Clapham, P., Coates, G., Fairley, S., Fitzgerald, S., et al. (2012). Ensembl 2012. Nucleic Acids Res. *40*, D84–D90.

Fritsch, O., Benvenuto, G., Bowler, C., Molinier, J., and Hohn, B. (2004). The INO80 protein controls homologous recombination in Arabidopsis thaliana. Mol. Cell *16*,

479–485.

Galas, D.J., and Schmitz, A. (1978). DNAse footprinting: a simple method for the detection of protein-DNA binding specificity. Nucleic Acids Res. *5*, 3157–3170.

Gangaraju, V.K., and Bartholomew, B. (2007). Dependency of ISW1a Chromatin Remodeling on Extranucleosomal DNA. Mol. Cell. Biol. *27*, 3217–3225.

Gerhold, C.B., and Gasser, S.M. (2014). INO80 and SWR complexes: relating structure to function in chromatin remodeling. Trends Cell Biol. *24*, 619–631.

Gerhold, C.-B., Hauer, M.H., and Gasser, S.M. (2015). INO80-C and SWR-C: guardians of the genome. J. Mol. Biol. *427*, 637–651.

Ghisletti, S., and Natoli, G. (2013). Deciphering cis-regulatory control in inflammatory cells. Philos. Trans. R. Soc. Lond. B. Biol. Sci. *368*, 20120370.

Ghisletti, S., Barozzi, I., Mietton, F., Polletti, S., De Santa, F., Venturini, E., Gregory, L., Lonie, L., Chew, A., Wei, C.-L., et al. (2010). Identification and characterization of enhancers controlling the inflammatory gene expression program in macrophages. Immunity *32*, 317–328.

Gilchrist, D. a, Dos Santos, G., Fargo, D.C., Xie, B., Gao, Y., Li, L., and Adelman, K. (2010). Pausing of RNA polymerase II disrupts DNA-specified nucleosome organization to enable precise gene regulation. Cell *143*, 540–551.

Giresi, P.G., and Lieb, J.D. (2009). Isolation of active regulatory elements from eukaryotic chromatin using FAIRE (Formaldehyde Assisted Isolation of Regulatory Elements). Methods *48*, 233–239.

Gkikopoulos, T., Schofield, P., Singh, V., Pinskaya, M., Mellor, J., Smolle, M., Workman, J.L., Barton, G.J., and Owen-Hughes, T. (2011a). A role for Snf2-related nucleosome-spacing enzymes in genome-wide nucleosome organization. Science *333*, 1758–1760.

Gkikopoulos, T., Schofield, P., Singh, V., Pinskaya, M., Mellor, J., Smolle, M., Workman, J.L., Barton, G.J., and Owen-Hughes, T. (2011b). A role for Snf2-related nucleosome-spacing enzymes in genome-wide nucleosome organization. Science *333*, 1758–1760.

Gosselin, D., Link, V.M., Romanoski, C.E., Fonseca, G.J., Eichenfield, D.Z., Spann, N.J., Stender, J.D., Chun, H.B., Garner, H., Geissmann, F., et al. (2014). Environment Drives Selection and Function of Enhancers Controlling Tissue-Specific Macrophage Identities. Cell *159*, 1327–1340.

Greaves, I.K., Rangasamy, D., Ridgway, P., and Tremethick, D.J. (2006). H2A.Z contributes to the unique 3D structure of the centromere. Proc. Natl. Acad. Sci. *104*, 525–530.

Gross, D.S., and Garrard, W.T. (1988). Nuclease hypersensitive sites in chromatin. Annu. Rev. Biochem. *57*, 159–197.

Grüne, T., Brzeski, J., Eberharter, A., Clapier, C.R., Corona, D.F. V, Becker, P.B., and Müller, C.W. (2003). Crystal structure and functional analysis of a nucleosome recognition module of the remodeling factor ISWI. Mol. Cell *12*, 449–460.

Guillemette, B., Bataille, A.R., Gévry, N., Adam, M., Blanchette, M., Robert, F., and Gaudreau, L. (2005a). Variant Histone H2A.Z Is Globally Localized to the Promoters of Inactive Yeast Genes and Regulates Nucleosome Positioning. PLoS Biol. *3*, e384.

Guillemette, B., Bataille, A.R., Gévry, N., Adam, M., Blanchette, M., Robert, F., and Gaudreau, L. (2005b). Variant histone H2A.Z is globally localized to the promoters of inactive yeast genes and regulates nucleosome positioning. PLoS Biol. *3*, e384.

Hall, J.A., and Georgel, P.T. (2007). CHD proteins: a diverse family with strong ties. Biochem. Cell Biol. *85*, 463–476.

Hardy, S., Jacques, P.-E., Gévry, N., Forest, A., Fortin, M.-E., Laflamme, L., Gaudreau, L., and Robert, F. (2009). The euchromatic and heterochromatic landscapes are shaped by antagonizing effects of transcription on H2A.Z deposition. PLoS Genet. *5*, e1000687.

Hargreaves, D.C., and Crabtree, G.R. (2011). ATP-dependent chromatin remodeling: genetics, genomics and mechanisms. Cell Res. *21*, 396–420.

Hargreaves, D.C., Horng, T., and Medzhitov, R. (2009). Control of inducible gene expression by signal-dependent transcriptional elongation. Cell *138*, 129–145.

Hassan, A.H., Prochasson, P., Neely, K.E., Galasinski, S.C., Chandy, M., Carrozza, M.J., and Workman, J.L. (2002). Function and selectivity of bromodomains in anchoring chromatin-modifying complexes to promoter nucleosomes. Cell *111*, 369–379.

He, H.H., Meyer, C.A., Shin, H., Bailey, S.T., Wei, G., Wang, Q., Zhang, Y., Xu, K., Ni, M., Lupien, M., et al. (2010). Nucleosome dynamics define transcriptional enhancers. Nat. Genet. *42*, 343–347.

Heintzman, N.D., Stuart, R.K., Hon, G., Fu, Y., Ching, C.W., Hawkins, R.D., Barrera, L.O., Van Calcar, S., Qu, C., Ching, K.A., et al. (2007). Distinct and predictive chromatin signatures of transcriptional promoters and enhancers in the human genome. Nat. Genet. *39*, 311–318.

Heintzman, N.D., Hon, G.C., Hawkins, R.D., Kheradpour, P., Stark, A., Harp, L.F., Ye, Z., Lee, L.K., Stuart, R.K., Ching, C.W., et al. (2009). Histone modifications at human enhancers reflect global cell-type-specific gene expression. Nature *459*, 108–112.

Heinz, S., Benner, C., Spann, N., Bertolino, E., Lin, Y.C., Laslo, P., Cheng, J.X., Murre, C., Singh, H., and Glass, C.K. (2010a). Simple Combinations of Lineage-Determining Transcription Factors Prime cis-Regulatory Elements Required for Macrophage and B Cell Identities. Mol. Cell *38*, 576–589.

Heinz, S., Benner, C., Spann, N., Bertolino, E., Lin, Y.C., Laslo, P., Cheng, J.X., Murre, C., Singh, H., and Glass, C.K. (2010b). Simple combinations of lineage-determining transcription factors prime cis-regulatory elements required for macrophage and B cell identities. Mol. Cell *38*, 576–589.

Heinz, S., Romanoski, C.E., Benner, C., and Glass, C.K. (2015). The selection and function of cell type-specific enhancers. Nat. Rev. Mol. Cell Biol. *16*, 144–154.

Hennig, B.P., Bendrin, K., Zhou, Y., and Fischer, T. (2012). Chd1 chromatin remodelers maintain nucleosome organization and repress cryptic transcription. EMBO Rep. *13*, 997–1003.

Herschman, H.R. (1991). Primary response genes induced by growth factors and tumor promoters. Annu. Rev. Biochem. *60*, 281–319.

Hesselberth, J.R., Chen, X., Zhang, Z., Sabo, P.J., Sandstrom, R., Reynolds, A.P., Thurman, R.E., Neph, S., Kuehn, M.S., Noble, W.S., et al. (2009a). Global mapping of protein-DNA interactions in vivo by digital genomic footprinting. *6*, 283–289.

Hesselberth, J.R., Chen, X., Zhang, Z., Sabo, P.J., Sandstrom, R., Reynolds, A.P., Thurman, R.E., Neph, S., Kuehn, M.S., Noble, W.S., et al. (2009b). Global mapping of protein-DNA interactions in vivo by digital genomic footprinting. Nat. Methods *6*, 283–289.

Hnisz, D., Abraham, B.J., Lee, T.I., Lau, A., Saint-André, V., Sigova, A.A., Hoke, H.A., and Young, R.A. (2013). Super-enhancers in the control of cell identity and disease. Cell *155*, 934–947.

Ho, L., Jothi, R., Ronan, J.L., Cui, K., Zhao, K., and Crabtree, G.R. (2009). An embryonic stem cell chromatin remodeling complex, esBAF, is an essential component of the core pluripotency transcriptional network. Proc. Natl. Acad. Sci. U. S. A. *106*, 5187–5191.

Hopfner, K.-P., Gerhold, C.-B., Lakomek, K., and Wollmann, P. (2012). Swi2/Snf2 remodelers: hybrid views on hybrid molecular machines. Curr. Opin. Struct. Biol. *22*, 225–233.

Hu, G., Cui, K., Northrup, D., Liu, C., Wang, C., Tang, Q., Ge, K., Levens, D., Crane-Robinson, C., and Zhao, K. (2013a). H2A.Z facilitates access of active and repressive complexes to chromatin in embryonic stem cell self-renewal and differentiation. Cell Stem Cell *12*, 180–192.

Hu, G., Cui, K., Northrup, D., Liu, C., Wang, C., Tang, Q., Ge, K., Levens, D., Crane-Robinson, C., and Zhao, K. (2013b). H2A.Z facilitates access of active and repressive complexes to chromatin in embryonic stem cell self-renewal and differentiation. Cell Stem Cell *12*, 180–192.

Hughes, A.L., and Rando, O.J. (2015). Comparative Genomics Reveals Chd1 as a Determinant of Nucleosome Spacing in Vivo. G3 (Bethesda). *5*, 1889–1897.

Imbalzano, A.N., Kwon, H., Green, M.R., and Kingston, R.E. (1994). Facilitated

binding of TATA-binding protein to nucleosomal DNA. Nature *370*, 481–485.

Iouzalen, N. (1996). H2A.ZI, a new variant histone expressed during Xenopus early development exhibits several distinct features from the core histone H2A. Nucleic Acids Res. *24*, 3947–3952.

Iwasaki, H., Somoza, C., Shigematsu, H., Duprez, E.A., Iwasaki-Arai, J., Mizuno, S.-I., Arinobu, Y., Geary, K., Zhang, P., Dayaram, T., et al. (2005). Distinctive and indispensable roles of PU.1 in maintenance of hematopoietic stem cells and their differentiation. Blood *106*, 1590–1600.

Jackson, J.D., and Gorovsky, M.A. (2000). Histone H2A.Z has a conserved function that is distinct from that of the major H2A sequence variants. Nucleic Acids Res. *28*, 3811–3816.

Jiang, C., and Pugh, B.F. (2009). Nucleosome positioning and gene regulation: advances through genomics. Nat. Rev. Genet. *10*, 161–172.

Jin, C., and Felsenfeld, G. (2007). Nucleosome stability mediated by histone variants H3.3 and H2A.Z. Genes Dev. *21*, 1519–1529.

Jin, C., Zang, C., Wei, G., Cui, K., Peng, W., Zhao, K., and Felsenfeld, G. (2009). H3.3/H2A.Z double variant-containing nucleosomes mark “nucleosome-free regions” of active promoters and other regulatory regions. Nat. Genet. *41*, 941–945.

John, S., Sabo, P.J., Johnson, T.A., Sung, M.-H., Biddie, S.C., Lightman, S.L., Voss, T.C., Davis, S.R., Meltzer, P.S., Stamatoyannopoulos, J.A., et al. (2008). Interaction of the glucocorticoid receptor with the chromatin landscape. Mol. Cell *29*, 611–624.

Kalocsay, M., Hiller, N.J., and Jentsch, S. (2009). Chromosome-wide Rad51 spreading and SUMO-H2A.Z-dependent chromosome fixation in response to a persistent DNA double-strand break. Mol. Cell *33*, 335–343.

Kaplan, N., Moore, I.K., Fondufe-Mittendorf, Y., Gossett, A.J., Tillo, D., Field, Y., LeProust, E.M., Hughes, T.R., Lieb, J.D., Widom, J., et al. (2009). The DNA-encoded nucleosome organization of a eukaryotic genome. Nature *458*, 362–366.

Kim, T.-K., Hemberg, M., Gray, J.M., Costa, A.M., Bear, D.M., Wu, J., Harmin, D.A., Laptewicz, M., Barbara-Haley, K., Kuersten, S., et al. (2010). Widespread transcription at neuronal activity-regulated enhancers. Nature *465*, 182–187.

Kobor, M.S., Venkatasubrahmanyam, S., Meneghini, M.D., Gin, J.W., Jennings, J.L., Link, A.J., Madhani, H.D., and Rine, J. (2004). A protein complex containing the conserved Swi2/Snf2-related ATPase Swr1p deposits histone variant H2A.Z into euchromatin. PLoS Biol. *2*, E131.

Kornberg, R. (1981). The location of nucleosomes in chromatin: specific or statistical. Nature *292*, 579–580.

Ku, M., Jaffe, J.D., Koche, R.P., Rheinbay, E., Endoh, M., Koseki, H., Carr, S.A., and Bernstein, B.E. (2012a). H2A.Z landscapes and dual modifications in pluripotent and multipotent stem cells underlie complex genome regulatory functions. Genome

Biol. *13*, R85.

Ku, M., Jaffe, J.D., Koche, R.P., Rheinbay, E., Endoh, M., Koseki, H., Carr, S.A., and Bernstein, B.E. (2012b). H2A.Z landscapes and dual modifications in pluripotent and multipotent stem cells underlie complex genome regulatory functions. Genome Biol. *13*, R85.

Kumar, S.V., and Wigge, P.A. (2010). H2A.Z-containing nucleosomes mediate the thermosensory response in Arabidopsis. Cell *140*, 136–147.

Kundaje, A., Kyriazopoulou-Panagiotopoulou, S., Libbrecht, M., Smith, C.L., Raha, D., Winters, E.E., Johnson, S.M., Snyder, M., Batzoglou, S., and Sidow, A. (2012). Ubiquitous heterogeneity and asymmetry of the chromatin environment at regulatory elements. Genome Res. *22*, 1735–1747.

Kusch, T. (2004). Acetylation by Tip60 Is Required for Selective Histone Variant Exchange at DNA Lesions. Science (80-.). *306*, 2084–2087.

Kwon, H., Imbalzano, A.N., Khavari, P.A., Kingston, R.E., and Green, M.R. (1994). Nucleosome disruption and enhancement of activator binding by a human SW1/SNF complex. Nature *370*, 477–481.

de la Cruz, X., Lois, S., S�nchez-Molina, S., and Mart�nez-Balb�s, M.A. (2005). Do protein motifs read the histone code? BioEssays *27*, 164–175.

Lai, D., Wan, M., Wu, J., Preston-Hurlburt, P., Kushwaha, R., Grundström, T., Imbalzano, A.N., and Chi, T. (2009). Induction of TLR4-target genes entails calcium/calmodulin-dependent regulation of chromatin remodeling. Proc. Natl. Acad. Sci. U. S. A. *106*, 1169–1174.

Lam, M.T.Y., Cho, H., Lesch, H.P., Gosselin, D., Heinz, S., Tanaka-Oishi, Y., Benner, C., Kaikkonen, M.U., Kim, A.S., Kosaka, M., et al. (2013). Rev-Erbs repress macrophage gene expression by inhibiting enhancer-directed transcription. Nature *498*, 511–515.

Langmead, B., Trapnell, C., Pop, M., and Salzberg, S.L. (2009). Ultrafast and memory-efficient alignment of short DNA sequences to the human genome. Genome Biol. *10*, R25.

Lantermann, A.B., Straub, T., Strålfors, A., Yuan, G.-C., Ekwall, K., and Korber, P. (2010). Schizosaccharomyces pombe genome-wide nucleosome mapping reveals positioning mechanisms distinct from those of Saccharomyces cerevisiae. Nat. Struct. Mol. Biol. *17*, 251–257.

Lavin, Y., Winter, D., Blecher-Gonen, R., David, E., Keren-Shaul, H., Merad, M., Jung, S., and Amit, I. (2014). Tissue-Resident Macrophage Enhancer Landscapes Are Shaped by the Local Microenvironment. Cell *159*, 1312–1326.

Lawrence, T., and Natoli, G. (2011). Transcriptional regulation of macrophage polarization: enabling diversity with identity. Nat. Rev. Immunol. *11*, 750–761.

Leddin, M., Perrod, C., Hoogenkamp, M., Ghani, S., Assi, S., Heinz, S., Wilson,

N.K., Follows, G., Schönheit, J., Vockentanz, L., et al. (2011). Two distinct auto-regulatory loops operate at the PU.1 locus in B cells and myeloid cells. Blood *117*, 2827–2838.

Li, B., Pattenden, S.G., Lee, D., Gutierrez, J., Chen, J., Seidel, C., Gerton, J., and Workman, J.L. (2005). Preferential occupancy of histone variant H2AZ at inactive promoters influences local histone modifications and chromatin remodeling. Proc. Natl. Acad. Sci. *102*, 18385–18390.

Li, B., Carey, M., and Workman, J.L. (2007). The role of chromatin during transcription. Cell *128*, 707–719.

Li, W., Nagaraja, S., Delcuve, G.P., Hendzel, M.J., and Davie, J.R. (1993). Effects of histone acetylation, ubiquitination and variants on nucleosome stability. Biochem. J. *296 (Pt 3*, 737–744.

Li, Z., Gadue, P., Chen, K., Jiao, Y., Tuteja, G., Schug, J., Li, W., and Kaestner, K.H. (2012). Foxa2 and H2A.Z mediate nucleosome depletion during embryonic stem cell differentiation. Cell *151*, 1608–1616.

Lichtinger, M., Ingram, R., Hannah, R., Müller, D., Clarke, D., Assi, S.A., Lie-A-Ling, M., Noailles, L., Vijayabaskar, M.S., Wu, M., et al. (2012). RUNX1 reshapes the epigenetic landscape at the onset of haematopoiesis. EMBO J. *31*, 4318–4333.

Liu, H., Kang, H., Liu, R., Chen, X., and Zhao, K. (2002). Maximal Induction of a Subset of Interferon Target Genes Requires the Chromatin-Remodeling Activity of the BAF Complex. Mol. Cell. Biol. *22*, 6471–6479.

Liu, N., Balliano, A., and Hayes, J.J. (2011). Mechanism(s) of SWI/SNF-induced nucleosome mobilization. Chembiochem *12*, 196–204.

Lopez-Perrote, A., Alatwi, H.E., Torreira, E., Ismail, A., Ayora, S., Downs, J.A., and Llorca, O. (2014). Structure of Yin Yang 1 Oligomers That Cooperate with RuvBL1-RuvBL2 ATPases. J. Biol. Chem. *289*, 22614–22629.

Luger, K., Mäder, A.W., Richmond, R.K., Sargent, D.F., and Richmond, T.J. (1997). Crystal structure of the nucleosome core particle at 2.8 A resolution. Nature *389*, 251–260.

Luger, K., Rechsteiner, T.J., and Richmond, T.J. (1999). Chromatin (Elsevier).

Luk, E., Ranjan, A., Fitzgerald, P.C., Mizuguchi, G., Huang, Y., Wei, D., and Wu, C. (2010). Stepwise histone replacement by SWR1 requires dual activation with histone H2A.Z and canonical nucleosome. Cell *143*, 725–736.

Malik, H.S., and Henikoff, S. (2003). Phylogenomics of the nucleosome. Nat. Struct. Biol. *10*, 882–891.

Mao, Z., Pan, L., Wang, W., Sun, J., Shan, S., Dong, Q., Liang, X., Dai, L., Ding, X., Chen, S., et al. (2014). Anp32e, a higher eukaryotic histone chaperone directs preferential recognition for H2A.Z. Cell Res.

Marfella, C.G.A., and Imbalzano, A.N. (2007). The Chd family of chromatin remodelers. Mutat. Res. *618*, 30–40.

Marques, M., Laflamme, L., Gervais, A.L., and Gaudreau, L. (2010). Reconciling the positive and negative roles of histone H2A.Z in gene transcription. Epigenetics 267–272.

Marzluff, W.F., Gongidi, P., Woods, K.R., Jin, J., and Maltais, L.J. (2002). The Human and Mouse Replication-Dependent Histone Genes. Genomics *80*, 487–498.

Marzluff, W.F., Wagner, E.J., and Duronio, R.J. (2008). Metabolism and regulation of canonical histone mRNAs: life without a poly(A) tail. Nat. Rev. Genet. *9*, 843–854.

Mavrich, T.N., Ioshikhes, I.P., Venters, B.J., Jiang, C., Tomsho, L.P., Qi, J., Schuster, S.C., Albert, I., and Pugh, B.F. (2008a). A barrier nucleosome model for statistical positioning of nucleosomes throughout the yeast genome. Genome Res. *18*, 1073–1083.

Mavrich, T.N., Jiang, C., Ioshikhes, I.P., Li, X., Venters, B.J., Zanton, S.J., Tomsho, L.P., Qi, J., Glaser, R.L., Schuster, S.C., et al. (2008b). Nucleosome organization in the Drosophila genome. Nature *453*, 358–362.

McKercher, S.R., Torbett, B.E., Anderson, K.L., Henkel, G.W., Vestal, D.J., Baribault, H., Klemsz, M., Feeney, A.J., Wu, G.E., Paige, C.J., et al. (1996). Targeted disruption of the PU.1 gene results in multiple hematopoietic abnormalities. EMBO J. *15*, 5647–5658.

Medzhitov, R., and Horng, T. (2009). Transcriptional control of the inflammatory response. Nat. Rev. Immunol. *9*, 692–703.

Mehta, M., Kim, H.-S., and Keogh, M.-C. (2010). Sometimes one just isn't enough: do vertebrates contain an H2A.Z hyper-variant? J. Biol. *9*, 3.

Meneghini, M.D., Wu, M., and Madhani, H.D. (2003). Conserved histone variant H2A.Z protects euchromatin from the ectopic spread of silent heterochromatin. Cell *112*, 725–736.

Millar, C.B. (2013). Organizing the genome with H2A histone variants. Biochem. J. *449*, 567–579.

Millau, J.-F., and Gaudreau, L. (2011). CTCF, cohesin, and histone variants: connecting the genome. Biochem. Cell Biol. *89*, 505–513.

Mizuguchi, G., Shen, X., Landry, J., Wu, W.-H., Sen, S., and Wu, C. (2004). ATP-driven exchange of histone H2AZ variant catalyzed by SWR1 chromatin remodeling complex. Science *303*, 343–348.

Mohrmann, L., and Verrijzer, C.P. (2005). Composition and functional specificity of SWI2/SNF2 class chromatin remodeling complexes. Biochim. Biophys. Acta - Gene Struct. Expr. *1681*, 59–73.

Mohrmann, L., Langenberg, K., Krijgsveld, J., Kal, A.J., Heck, A.J.R., and Verrijzer,

C.P. (2004). Differential Targeting of Two Distinct SWI/SNF-Related Drosophila Chromatin-Remodeling Complexes. Mol. Cell. Biol. *24*, 3077–3088.

Morris, S.A., Baek, S., Sung, M.-H., John, S., Wiench, M., Johnson, T.A., Schiltz, R.L., and Hager, G.L. (2013). Overlapping chromatin-remodeling systems collaborate genome wide at dynamic chromatin transitions. Nat. Struct. Mol. Biol. *advance on*.

Moshkin, Y.M., Chalkley, G.E., Kan, T.W., Reddy, B.A., Ozgur, Z., van Ijcken, W.F.J., Dekkers, D.H.W., Demmers, J.A., Travers, A.A., and Verrijzer, C.P. (2012). Remodelers organize cellular chromatin by counteracting intrinsic histone-DNA sequence preferences in a class-specific manner. Mol. Cell. Biol. *32*, 675–688.

Mueller-Planitz, F., Klinker, H., and Becker, P.B. (2013). Nucleosome sliding mechanisms: new twists in a looped history. Nat. Struct. Mol. Biol. *20*, 1026–1032.

Narlikar, G.J., Phelan, M.L., and Kingston, R.E. (2001). Generation and Interconversion of Multiple Distinct Nucleosomal States as a Mechanism for Catalyzing Chromatin Fluidity. Mol. Cell *8*, 1219–1230.

Natoli, G. (2010). Maintaining Cell Identity through Global Control of Genomic Organization. Immunity *33*, 12–24.

Neigeborn, L., and Carlson, M. (1984). Genes affecting the regulation of SUC2 gene expression by glucose repression in Saccharomyces cerevisiae. Genetics *108*, 845–858.

Nekrasov, M., Amrichova, J., Parker, B.J., Soboleva, T.A., Jack, C., Williams, R., Huttley, G.A., and Tremethick, D.J. (2012). Histone H2A.Z inheritance during the cell cycle and its impact on promoter organization and dynamics. Nat. Struct. Mol. Biol. *19*, 1076–1083.

Nelson, H.C.M., Finch, J.T., Luisi, B.F., and Klug, A. (1987). The structure of an oligo(dA)•oligo(dT) tract and its biological implications. Nature *330*, 221–226.

Neph, S., Vierstra, J., Stergachis, A.B., Reynolds, A.P., Haugen, E., Vernot, B., Thurman, R.E., John, S., Sandstrom, R., Johnson, A.K., et al. (2012a). An expansive human regulatory lexicon encoded in transcription factor footprints. Nature *489*, 83–90.

Neph, S., Stergachis, A.B., Reynolds, A., Sandstrom, R., Borenstein, E., and Stamatoyannopoulos, J.A. (2012b). Circuitry and dynamics of human transcription factor regulatory networks. Cell *150*, 1274–1286.

Nerlov, C., and Graf, T. (1998). PU.1 induces myeloid lineage commitment in multipotent hematopoietic progenitors. Genes Dev. *12*, 2403–2412.

Nishi, R., Wijnhoven, P., le Sage, C., Tjeertes, J., Galanty, Y., Forment, J. V, Clague, M.J., Urbé, S., and Jackson, S.P. (2014). Systematic characterization of deubiquitylating enzymes for roles in maintaining genome integrity. Nat. Cell Biol. *16*, 1016–1026, 1–8.

Obri, A., Ouararhni, K., Papin, C., Diebold, M.-L., Padmanabhan, K., Marek, M., Stoll, I., Roy, L., Reilly, P.T., Mak, T.W., et al. (2014). ANP32E is a histone chaperone that removes H2A.Z from chromatin. Nature.

Ostuni, R., Piccolo, V., Barozzi, I., Polletti, S., Termanini, A., Bonifacio, S., Curina, A., Prosperini, E., Ghisletti, S., and Natoli, G. (2013). Latent enhancers activated by stimulation in differentiated cells. Cell *152*, 157–171.

Papamichos-Chronakis, M., Watanabe, S., Rando, O.J., and Peterson, C.L. (2011). Global regulation of H2A.Z localization by the INO80 chromatin-remodeling enzyme is essential for genome integrity. Cell *144*, 200–213.

Papoulas, O., Beek, S.J., Moseley, S.L., McCallum, C.M., Sarte, M., Shearn, A., and Tamkun, J.W. (1998). The Drosophila trithorax group proteins BRM, ASH1 and ASH2 are subunits of distinct protein complexes. Development *125*, 3955–3966.

Park, Y.-J., Dyer, P.N., Tremethick, D.J., and Luger, K. (2004). A New Fluorescence Resonance Energy Transfer Approach Demonstrates That the Histone Variant H2AZ Stabilizes the Histone Octamer within the Nucleosome. J. Biol. Chem. *279*, 24274–24282.

Parker, S.C.J., Stitzel, M.L., Taylor, D.L., Orozco, J.M., Erdos, M.R., Akiyama, J.A., van Bueren, K.L., Chines, P.S., Narisu, N., Black, B.L., et al. (2013). Chromatin stretch enhancer states drive cell-specific gene regulation and harbor human disease risk variants. Proc. Natl. Acad. Sci. U. S. A. *110*, 17921–17926.

Parnell, T.J., Schlichter, A., Wilson, B.G., and Cairns, B.R. (2015). The chromatin remodelers RSC and ISW1 display functional and chromatin-based promoter antagonism. Elife *4*, e06073.

Petter, M., Lee, C.C., Byrne, T.J., Boysen, K.E., Volz, J., Ralph, S.A., Cowman, A.F., Brown, G. V, and Duffy, M.F. (2011). Expression of P. falciparum var genes involves exchange of the histone variant H2A.Z at the promoter. PLoS Pathog. *7*, e1001292.

Piper, J., Elze, M.C., Cauchy, P., Cockerill, P.N., Bonifer, C., and Ott, S. (2014). Wellington: a novel method for the accurate identification of digital genomic footprints from DNase-seq data. Nucleic Acids Res. gku727 – .

Platt, R.J., Chen, S., Zhou, Y., Yim, M.J., Swiech, L., Kempton, H.R., Dahlman, J.E., Parnas, O., Eisenhaure, T.M., Jovanovic, M., et al. (2014). CRISPR-Cas9 Knockin Mice for Genome Editing and Cancer Modeling. Cell *159*, 440–455.

Pombo, A., and Dillon, N. (2015). Three-dimensional genome architecture: players and mechanisms. Nat. Rev. Mol. Cell Biol. *16*, 245–257.

Pott, S., and Lieb, J.D. (2015). What are super-enhancers? Nat. Genet. *47*, 8–12.

Quinlan, A.R., and Hall, I.M. (2010). BEDTools: a flexible suite of utilities for comparing genomic features. Bioinformatics *26*, 841–842.

Racki, L.R., Naber, N., Pate, E., Leonard, J., Cooke, R., and Narlikar, G.J. (2014).

The histone H4 tail regulates the conformation of the ATP-binding pocket in the SNF2h chromatin remodeling enzyme. J. Mol. Biol.

Rada-Iglesias, A., Bajpai, R., Swigut, T., Brugmann, S.A., Flynn, R.A., and Wysocka, J. (2011). A unique chromatin signature uncovers early developmental enhancers in humans. Nature *470*, 279–283.

Raisner, R.M., Hartley, P.D., Meneghini, M.D., Bao, M.Z., Liu, C.L., Schreiber, S.L., Rando, O.J., and Madhani, H.D. (2005). Histone Variant H2A.Z Marks the 5′ Ends of Both Active and Inactive Genes in Euchromatin. Cell *123*, 233–248.

Ramirez-Carrozzi, V.R., Nazarian, A.A., Li, C.C., Gore, S.L., Sridharan, R., Imbalzano, A.N., and Smale, S.T. (2006). Selective and antagonistic functions of SWI/SNF and Mi-2beta nucleosome remodeling complexes during an inflammatory response. Genes Dev. *20*, 282–296.

Ramirez-Carrozzi, V.R., Braas, D., Bhatt, D.M., Cheng, C.S., Hong, C., Doty, K.R., Black, J.C., Hoffmann, A., Carey, M., and Smale, S.T. (2009). A unifying model for the selective regulation of inducible transcription by CpG islands and nucleosome remodeling. Cell *138*, 114–128.

Ran, F.A., Hsu, P.D., Wright, J., Agarwala, V., Scott, D.A., and Zhang, F. (2013). Genome engineering using the CRISPR-Cas9 system. Nat. Protoc. *8*, 2281–2308.

Ren, Q., and Gorovsky, M.A. (2001). Histone H2A.Z acetylation modulates an essential charge patch. Mol. Cell *7*, 1329–1335.

Ridgway, P., Brown, K.D., Rangasamy, D., Svensson, U., and Tremethick, D.J. (2004). Unique residues on the H2A.Z containing nucleosome surface are important for Xenopus laevis development. J. Biol. Chem. *279*, 43815–43820.

Rippe, K., Schrader, A., Riede, P., Strohner, R., Lehmann, E., and Längst, G. (2007). DNA sequence- and conformation-directed positioning of nucleosomes by chromatin-remodeling complexes. Proc. Natl. Acad. Sci. U. S. A. *104*, 15635–15640.

De Rop, V., Padeganeh, A., and Maddox, P.S. (2012). CENP-A: the key player behind centromere identity, propagation, and kinetochore assembly. Chromosoma *121*, 527–538.

Ruhl, D.D., Jin, J., Cai, Y., Swanson, S., Florens, L., Washburn, M.P., Conaway, R.C., Conaway, J.W., and Chrivia, J.C. (2006a). Purification of a Human SRCAP Complex That Remodels Chromatin by Incorporating the Histone Variant H2A.Z into Nucleosomes †. Biochemistry *45*, 5671–5677.

Ruhl, D.D., Jin, J., Cai, Y., Swanson, S., Florens, L., Washburn, M.P., Conaway, R.C., Conaway, J.W., and Chrivia, J.C. (2006b). Purification of a human SRCAP complex that remodels chromatin by incorporating the histone variant H2A.Z into nucleosomes. Biochemistry *45*, 5671–5677.

Sabo, P.J., Kuehn, M.S., Thurman, R., Johnson, B.E., Johnson, E.M., Cao, H., Yu,

M., Rosenzweig, E., Goldy, J., Haydock, A., et al. (2006). Genome-scale mapping of DNase I sensitivity in vivo using tiling DNA microarrays © 2 0 0 6 N a t u r e P u b l i s h i n g G r o u p h t t p : / / w w w . n a t u r e . c o m / n a t u r e m e t h o d s. *3*.

Saha, A., Wittmeyer, J., and Cairns, B.R. (2006). Chromatin remodelling: the industrial revolution of DNA around histones. Nat. Rev. Mol. Cell Biol. *7*, 437–447.

Salmon-Divon, M., Dvinge, H., Tammoja, K., and Bertone, P. (2010). PeakAnalyzer: Genome-wide annotation of chromatin binding and modification loci. BMC Bioinformatics *11*, 415.

De Santa, F., Narang, V., Yap, Z.H., Tusi, B.K., Burgold, T., Austenaa, L., Bucci, G., Caganova, M., Notarbartolo, S., Casola, S., et al. (2009). Jmjd3 contributes to the control of gene expression in LPS-activated macrophages. EMBO J. *28*, 3341–3352.

De Santa, F., Barozzi, I., Mietton, F., Ghisletti, S., Polletti, S., Tusi, B.K., Muller, H., Ragoussis, J., Wei, C.-L., and Natoli, G. (2010). A large fraction of extragenic RNA pol II transcription sites overlap enhancers. PLoS Biol. *8*, e1000384.

Santisteban, M.S., Kalashnikova, T., and Smith, M.M. (2000). Histone H2A.Z regulats transcription and is partially redundant with nucleosome remodeling complexes. Cell *103*, 411–422.

Santisteban, M.S., Hang, M., and Smith, M.M. (2011). Histone variant H2A.Z and RNA polymerase II transcription elongation. Mol. Cell. Biol. *31*, 1848–1860.

Sarcinella, E., Zuzarte, P.C., Lau, P.N.I., Draker, R., and Cheung, P. (2007). Monoubiquitylation of H2A.Z distinguishes its association with euchromatin or facultative heterochromatin. Mol. Cell. Biol. *27*, 6457–6468.

Schaffner, W., Kunz, G., Daetwyler, H., Telford, J., Smith, H.O., and Birnstiel, M.L. (1978). Genes and spacers of cloned sea urchin histone DNA analyzed by sequencing. Cell *14*, 655–671.

Schep, A.N., Buenrostro, J.D., Denny, S.K., Schwartz, K., Sherlock, G., and Greenleaf, W.J. (2015). Structured nucleosome fingerprints enable high-resolution mapping of chromatin architecture within regulatory regions. Genome Res.

Schnetz, M.P., Bartels, C.F., Shastri, K., Balasubramanian, D., Zentner, G.E., Balaji, R., Zhang, X., Song, L., Wang, Z., Laframboise, T., et al. (2009). Genomic distribution of CHD7 on chromatin tracks H3K4 methylation patterns. Genome Res. *19*, 590–601.

Schones, D.E., Cui, K., Cuddapah, S., Roh, T.-Y., Barski, A., Wang, Z., Wei, G., and Zhao, K. (2008). Dynamic regulation of nucleosome positioning in the human genome. Cell *132*, 887–898.

Schönheit, J., Kuhl, C., Gebhardt, M.L., Klett, F.F., Riemke, P., Scheller, M., Huang, G., Naumann, R., Leutz, A., Stocking, C., et al. (2013). PU.1 level-directed

chromatin structure remodeling at the Irf8 gene drives dendritic cell commitment. Cell Rep. *3*, 1617–1628.

Scott, E.W., Simon, M.C., Anastasi, J., and Singh, H. (1994). Requirement of transcription factor PU.1 in the development of multiple hematopoietic lineages. Science *265*, 1573–1577.

Segal, E., and Widom, J. (2009). Poly(dA:dT) tracts: major determinants of nucleosome organization. Curr. Opin. Struct. Biol. *19*, 65–71.

Segal, E., Fondufe-Mittendorf, Y., Chen, L., Thåström, A., Field, Y., Moore, I.K., Wang, J.-P.Z., and Widom, J. (2006). A genomic code for nucleosome positioning. Nature *442*, 772–778.

Sevilla, A., and Binda, O. (2014). Post-translational modifications of the histone variant H2AZ. Stem Cell Res. *12*, 289–295.

Sherwood, R.I., Hashimoto, T., O'Donnell, C.W., Lewis, S., Barkal, A.A., van Hoff, J.P., Karun, V., Jaakkola, T., and Gifford, D.K. (2014). Discovery of directional and nondirectional pioneer transcription factors by modeling DNase profile magnitude and shape. Nat. Biotechnol. *32*, 171–178.

Siegel, T.N., Hekstra, D.R., Kemp, L.E., Figueiredo, L.M., Lowell, J.E., Fenyo, D., Wang, X., Dewell, S., and Cross, G.A.M. (2009). Four histone variants mark the boundaries of polycistronic transcription units in Trypanosoma brucei. Genes Dev. *23*, 1063–1076.

Smale, S.T., and Natoli, G. (2014). Transcriptional Control of Inflammatory Responses. Cold Spring Harb. Perspect. Biol. *6*, a016261–a016261.

Smith, C.L., Horowitz-Scherer, R., Flanagan, J.F., Woodcock, C.L., and Peterson, C.L. (2003). Structural analysis of the yeast SWI/SNF chromatin remodeling complex. Nat. Struct. Biol. *10*, 141–145.

Soboleva, T.A., Nekrasov, M., Pahwa, A., Williams, R., Huttley, G.A., and Tremethick, D.J. (2012). A unique H2A histone variant occupies the transcriptional start site of active genes. Nat. Struct. Mol. Biol. *19*, 25–30.

Song, L., and Crawford, G.E. (2010). DNase-seq: a high-resolution technique for mapping active gene regulatory elements across the genome from mammalian cells. Cold Spring Harb. Protoc. *2010*, pdb.prot5384.

Song, L., Zhang, Z., Grasfeder, L.L., Boyle, A.P., Giresi, P.G., Lee, B.-K., Sheffield, N.C., Gräf, S., Huss, M., Keefe, D., et al. (2011a). Open chromatin defined by DNaseI and FAIRE identifies regulatory elements that shape cell-type identity. Genome Res. *21*, 1757–1767.

Song, L., Zhang, Z., Grasfeder, L.L., Boyle, A.P., Giresi, P.G., Lee, B.-K., Sheffield, N.C., Gräf, S., Huss, M., Keefe, D., et al. (2011b). Open chromatin defined by DNaseI and FAIRE identifies regulatory elements that shape cell-type identity. Genome Res. *21*, 1757–1767.

Song, L., Zhang, Z., Grasfeder, L.L., Lee, B., Bhinge, A.A., Battenhouse, A., Boyle, A.P., Giresi, P.G., Sheffield, N.C., Gra, S., et al. (2011c). elements that shape cell-type identity Open chromatin defined by DNaseI and FAIRE identifies regulatory elements that shape cell-type identity. 1757–1767.

Soufi, A., Garcia, M.F., Jaroszewicz, A., Osman, N., Pellegrini, M., and Zaret, K.S. (2015). Pioneer Transcription Factors Target Partial DNA Motifs on Nucleosomes to Initiate Reprogramming. Cell *161*, 555–568.

Spitz, F., and Furlong, E.E.M. (2012). Transcription factors: from enhancer binding to developmental control. Nat. Rev. Genet. *13*, 613–626.

Staber, P.B., Zhang, P., Ye, M., Welner, R.S., Nombela-Arrieta, C., Bach, C., Kerenyi, M., Bartholdy, B.A., Zhang, H., Alberich-Jordà, M., et al. (2013). Sustained PU.1 Levels Balance Cell-Cycle Regulators to Prevent Exhaustion of Adult Hematopoietic Stem Cells. Mol. Cell *49*, 934–946.

Stergachis, A.B., Neph, S., Reynolds, A., Humbert, R., Miller, B., Paige, S.L., Vernot, B., Cheng, J.B., Thurman, R.E., Sandstrom, R., et al. (2013). Developmental Fate and Cellular Maturity Encoded in Human Regulatory DNA Landscapes. Cell *154*, 888–903.

Stern, M., Jensen, R., and Herskowitz, I. (1984). Five SWI genes are required for expression of the HO gene in yeast. J. Mol. Biol. *178*, 853–868.

Su, W., Jackson, S., Tjian, R., and Echols, H. (1991). DNA looping between sites for transcriptional activation: self-association of DNA-bound Sp1. Genes Dev. *5*, 820–826.

Sung, M.-H., Guertin, M.J., Baek, S., and Hager, G.L. (2014). DNase Footprint Signatures Are Dictated by Factor Dynamics and DNA Sequence. Mol. Cell.

Sutcliffe, E.L., Parish, I.A., He, Y.Q., Juelich, T., Tierney, M.L., Rangasamy, D., Milburn, P.J., Parish, C.R., Tremethick, D.J., and Rao, S. (2009). Dynamic Histone Variant Exchange Accompanies Gene Induction in T Cells. Mol. Cell. Biol. *29*, 1972–1986.

Szenker, E., Ray-Gallet, D., and Almouzni, G. (2011). The double face of the histone variant H3.3. Cell Res. *21*, 421–434.

Talbert, P.B., and Henikoff, S. (2010). Histone variants--ancient wrap artists of the epigenome. Nat. Rev. Mol. Cell Biol. *11*, 264–275.

Talbert, P.B., and Henikoff, S. (2014). Environmental responses mediated by histone variants. Trends Cell Biol.

Teif, V.B., Vainshtein, Y., Caudron-Herger, M., Mallm, J.-P., Marth, C., Höfer, T., and Rippe, K. (2012). Genome-wide nucleosome positioning during embryonic stem cell development. Nat. Struct. Mol. Biol. *19*, 1185–1192.

Tewhey, R., Nakano, M., Wang, X., Pabón-Peña, C., Novak, B., Giuffre, A., Lin, E., Happe, S., Roberts, D.N., LeProust, E.M., et al. (2009). Enrichment of sequencing

targets from the human genome by solution hybridization. Genome Biol. *10*, R116.

Thakar, A., Gupta, P., McAllister, W.T., and Zlatanova, J. (2010). Histone variant H2A.Z inhibits transcription in reconstituted nucleosomes. Biochemistry *49*, 4018–4026.

Thambirajah, A.A., Dryhurst, D., Ishibashi, T., Li, A., Maffey, A.H., and Ausio, J. (2006). H2A.Z Stabilizes Chromatin in a Way That Is Dependent on Core Histone Acetylation. J. Biol. Chem. *281*, 20036–20044.

Thatcher, T.H., and Gorovsky, M.A. (1994). Phylogenetic analysis of the core histones H2A, H2B, H3, and H4. Nucleic Acids Res. *22*, 174–179.

Thurman, R.E., Rynes, E., Humbert, R., Vierstra, J., Maurano, M.T., Haugen, E., Sheffield, N.C., Stergachis, A.B., Wang, H., Vernot, B., et al. (2012). The accessible chromatin landscape of the human genome. Nature *489*, 75–82.

Tillo, D., and Hughes, T.R. (2009). G+C content dominates intrinsic nucleosome occupancy. BMC Bioinformatics *10*, 442.

Tirosh, I., Sigal, N., and Barkai, N. (2010). Widespread remodeling of mid-coding sequence nucleosomes by Isw1. Genome Biol. *11*, R49.

Torchy, M.P., Hamiche, A., and Klaholz, B.P. (2015). Structure and function insights into the NuRD chromatin remodeling complex. Cell. Mol. Life Sci. *72*, 2491–2507.

Tsukuda, T., Fleming, A.B., Nickoloff, J.A., and Osley, M.A. (2005). Chromatin remodelling at a DNA double-strand break site in Saccharomyces cerevisiae. Nature *438*, 379–383.

Tsukuda, T., Lo, Y.-C., Krishna, S., Sterk, R., Osley, M.A., and Nickoloff, J.A. (2009). INO80-dependent chromatin remodeling regulates early and late stages of mitotic homologous recombination. DNA Repair (Amst). *8*, 360–369.

Valdés-Mora, F., Song, J.Z., Statham, A.L., Strbenac, D., Robinson, M.D., Nair, S.S., Patterson, K.I., Tremethick, D.J., Stirzaker, C., and Clark, S.J. (2012). Acetylation of H2A.Z is a key epigenetic modification associated with gene deregulation and epigenetic remodeling in cancer. Genome Res. *22*, 307–321.

Valouev, A., Johnson, S.M., Boyd, S.D., Smith, C.L., Fire, A.Z., and Sidow, A. (2011). Determinants of nucleosome organization in primary human cells. Nature *474*, 516–520.

Visel, A., Rubin, E.M., and Pennacchio, L.A. (2009a). Genomic views of distant-acting enhancers. Nature *461*, 199–205.

Visel, A., Blow, M.J., Li, Z., Zhang, T., Akiyama, J.A., Holt, A., Plajzer-Frick, I., Shoukry, M., Wright, C., Chen, F., et al. (2009b). ChIP-seq accurately predicts tissue-specific activity of enhancers. Nature *457*, 854–858.

van Vugt, J.J.F.A., de Jager, M., Murawska, M., Brehm, A., van Noort, J., and Logie, C. (2009). Multiple aspects of ATP-dependent nucleosome translocation by RSC

and Mi-2 are directed by the underlying DNA sequence. PLoS One *4*, e6345.

Wang, L., Du, Y., Ward, J.M., Shimbo, T., Lackford, B., Zheng, X., Miao, Y., Zhou, B., Han, L., Fargo, D.C., et al. (2014). INO80 Facilitates Pluripotency Gene Activation in Embryonic Stem Cell Self-Renewal, Reprogramming, and Blastocyst Development. Cell Stem Cell *14*, 575–591.

Wang, W., Côté, J., Xue, Y., Zhou, S., Khavari, P.A., Biggar, S.R., Muchardt, C., Kalpana, G. V, Goff, S.P., Yaniv, M., et al. (1996). Purification and biochemical heterogeneity of the mammalian SWI-SNF complex. EMBO J. *15*, 5370–5382.

Watanabe, S., and Peterson, C.L. (2010). The INO80 family of chromatin-remodeling enzymes: regulators of histone variant dynamics. Cold Spring Harb. Symp. Quant. Biol. *75*, 35–42.

Watanabe, S., Radman-Livaja, M., Rando, O.J., and Peterson, C.L. (2013). A histone acetylation switch regulates H2A.Z deposition by the SWR-C remodeling enzyme. Science *340*, 195–199.

Weber, C.M., and Henikoff, S. (2014). Histone variants: dynamic punctuation in transcription. Genes Dev. *28*, 672–682.

Weber, C.M., Ramachandran, S., and Henikoff, S. (2014). Nucleosomes Are Context-Specific, H2A.Z-Modulated Barriers to RNA Polymerase. Mol. Cell *53*, 819–830.

Wei, G.-H., Badis, G., Berger, M.F., Kivioja, T., Palin, K., Enge, M., Bonke, M., Jolma, A., Varjosalo, M., Gehrke, A.R., et al. (2010). Genome-wide analysis of ETS-family DNA-binding in vitro and in vivo. EMBO J. *29*, 2147–2160.

Weiner, A., Hughes, A., Yassour, M., Rando, O.J., and Friedman, N. (2010). High-resolution nucleosome mapping reveals transcription-dependent promoter packaging. 90–100.

West, M.H., and Bonner, W.M. (1980). Histone 2A, a heteromorphous family of eight protein species. Biochemistry *19*, 3238–3245.

Whitehouse, I., and Tsukiyama, T. (2006). Antagonistic forces that position nucleosomes in vivo. Nat. Struct. Mol. Biol. *13*, 633–640.

Whittle, C.M., McClinic, K.N., Ercan, S., Zhang, X., Green, R.D., Kelly, W.G., and Lieb, J.D. (2008). The genomic distribution and function of histone variant HTZ-1 during C. elegans embryogenesis. PLoS Genet. *4*, e1000187.

Whyte, W.A., Orlando, D.A., Hnisz, D., Abraham, B.J., Lin, C.Y., Kagey, M.H., Rahl, P.B., Lee, T.I., and Young, R.A. (2013). Master transcription factors and mediator establish super-enhancers at key cell identity genes. Cell *153*, 307–319.

Wimalarathna, R.N., Pan, P.Y., and Shen, C.-H. (2014). Co-dependent recruitment of Ino80p and Snf2p is required for yeast CUP1 activation. Biochem. Cell Biol. *92*, 69–75.

Wu, W.-H., Alami, S., Luk, E., Wu, C.-H., Sen, S., Mizuguchi, G., Wei, D., and Wu, C. (2005). Swc2 is a widely conserved H2AZ-binding module essential for ATP-dependent histone exchange. Nat. Struct. Mol. Biol. *12*, 1064–1071.

Xu, Y., Ayrapetov, M.K., Xu, C., Gursoy-Yuzugullu, O., Hu, Y., and Price, B.D. (2012). Histone H2A.Z controls a critical chromatin remodeling step required for DNA double-strand break repair. Mol. Cell *48*, 723–733.

Yardımcı, G.G., Frank, C.L., Crawford, G.E., and Ohler, U. (2014). Explicit DNase sequence bias modeling enables high-resolution transcription factor footprint detection. Nucleic Acids Res. gku810 – .

Yen, K., Vinayachandran, V., Batta, K., Koerber, R.T., and Pugh, B.F. (2012). Genome-wide nucleosome specificity and directionality of chromatin remodelers. Cell *149*, 1461–1473.

Yen, K., Vinayachandran, V., and Pugh, B.F. (2013). SWR-C and INO80 chromatin remodelers recognize nucleosome-free regions near +1 nucleosomes. Cell *154*, 1246–1256.

Yigit, E., Zhang, Q., Xi, L., Grilley, D., Widom, J., Wang, J.-P., Rao, A., and Pipkin, M.E. (2013). High-resolution nucleosome mapping of targeted regions using BAC-based enrichment. Nucleic Acids Res. *41*, e87.

Yildirim, O., Li, R., Hung, J.-H., Chen, P.B., Dong, X., Ee, L.-S., Weng, Z., Rando, O.J., and Fazzio, T.G. (2011). Mbd3/NURD complex regulates expression of 5-hydroxymethylcytosine marked genes in embryonic stem cells. Cell *147*, 1498–1510.

Yodh, J. (2013). ATP-Dependent Chromatin Remodeling. Adv. Exp. Med. Biol. *767*, 263–295.

Yuan, G.-C., and Liu, J.S. (2008). Genomic Sequence Is Highly Predictive of Local Nucleosome Depletion. PLoS Comput. Biol. *4*, e13.

Yuan, J., Adamski, R., and Chen, J. (2010). Focus on histone variant H2AX: to be or not to be. FEBS Lett. *584*, 3717–3724.

Yukawa, M., Akiyama, T., Franke, V., Mise, N., Isagawa, T., Suzuki, Y., Suzuki, M.G., Vlahovicek, K., Abe, K., Aburatani, H., et al. (2014). Genome-Wide Analysis of the Chromatin Composition of Histone H2A and H3 Variants in Mouse Embryonic Stem Cells. PLoS One *9*, e92689.

Zambelli, F., Pesole, G., and Pavesi, G. (2009). Pscan: finding over-represented transcription factor binding site motifs in sequences from co-regulated or co-expressed genes. Nucleic Acids Res. *37*, W247–W252.

Zaret, K.S., and Carroll, J.S. (2011). Pioneer transcription factors: establishing competence for gene expression. Genes Dev. *25*, 2227–2241.

Zentner, G.E., and Henikoff, S. (2013). Regulation of nucleosome dynamics by histone modifications. Nat. Struct. Mol. Biol. *20*, 259–266.

Zentner, G.E., Tsukiyama, T., and Henikoff, S. (2013). ISWI and CHD chromatin remodelers bind promoters but act in gene bodies. PLoS Genet. *9*, e1003317.

Zhang, H., Roberts, D.N., and Cairns, B.R. (2005). Genome-wide dynamics of Htz1, a histone H2A variant that poises repressed/basal promoters for activation through histone loss. Cell *123*, 219–231.

Zhang, Y., Liu, T., Meyer, C.A., Eeckhoute, J., Johnson, D.S., Bernstein, B.E., Nussbaum, C., Myers, R.M., Brown, M., Li, W., et al. (2008). Model-based Analysis of ChIP-Seq (MACS). Genome Biol. *9*, R137.

Zhang, Y., Moqtaderi, Z., Rattner, B.P., Euskirchen, G., Snyder, M., Kadonaga, J.T., Liu, X.S., and Struhl, K. (2009). Intrinsic histone-DNA interactions are not the major determinant of nucleosome positions in vivo. Nat. Struct. Mol. Biol. *16*, 847–852.

Zhang, Z., Wippo, C.J., Wal, M., Ward, E., Korber, P., and Pugh, B.F. (2011). A packing mechanism for nucleosome organization reconstituted across a eukaryotic genome. Science *332*, 977–980.

Zhou, V.W., Goren, A., and Bernstein, B.E. (2011). Charting histone modifications and the functional organization of mammalian genomes. Nat. Rev. Genet. *12*, 7–18.

Zilberman, D., Coleman-Derr, D., Ballinger, T., and Henikoff, S. (2008). Histone H2A.Z and DNA methylation are mutually antagonistic chromatin marks. Nature *456*, 125–129.

Zlatanova, J., and Thakar, A. (2008). H2A.Z: View from the Top. Structure *16*, 166–179.

Zuber, J., McJunkin, K., Fellmann, C., Dow, L.E., Taylor, M.J., Hannon, G.J., and Lowe, S.W. (2011). Toolkit for evaluating genes required for proliferation and survival using tetracycline-regulated RNAi. Nat. Biotechnol. *29*, 79–83.